

Linear and Non-linear Analysis of Dust Acoustic Waves in Electronegative Halley Comet Plasma

by

Muhammad Younas Khan

A thesis
submitted in partial fulfillment of the
requirements for the degree of
Master of Science
in
Physics


Supervised by
Dr. Muddasir Ali Shah



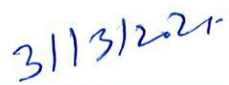
School of Natural Sciences,
National University of Sciences and Technology,
H-12, Islamabad, Pakistan
January, 2021

National University of Sciences & Technology**MS THESIS WORK**

We hereby recommend that the dissertation prepared under our supervision by: Muhammad Younas Khan, Regn No. 00000203240 Titled: **Linear and Non-linear Analysis of Dust Acoustic Waves in Electronegative Halley Comet Plasma** accepted in partial fulfillment of the requirements for the award of **MS** degree.

Examination Committee Members1. Name: Dr. M. ALI PARACHASignature: 2. Name: DR. AEYSHA KHALIQUESignature: External Examiner: DR. Muhammad ShahidSignature: Supervisor's Name: DR. MUDDASIR ALI SHAHSignature: 


 Head of Department



 Date
COUNTERSIGNEDDate: 01/04/2021


 Dean/Principal

Dedicated

to

My Beloved Late Mother

Acknowledgements

All Praises to Almighty Allah, the most benevolent and merciful, who enabled me to complete this research work successfully. And pay my innumerable homage to our beloved Prophet MUHAMMAD (SAW).

First and foremost I would like to express my sincere gratitude to my supervisor **Dr. Muddasir Ali Shah**, Assistant Professor (SNS, NUST) for his invaluable guidance and supervision during the completion of this thesis. His passion and support for research was always motivational for me even during tough times in my M.S pursuit. Without his encouragement, patience, and instructions, this thesis would not have been completed.

I am also pleased to all the SNS faculty members and administration for their support, especially I would deeply thank to my committee members **Dr. Muhammad Ali Paracha** and **Dr. Aeysha Khalique**, for guidance, encouragement and cooperation. I would like to express my sincere gratitude to **Prof. Dr. Mushtaq Ahmad**, department of physics, FBAS, International Islamic University (IIUI), Islamabad. The countless discussions we have had and the explanations, the original ideas he shared with me were an invaluable contribution to this thesis. I could not have imagined having a better mentor. I am much obliged to **Dr. Zahida Ehsan** from CIIT, Lahore campus for here guidance and always being so supportive. I am particularly indebted to **Mr. Muhammad Kundi** who has provided me extensive personal and professional guidance and taught me a great deal about both scientific research and life in general. My heartiest thanks to all members of Plasma Physics Group at School of Natural Sciences (SNS), Physics Department. My cordial thanks to all my friends specially **Muhammad Ismail, Dr. Amjad Ali Khan, Dr. Mehar Ali Malik, Dr. Mureed**

Hussain, Mr. Akhtar Munir Khan, Mr. Saad Ghaffar, Ahzaz Khan Jadoon, Farman Ullah Khan, Kifayat Ullah Shah, Imran Khan, Safeer Ullah, Zaheer Khan and Naveed Khan for their cooperation.

Finally, I sincerely pray for my late mother. May ALLAH grant here the highest place in jannat-ul-firdos. I express my deep love for my father , brother and sister. Their affection and prayers kept me strong and resilient.

Muhammad Younas Khan

Abstract

In this thesis, we have discussed linear and non-linear effects on dust acoustic waves (DAWs) in a magnetized electronegative dusty plasma. By electronegative dusty plasma, we mean the plasma having electrons, positive ions, negative ions, and dust particulates constituents. In the linear analysis regime, in the absence of dust charge fluctuations, the Doppler's frequency and growth rate are our main focus. The Doppler's frequency variation has been discussed with the effects of Cairns distributed positive ions, obliqueness of the magnetic field, density ratio of electrons versus energetic positive ions, and normalized dust cyclotron frequency or magnitude of the magnetic field. It was found that for dust acoustic waves these parameters affect the Doppler's frequency. Similarly, the growth rate variations have been discussed with the effects of Cairns distributed positive ions, obliqueness of the magnetic field, normalized dust cyclotron frequency, density ratio of electrons versus energetic positive ions, and density ratio of negative ions versus energetic positive ions. It was observed that for dust acoustic waves these parameters affect the growth rate. While in the same regime we also considered the dust charge fluctuation and derived a linear expression.

On the other hand, in the non-linear regime, DAWs have been investigated. Since we are studying the low-frequency wave, therefore, we have to enlarge the space and time coordinates by stretching the coordinates. By using the Reductive Perturbation Technique (RPT), the Korteweg-de Vries Burger equation is derived for the small but finite amplitude non-linear dust acoustic wave (DAWs) bearing non-thermality (Cairns distributed) in the positive ions. In our case, the non-linear KdVB equation in the absence of the dust charge fluctuation, the dissipative term vanishes, and the non-linear KdVB equation is reduced to the KdV equation which admits solitary wave solution. While

for the parallel propagation, i.e., $\theta = 0$ (no obliqueness in the magnetic field) under certain boundary conditions, i.e., $N_d^{(1)}(\xi, \tau), \frac{dN_d^{(1)}(\xi, \tau)}{d\eta} \rightarrow 0$ as $\eta \rightarrow -\infty$, the non-linear dust acoustic wave is governed by Burger equation which admits the monotonic shock solution. In this analysis, the amplitude, as well as the width of the soliton, has been discussed with effects of obliqueness, Cairns distributed positive ions, density ratio of electrons versus Cairns distributed positive ions and density ratio of negative ions versus Cairns distributed positive ions. It was found that for dust acoustic waves these parameters affect the propagation properties of solitary waves. Similarly, the amplitude of the monotonic shock has been discussed with the effects of Cairns distributed positive ions, density ratio of electrons versus energetic positive ions, and density ratio of negative ions versus energetic positive ions, it is found that for dust acoustic waves these parameters affect the monotonic shock structure.

Contents

List of Figures	x
List of Tables	xv
1 Introduction	1
1.1 What is Plasma	1
1.1.1 Criteria for Plasmas	3
1.2 Non-Degenerate or Classical Plasmas Regime	3
1.3 Magnetized Plasma	4
1.4 Dusty Plasma	5
1.5 Characteristics of Dusty Plasma	6
1.5.1 Macroscopic Neutrality	8
1.5.2 Debye Shielding	8
1.5.3 Characteristic Frequencies	10
1.6 Dust Charging Processes	12
1.7 Isolated Dust Grains	14
1.7.1 Collection of Plasma Particles	14
1.7.2 Photo-emission	16
1.7.3 Radioactivity	17
1.8 Non-isolated Dust Grains	18
1.9 Different types of Non-linear Structures	19

1.9.1	Solitons	19
1.9.2	Shock Waves	21
1.10	Dusty Plasma in Space	23
1.10.1	Interplanetary Space	24
1.10.2	Comets	24
1.10.3	Jupiter's Ring System	26
1.10.4	Saturn's Ring System	27
1.10.5	Uranian Ring System	28
1.10.6	Earth's Atmosphere	28
1.11	Dusty Plasmas in Laboratories	29
1.11.1	DC and RF Discharge	29
1.11.2	Fusion Plasma Devices	30
2	Mathematical Model	32
2.1	Mathematical Model	32
2.1.1	Reductive Perturbative Method	33
2.2	Korteweg de-Vries (KdV) Equation	34
2.2.1	Exact Solution of Kd-V equation	35
2.3	Burger Equation	38
2.3.1	Solution of Burger Equation	38
2.4	Distribution Functions	41
2.4.1	Maxwellian Distribution Function	42
2.4.2	Cairns Distribution Function	43
2.5	Linear Analysis of Plasma Waves	45
2.5.1	Dust Acoustic Waves	46
2.5.2	Dust Ion Acoustic Waves	48
2.6	Non-linear Analysis of Plasma Waves	49
2.6.1	Dust Acoustic Solitary Waves	50
2.6.2	Dust Acoustic Shock Waves	55
2.6.3	Dust Ion Acoustic Shock Waves	57

3	Linear and Non-linear Analysis of Dust Acoustic Waves in Electronegative Halley Comet Plasma	61
3.1	Introduction	61
3.2	Physical Assumptions	63
3.3	Model Equations	66
3.4	Linear Analysis	69
3.4.1	DAWs in the Absence of Dust Charge Fluctuations	69
3.4.2	Growth Rate	70
3.4.3	DAWs in the Presence of Dust Charge Fluctuations	75
3.5	Derivation of Non-linear Evaluation Equation	78
3.6	Stationary Solution: Generation of Shock Wave	84
3.7	Parametric Analysis	86
4	Discussions and Conclusions	88
4.1	Discussions	88
4.2	Conclusions	91
	Bibliography	101
	Appendix	108

List of Figures

1.1	A view of comet Hale-Bopp showing.	25
1.2	A view of comet Hale-Bopp showing two distinct tails.	30
2.1	Propagation of KdV Solitons for two different values (a) Solid curves $\beta = 1$ and (b) Dashed lines $t = 2$	37
2.2	Maxwell Distribution Function	43
2.3	Cairn Distribution Function	44
3.1	Variation of Doppler frequency (ω_D) against wave number (k) for differ- ent value of non-thermal parameter " a ".	70
3.2	Variation of Doppler frequency (ω_D) against wave number (k) for differ- ent value of obliqueness of the magnetic field θ	71
3.3	Variation of Doppler frequency (ω_D) against wave number (k) for differ- ent value of non-thermal parameter " a " at fixed obliqueness of magnetic field θ . The left panel represents $\theta = 5$ and the right panel represents $\theta = 30$	72
	(a)	72
	(b)	72
3.4	The profile of Doppler frequency (ω_D) against wave number (k) for dif- ferent value of density ratio δ_p . The other parameters are $\theta = 30$ and a $= 0$	72
3.5	The behavior of Doppler frequency (ω_D) versus wave number (k) for dif- ferent values of non-thermal parameter " a " with fixed density ratio δ_p . The left panel shows $\delta_p = 0.1$ and right panel shows $\delta_p = 0.3$	73

(a)	73
(b)	73
3.6	The profile of Doppler frequency (ω_D) against wave number (k) for different value of normalized dust cyclotron frequency ω_{cd} . The other parameters are $\theta = 30$ and $a = 0$	73
3.7	The profile of Doppler frequency (ω_D) against wave number (k) for different values of non-thermal parameter "a" with fixed normalized dust cyclotron frequency ω_{cd} . The left panel shows the $\omega_{cd} = 0.011$ and right panel shows the $\omega_{cd} = 0.033$	74
(a)	74
(b)	74
3.8	Plot of growth rate (γ) as a function of wave number (k) for different values of non-thermal parameter "a".	74
3.9	Plot of growth rate (γ) as a function of wave number (k) for different values of magnetic field obliqueness θ	75
3.10	The behavior of growth rate (γ) against wave number (k) for different value of non-thermal parameter "a" with fixed magnetic field obliqueness θ . The left panel shows $\theta = 15$ and right panel shows $\theta = 30$	76
(a)	76
(b)	76
3.11	The variation of growth rate (γ) versus wave number (k) for different values of normalized dust cyclotron frequency ω_{cd}	76
3.12	The variation of growth rate (γ) as a function of wave number (k) for different values of non-thermal parameter "a" at fixed normalized dust cyclotron frequency ω_{cd} . The left panel shows $\omega_{cd} = 0.011$ and the right panel shows $\omega_{cd} = 0.033$	77
(a)	77
(b)	77

3.13	Plot of growth rate (γ) versus wave number (k) for different values of density ratio δ_n	77
3.14	The behavior of growth rate (γ) versus wave number (k) for different values of non-thermal parameter "a" at fixed density ratio δ_n . The left plot shows $\delta_n = 0.1$ and the right plot shows $\delta_n = 0.3$	78
	(a)	78
	(b)	78
3.15	The profile of growth rate (γ) against wave number (k) for different value of density ratio δ_p . The other parameters are $\theta = 30$ and $a = 0$	78
3.16	The profile of growth rate (γ) versus wave number (k) for different value of non-thermal parameter "a" at fixed density ratio δ_p . The left panel shows $\delta_p = 0.1$ and the right panel shows $\delta_p = 0.3$	79
	(a)	79
	(b)	79
3.17	Variation of dissipative term (μ_{ch}) against density ratio (δ_n) for different value of density ratio δ_p . The other parameters are $\theta = 30$ and $a = 0$	87
3.18	Plot of dissipative term (μ_{ch}) against density ratio (δ_n) for different values of non-thermal parameter "a" at fixed density ratio δ_p . The plot (a) shows $\delta_p = 0.1$ and plot (b) shows $\delta_p = 0.3$	87
	(a)	87
	(b)	87
4.1	The effect of dissipative term (μ_{ch}) against density ratio (δ_n) for different values of obliqueness of magnetic field θ	91
4.2	The effect of dissipative term (μ_{ch}) versus density ratio (δ_n) for different value of different values of non-thermal parameter "a" at fixed magnetic field obliqueness θ . The left panel shows $\theta = 6$ and right panel shows $\theta = 44$	92
	(a)	92

	(b)	92
4.3	The KdV solitons are plotted for different values of non-thermal parameter "a" at fixed obliqueness of magnetic field $\theta = 30$	92
4.4	The profile of KdV solitons for different value of non-thermal parameter "a" at fixed obliqueness of magnetic field that is $\theta = 30$	93
4.5	The profile of KdV solitons for different value of non-thermal parameter "a" at fixed normalized dust cyclotron frequency ω_{cd} . The plot (a) shows $\omega_{cd} = 0.011$ and plot (b) shows $\omega_{cd} = 0.013$	94
	(a)	94
	(b)	94
4.6	The behavior of KdV solitons are plotted for different values of negative ions and positive ions density ratio δ_n . The blue solid curve corresponds to $\delta_n = 0.1$, the red solid curve corresponds to $\delta_n = 0.5$ and the black solid curve corresponds to $\delta_n = 1$ at fixed obliqueness of magnetic field $\theta = 30$	94
4.7	The behavior of KdV solitons for different values of non-thermal parameter "a" at fixed negative ions and positive ions density ratio δ_n . The left panel shows $\delta_n = 0.1$ and right panel shows $\delta_n = 1.0$	95
	(a)	95
	(b)	95
4.8	The profile of KdV solitons for different value of electrons and positive ions density ratio δ_p at fixed obliqueness of magnetic field $\theta = 30$	95
4.9	The profile of KdV solitons for different values of non-thermal parameter "a" at fixed electrons and positive ions density ratio δ_p . The left panel shows $\delta_p = 0.1$ and right panel shows $\delta_p = 1.0$	96
	(a)	96
	(b)	96
4.10	The profile of KdV solitons are plotted for different values of obliqueness of magnetic field θ	96

4.11	The profile KdV solitons are plotted for different value of obliqueness of magnetic field θ . The left panel shows $\theta = 20$ and right panel shows $\theta = 44$	97
	(a)	97
	(b)	97
4.12	The profile of monotonic dust-acoustic shocks are plotted for different value of non-thermal parameter " a ".	97
4.13	The behavior of monotonic dust-acoustic shocks are plotted for different value of negative and positive ions density ratio δ_n at fixed non-thermal parameter $a = 0.07$	98
4.14	The behavior of monotonic dust-acoustic shocks are plotted for different values of non-thermal parameter " a " at fixed density ratio δ_n	99
	(a)	99
	(b)	99
4.15	The profile of monotonic dust-acoustic shocks are plotted for different values of electrons and positive ions density ratio δ_p at fixed non-thermal parameter $a = 0.07$	99
4.16	The profile of monotonic dust-acoustic shocks are plotted for different value of non-thermal parameter " a " at fixed electrons and positive ions density ratio δ_p . The left plot shows $\delta_p = 0.1$ and right plot shows $\delta_p = 0.9$. . .	100
	(a)	100
	(b)	100

List of Tables

Chapter 1

Introduction

1.1 What is Plasma

The word "plasma" is derived from the Greek which means something molded or fabricated. For the very first time in 1929, it was Irving Langmuir an American scientist and a Nobel laureate who proposed that an ionized gas comprising of the ions, electrons, and neutrals could be considered as fluid and called this fluid medium plasma [1]. After 1929, the research in the plasma field widely spread in many directions like the development of radio broadcasting which led to the discovery of the Earth's ionosphere (a layer in the upper atmosphere which is partially ionized), which absorbs the radio waves and also distorts the same radio waves [2]. We have already familiar with the three states of matter but not so much familiar with the fourth state of matter that is a "plasma" state. Thus, plasma is considered the fourth state of matter. By giving sufficient heat to gas, it can be converted into ionized gas and under certain conditions it becomes plasma. These conditions under which the ionized gas becomes plasma will be discussed later. Firstly, we define plasma in such a way that it is "a quasineutral gas of charged and neutral particles which exhibits collective behavior" [3]. By "quasineutrality" we mean that their is an equivalency of negative charge density (n_-) and positive charge density (n_+) that is $n_- \approx n_+ = n$, where n is the common plasma density. But here one thing is most important that the plasma cannot be considered a neutral mixture of electrons and ions but a small deviation from neutrality is developed on a very small scale called Debye length, therefore, the plasma must be

quasi-neutral on a length scale larger than Debye length. By the word "collective", we mean the interaction between the positive and negative charge due to long-range electromagnetic forces which predominates the collisions. Therefore, the motion of the charged particles not only depends on local conditions but the state of plasma in the remote region as well. In plasma, the electrostatic interaction can be described by the Coulomb force which is also a long-range force and decays with the distance r^{-2} . On the other hand in neutral gas dynamics, the particle interaction is through short-range Vander Waal's force during collisions. This force decays very rapidly with the distance r^{-6} [4].

At the time of the Big Bang, the temperature is excessively high that the whole universe was in the state of plasma. And due to very much high temperature, the plasma at that time was a quark-gluon plasma. As time passes the temperature of the plasma decreases and the well-known states of matter that is gas, liquid and solids are began to form. However, most of the matter in the universe is still in a plasma state, it is estimated to be 99 percent of the plasma [3]. Therefore, the temperature is one of the fundamental parameters of a plasma. Besides temperature, the particles (electron and ion) per unit volume known as number density is also an important parameter. Since we considered the simple plasma situation contained only two species that is electrons and positive ions. But there is a certain environment that contains other species like positrons, negative ions, dust particles, etc. Each of these species responds to electromagnetic forces differently, so their number density could be considered as an independent variable. Therefore, the range of the temperature and density is different from space plasma to laboratory plasma. For example, the interstellar gases have a typical density of 10^6 m^{-3} and temperature of about 10^4 K . Space plasma in the solar wind and the vicinity of the earth has particle densities in the range of 10^7 m^{-3} to 10^{11} m^{-3} and temperature in the range of 10^3 K to 10^5 K [5].

1.1.1 Criteria for Plasmas

The ionized gases must satisfied certain criteria to become a plasma. These criterias are

- $\lambda_D \ll L$
- $N_D \gg 1$
- $\omega\tau > 1$

These are the basic criteria to be followed by ionized gases to become plasma where L is the dimension of the plasma and λ_D is the length of the Debye sphere called Debye length and can be expressed as

$$\lambda_D = \sqrt{\frac{\epsilon_0 K_B T}{ne^2}}, \quad (1.1)$$

here n , e and T are equilibrium plasma number density, charge of electron and plasma temperature respectively, and ϵ_0 and K_B are the Boltzmann constant and permittivity of the free space respectively. In the second criteria, their is N_D which represents the number of particles present in the Debye sphere of radius λ_D . Although,

$$\omega \simeq \omega_p = \sqrt{\frac{ne^2}{\epsilon_0 m}}, \quad (1.2)$$

is the characteristic oscillation frequency of a plasma, where m is mass of the plasma specie. For different species, the plasma frequency is different. However, the fast specie frequency in the plasma that is electron frequency is referred to be the plasma frequency. In the third criteria, τ is the mean time of collisions among charged particles and neutrals. [3].

1.2 Non-Degenerate or Classical Plasmas Regime

The temperature and particle number density are the most important parameters in plasma. The non-degenerate or classical plasma regime can be characterized by a low

number of density and high temperature. And to handle such type of plasma dynamics, the classical laws with Maxwell-Boltzmann statistics are sufficient to elaborate the dynamical response of the plasma and the energy distribution of classical plasma species that are at thermal equilibrium. However, the non-degenerate or classical plasma can be defined by the coupling parameter as

$$g_c = \frac{e^2 n^{\frac{1}{3}}}{\epsilon_0 K_B T}. \quad (1.3)$$

The coupling parameter is the ratio between interaction energy to the average kinetic energy i.e $g_c = \frac{E_{int}}{E_{kin}}$, and therefore, it is a dimensionless parameter. The interaction energy i.e E_{int} is of the order of electric energy $\frac{e^2 n^{\frac{1}{3}}}{\epsilon_0}$, here the mean distance between the two charged particles is $n^{-\frac{1}{3}}$.

If $g_c \ll 1$, then it means that thermal energy is greater than the interaction energy, and the plasma is weakly coupled called collision-less plasma. In this plasma environment, the particle collisions or Coulomb interaction between two particles are negligible and hence neglected. Whenever, $g_c \simeq 1$ or larger than one the collision factors dominate and cannot be ignored, and thus the plasma is strongly coupled [6].

1.3 Magnetized Plasma

A plasma is said to be magnetized if the strength of the magnetic field B is strong enough to change the trajectories of the plasma species. This magnetic field changes the plasma nature to anisotropic and therefore, the plasma responds differently to forces that are parallel and perpendicular to the magnetic field direction. As the magnetic field strength increases the decrease in the helical orbits occurs and finally these helical orbits become very tightly wound and tying particles to the magnetic field lines effectively. However, the magnetic field has a direct impact on the particles gyrating in the magnetic field, so the Larmor radius (gyro-radius) and cyclotron frequency (gyro-frequency) are also effected. The Larmor radius (gyro-radius) and cyclotron frequency (gyro-frequency) are expressed as:

$$\rho = \frac{V_t}{\omega_c}, \quad (1.4)$$

$$\omega_c = \frac{|q| B}{m}, \quad (1.5)$$

where ρ and ω_c is the Larmor radius (gyro-radius) and cyclotron frequency (gyro-frequency), respectively. Whereas, m and q is the mass and charge of the plasma species, and for each plasma species there is a distinct gyro-radius[3]. If species temperature is comparable then the ion gyro-radius is larger than electron gyro-radius and vice versa,

$$\rho_e \sim \left(\frac{m_e}{m_i}\right)^2 \rho_i. \quad (1.6)$$

Consider L as a characteristic length scale, and when this length L is very small as compare to gyro-radius i.e $\rho \gg L$, then the trajectory of the particle is a straight line. While on the other hand if $\rho \ll L$, then the plasma system is said to be magnetized. The magnetization in a plasma can be measured by magnetization parameter denoted by δ and defined as

$$\delta \equiv \frac{\rho}{L}. \quad (1.7)$$

Sometime in a plasma the ion species are magnetized but electron species is not magnetized, but ignoring these type of situation and take both species of the plasma as a magnetized species. This state is generally achieved when

$$\delta_i \equiv \frac{\rho_i}{L} \ll 1. \quad (1.8)$$

1.4 Dusty Plasma

In most cases, a plasma which is usually the combination of electrons and ions species co-exists with micron or sub-micron additional charged constituents (called dust particles). These charged constituents are either positively or negatively charged depend-

ing on the plasma's surrounding environment . Thus the mixture of electrons, ions, dust particles, and sometimes neutrals forms a "dusty plasma".

For the very first time when the research on the space plasma is started, the dust particle is considered as an impurity that does not change the behavior of the plasma. They just considered the effect of the dust component to be the sum of the effects occurring for individual grains. But after that, it was understood that such a consideration is not complete, but we have to count the new effects of collective behavior of plasmas containing dust grains. In Space plasma, dust is almost present in all environments including earth's upper atmosphere and magnetosphere, interstellar clouds, and in cometary tails, etc. The dust also plays an important role in the dynamics of stellar wind, explosions in nova and supernova, and in the formation of stars and planets [7]. Likewise, the worth of the dusty plasma received a very huge improvement in the research of the zodiacal light clouds and when Jupiter's ring was discovered and the active volcanism on Io, with its ejection of fine ash into the Jovian magnetosphere was first detected by the detector aboard the Voyager spacecraft [8]. Historically , the main interest of the problems of the plasmas containing dust was not only related to the industrial aspects of the dusty plasma but also space plasma. The dusty plasma has the main role in space plasma and was realized a century ago [9].

1.5 Characteristics of Dusty Plasma

A dusty plasma loosely defines as "a plasma having, electrons and ions species with an additionally charged constituent called dust particle". This extra component increases the complexity of the plasma system, that's why the dusty plasma is also called complex plasma. Dust grains are very massive i.e., billion times heavier than protons and their size range from nano-meters (10^{-9} m) to millimeters (10^{-3} m). The size and shape of the dust grains are different and they can be metallic, conducting, or made of ice particulates.

A plasma with additional dust grains or particles titled as either "dust in a plasma" or "dusty plasma" depending on the characteristic lengths, i.e., the dust grain radius (r_d), average inter-grain distance (a), the Debye radius (λ_D) and the dust plasma dimension. The condition for the "dust in a plasma" is:

$$r_d \ll \lambda_D < a, \quad (1.9)$$

in this situation the dust charged particles are considered as a collection of isolated grains, they cannot participate in collective behavior and then the local inhomogeneities cannot be ignored. On the other hand, the condition for the "dusty plasma" is

$$r_d \ll a < \lambda_D, \quad (1.10)$$

in this situation, the charged dust particles participate in the collective behavior and here we take the dust grains as massive charged particles similar to charged negative or positive ions. Due to the presence of the charged dust grains in plasma, the existing low-frequency waves are modified, i.e.,

- Ion-acoustic waves (IAW)
- Lower-hybrid waves (LHW)
- Ion-acoustic (IA) solitons
- Ion-acoustic (IA) shocks etc.

However, some new kinds of low-frequency dust related waves are also indicated, i.e.,

- Dust-acoustic waves (DAW)
- Dust-ion acoustic waves (DIAW)
- Dust-ion acoustic (DIA) solitons

- Dust-ion acoustic (DIA) shocks
- Dust-acoustic (DA) solitons
- Dust-acoustic (DA) shocks

1.5.1 Macroscopic Neutrality

A dusty plasma is said to be macroscopically neutral when there is no external disturbance present. In this condition, the electric charge is zero because no external forces are present and the dusty plasma is in equilibrium. Therefore, the equilibrium charge neutrality condition is

$$q_i n_{i0} = e n_{e0} - q_d n_{d0}, \quad (1.11)$$

where n_{i0} , n_{e0} , n_{d0} , are the unperturbed number densities of the ions, electrons and dust grains respectively and e is the magnitude of the electron charge. However, q_i is the ion charge and can be expressed as $q_i = Z_i e$, where $Z_i = 1$, and $q_d = Z_d e$ or $(-Z_d e)$ is the dust particle charge when the dust grains are positively or negatively charged, and Z_d is the number of charges resides on the dust grain surface.

Usually, one thousand to several thousand elementary charges are collected on the dust grain surface and $Z_d n_{d0}$ approaches to n_{i0} even when the unperturbed density of dust grain is very much less than ion unperturbed density. When the background electrons take part in the charging process of the dust particles then we cannot ignore the depletion of electron number density, but actually, complete depletion of electrons is not possible. Consequently, for negatively charged dust grains equation (1.11) becomes

$$n_{i0} \approx Z_d n_{d0}. \quad (1.12)$$

1.5.2 Debye Shielding

The influence of the electric field of an individual charged particle and surface that has some potential is observed by other charged particles inside the plasma at a distance called Debye radius.

Let us put a small charged ball inside a dusty plasma whose species are electrons, positive ions, and dust particles (positive or negative). The ball would attract particles of opposite sign, so if the ball is positively charged then it would be shielded by the electrons and negatively charged dust particles. Similarly, if the ball is negatively charged then it would be shielded by positive ions and positively charged dust particles. If the dusty plasma is cold and there are no thermal motions, then there would be just as many changes in the cloud as in the ball, this is referred to as a perfect shielding, and there would be no electric field present outside the cloud. On the other hand, when plasma is not cold then the edge of the cloud occurs at the radius where the thermal energy of the particles and potential energy is approximately equal, while particles at the edges of the cloud have enough thermal energy to escape from the cloud.

Now we are going to calculate the approximate thickness of a charged cloud under some assumptions, i.e. the potential $\phi_s(r)$ at center ($r = 0$) of the cloud is ϕ_{s0} and the dust-ion mass ratio $\frac{m_d}{m_i} \gg 1$. Hence dust particles prevent ions to move significantly. The electrons and ions in the dusty plasma are assumed to be in local thermodynamic equilibrium. The number density of electrons (n_e) and positive ions (n_i) obey the Boltzmann distribution, i.e.,

$$n_e = n_{e0} \exp\left(\frac{e\phi_s}{K_B T_e}\right), \quad (1.13)$$

and

$$n_i = n_{i0} \exp\left(-\frac{e\phi_s}{K_B T_i}\right), \quad (1.14)$$

where n_{e0} , n_{i0} are the electron and ion number densities respectively at equilibrium, while T_e , T_i are the electron and ion temperature, respectively. For the current situation, the Poisson's equation can be written as:

$$\nabla^2 \phi_s = 4\pi(e n_e - e n_i - q_d n_d), \quad (1.15)$$

where n_d is the number density of dust particles. According to our consideration, inside and outside the cloud the particle number density is same, i.e. $q_d n_d = q_d n_{d0} = e n_{e0} - e n_{i0}$. Now putting equations (1.13) and (1.14) into equation (1.15), we get

$$\nabla^2 \phi_s = 4\pi \left(\frac{e^2 n_{e0} \phi_s}{K_B T_e} + e n_{e0} \left(\frac{e\phi_s}{K_B T_e} \right)^2 + \frac{e^2 n_{i0} \phi_s}{K_B T_i} - e n_{i0} \left(\frac{e\phi_s}{K_B T_i} \right)^2 \right). \quad (1.16)$$

Thus, under the approximation $\frac{e\phi_s}{K_B T_e} \ll 1$ and $\frac{e\phi_s}{K_B T_i} \ll 1$, equation (1.16) becomes

$$\nabla^2 \phi_s = \left(\frac{1}{\lambda_{De}^2} + \frac{1}{\lambda_{Di}^2} \right) \phi_s, \quad (1.17)$$

where $\lambda_{De} = \left(\frac{K_B T_e}{4\pi n_{e0} e^2} \right)^{\frac{1}{2}}$ and $\lambda_{Di} = \left(\frac{K_B T_e}{4\pi n_{i0} e^2} \right)^{\frac{1}{2}}$ are electron and ion Debye radius, respectively. Our approximations, i.e. $\frac{e\phi_s}{K_B T_e} \ll 1$ and $\frac{e\phi_s}{K_B T_i} \ll 1$, cannot be effective near the region $r = 0$ (this region is called sheath). In this region the potential drops very quickly and cannot contribute to the thickness of the cloud. Now we consider some value of the potential, i.e. $\phi_s = \phi_{s0} \exp(-\frac{r}{\lambda_D})$, and finally we obtain the dusty plasma Debye radius from equation (1.16),

$$\lambda_D = \frac{\lambda_{De} \lambda_{Di}}{\sqrt{\lambda_{De}^2 + \lambda_{Di}^2}}. \quad (1.18)$$

Equation (1.18) represents the shielding distance in a dusty plasma. If we have negatively charged dust grains then the particle number density at equilibrium and temperature of electrons and ions are related as $n_{e0} \ll n_{i0}$ and $T_e \geq T_i$, i.e. $\lambda_{Di} \ll \lambda_{De}$. Thus from equation (1.18) it is clear that $\lambda_D \simeq \lambda_{Di}$. From this result: it is clear that temperature and the number density of ions governs the shielding distance or thickness of the sheath in a dusty plasma.

On the other hand, if dust particles are positively charged which indicates that most of the positively charged ions are attached on the dust grains surface, then we obtain a relation between temperature and equilibrium particle number densities, i.e., $T_e n_{i0} \ll T_i n_{e0}$, which indicates that $\lambda_{De} \ll \lambda_{Di}$ and from equation (1.18), we get $\lambda_D \simeq \lambda_{De}$. Thus, in a dusty plasma where dust particles are positively charged the shielding distance is usually governed by the temperature and the density of electrons.

1.5.3 Characteristic Frequencies

Frequencies have a significant role when we study waves and especially when these waves are generated in a plasma environment. When a plasma is slightly disturbed from its equilibrium position it gives rise to collective particle motion and the electric field will be established in such a direction to restore the charge neutrality and

pull the charges back to their equilibrium position. But due to the inertia of the particles, they overshoot the equilibrium position, and then the field changes its polarity and pushes particles back to the equilibrium position. These particle motion about their mean position with a characteristic frequency called plasma frequency (ω_p).

Now we obtained an expression for the plasma frequency (ω_p), under the following assumptions, i.e., our dusty plasma environment is:

- Uniform
- Cold (mean there are no thermal motions, i.e., $K_B T = 0$)
- Unmagnetized
- No sources and sinks
- No pressure gradient forces

For this situation our governing equations are:

Continuity equation

$$\partial_t n_s + \nabla \cdot (n_s v_s) = 0, \quad (1.19)$$

Equation of motion

$$\partial_t v_s + (v_s \cdot \nabla) v_s = -\left(\frac{q_s}{m_s}\right) \nabla \phi, \quad (1.20)$$

and Poisson's equation

$$\nabla^2 \phi = -4\pi \sum_s q_s n_s. \quad (1.21)$$

Note that by ∂_t we mean $\frac{\partial}{\partial t}$ and ∇ is the three dimensional space operator. To make the linear theory valid, we assume small amplitude oscillations. Therefore, the terms containing higher-order amplitudes are neglected.

By linearizing equations (1.19), (1.20), (1.21), we consider $n_s = n_{s0} + n_{s1}$, where $n_{s1} \ll n_{s0}$. Under these assumptions we obtained a relation

$$\partial_t^2 \nabla^2 \phi = -4\pi \sum_s \left(\frac{n_{s0} q_s^2}{m_s}\right) \nabla^2 \phi, \quad (1.22)$$

where ϕ , q_s is the dusty plasma potential and charge of the species (i.e. electrons, positive ions and dust particles), and n_{s0} , m_s are the equilibrium number density of the dusty plasma species (i.e. electrons, positive ions and dust particles) and mass of the plasma species, respectively.

Now, integrate the equation (1.22) twice over space (three dimensional space) under suitable boundary condition, i.e. $\phi=0$ at $r=0$ (at equilibrium). Then equation (1.22) will be transformed and become second order ordinary differential equation. Thus, we replace $\frac{\partial}{\partial t}$ by $\frac{d}{dt}$

$$\frac{d^2\phi}{dt^2} + \omega_p^2\phi = 0. \quad (1.23)$$

In this equation ω_p is the plasma frequency related with plasma species given as

$$\omega_p^2 = \sum_s \frac{4\pi n_{s0} q_s^2}{m_s}. \quad (1.24)$$

The plasma frequency is not same for all species but depends on the charge and mass of the specie. Therefore, following are plasma frequencies for electron, positive ion and dust particle, respectively,

- Electron plasma frequency (here electrons oscillate around ions having this frequency), $\omega_{pe} = \left(\frac{4\pi n_{e0} e^2}{m_e}\right)^{\frac{1}{2}}$.
- Positive ion plasma frequency (here ions oscillates around dust grains having the following frequency), $\omega_{pi} = \left(\frac{4\pi n_{i0} e^2}{m_i}\right)^{\frac{1}{2}}$.
- Dust plasma frequency (dust particles oscillates around their equilibrium position), $\omega_{pd} = \left(\frac{4\pi n_{d0} Z_d^2 e^2}{m_d}\right)^{\frac{1}{2}}$.

1.6 Dust Charging Processes

The main thing of dusty plasma is to understand the charging process of dust grains. The elementary process of dust grains charging is somehow complicated and depend on the surrounding plasma environment. The basic charging processes are

- Interaction of dust grains with gaseous plasma particles,

- Interaction of dust grain with energetic particles, i.e., electrons or ions,
- Interaction of dust grain with photons.

When dust grains are introduced in a plasma environment, then plasma species (electrons and ions) are collected by the dust grains. This collection of plasma species on dust grains act as a probe. Therefore, the dust grains are charged by the surrounding plasma environment. Currents are produced due to the plasma species collection on the dust grains surface, so the dust grain charge (q_d) is determined by the equation $\frac{dq_d}{dt} = \sum_j I_j$. In this equation, I_j represents the current related with j plasma species (electrons and ions). But at equilibrium, there will be no current on the dust grains surface, i.e $\sum_j I_{j0} = 0$, here I_{j0} represents the equilibrium current. This will lead to the conclusion that dust grain surface grab some potential ϕ_g (ϕ_g represents the grain potential), which is $-2.5 \frac{K_B T}{e}$ (where $T = T_e \simeq T_i$) for simple hydrogen plasma and $-3.6 \frac{K_B T}{e}$ for simple oxygen plasma [17]. This indicates that whenever dust grains appear in a plasma it usually gets negatively charged.

Besides the interaction of dust grains with gaseous plasma particles, there is also the interaction of energetic particles with the dust grain surface. There are two possibilities, i.e., (i) the energetic plasma particles will be back-scattered or reflected, and (ii) these energetic particles will pass through the dust grain material. So, when the energetic particles pass through the dust grain material then the particles either lose their energy partially or totally. During the process when energetic particles lose partial energy, then a part of the energy can accelerate further electrons which are then able to escape from the material (known as secondary electron emission). Finally, the dust grain material becomes positively charged after secondary electron emissions.

When photons stick to the dust grain surface, it causes photo-emission and makes the dust grain surface positive due to the emission of electrons. These emitted electrons are then trapped onto some other grains which become negatively charged. There are so many other charging mechanisms, namely

- Thermionic emission

- Field emission
- Radioactivity
- Impact ionization etc.

To discuss all these processes simultaneously is a complex job, therefore, we take a simple way by considering the dust grain as an isolated dust grain. After that, a detail explanation of non-isolated dust grains will be provided.

1.7 Isolated Dust Grains

If the plasma with dust constituent obeying the relation $r_d \ll \lambda_D \ll a$, where r_d , λ_D and " a " are the dust grain radius, plasma Debye radius and average inter-grain distance respectively, then the plasma is called "dust in plasma". Therefore, some important mechanisms of dust charging in "dust in plasma" are discussed below.

1.7.1 Collection of Plasma Particles

Considered an unmagnetized plasma whose species are electrons and ions and a finite size neutral dust particles. The electrons reached very quickly onto the dust grain surface than ions because the thermal speed of electrons are much more than ions and make the dust grain surface potential negative. While the plasma ions absorption makes the dust grain charge and potential positive. The electron and ion current gets affected by the potential of the dust grain surface, and it also depends on the relative speed between plasma and dust grain. Therefore, for the negative surface potential of the dust grain, the ions are attracted and electrons are repelled. When the surface potential of a dust grain is positive then it will attract the electrons and current transfer by electrons increases, and similarly, it will repel the ions and current due to ions decreases.

Now, these charging currents (I_j) can be calculated by using orbit limited motion (OLM) approach [18, 21]. Let us considered a j plasma particle come closer to a spherical dust grain of radius " r_d " and " q_d " charge. When the plasma particle

j enters the spherical dust grain's Debye sphere the effect of the electrostatic forces will be felt by the particle and thus change its trajectory and just grazing collision can occurs. Let's consider the speed of plasma particle before and after grazing collision with dust particle is v_j and v_{gj} respectively and impact parameter is b_j . The cross-section for the collision between the dust and the plasma particle j is

$$\sigma_j^d = \pi b_j^2. \quad (1.25)$$

In grazing collision, the conservation of momentum and energy has a key role and can be expressed as

$$M_j v_j b_j = M_j v_{gj} r_d, \quad (1.26)$$

and

$$\frac{1}{2} M_j v_j^2 = \frac{1}{2} M_j v_{gj}^2 + \frac{Q_j q_d}{r_d}, \quad (1.27)$$

where q_d and Q_j are the charge on dust particle and charge on j plasma particle respectively. Also $q_d = C \phi_D$, where C is the capacitance of spherical dust grain and ϕ_D is the potential difference between dust grain potential (ϕ_g) and the plasma potential (ϕ_P), i.e., $\phi_D = \phi_g - \phi_P$. The capacitance of spherical dust grain is expressed as $C = r_d \exp(-\frac{r_d}{\lambda_D})$. When we assume that $\lambda_D \ll r_d$ then $C \simeq r_d$. Using equation (1.25) in equation (1.27), we get

$$1 - \frac{2Q_j \phi_D}{M_j v_j^2} = \frac{v_{gj}^2}{v_j^2}. \quad (1.28)$$

By simplification of equation (1.26), we get

$$b_j^2 = r_d^2 \frac{v_{gj}^2}{v_j^2}. \quad (1.29)$$

Now, multiply equation (1.28) with r_d^2 and put it in equation (1.25),. Finally, we get the expression for the cross section,

$$\sigma_d^d = \pi r_d^2 \left(1 - \frac{2Q_j \phi_D}{m_j v_j^2}\right). \quad (1.30)$$

The dust grain charging current (I_j) carried by j plasma species with velocity distribution can be expressed as

$$I_j = Q_j \int_{v_j^m}^{\infty} v_j \sigma_j^d f_j(v_j) dv_j. \quad (1.31)$$

Where $f_j(v_j)$ is the velocity distribution function and v_j^m is the minimum velocity required by the plasma particle to hit the dust grain.

For the lower limit of integration, assume two kind of situation, i.e., $Q_j\phi_D < 0$ and $Q_j\phi_D > 0$. For the first situation ($Q_j\phi_D < 0$) there is a force of attraction between dust grain and plasma particles, thus the integration of equation (1.31) will be performed on the whole velocity domain. While in second situation ($Q_j\phi_D > 0$) there is a force of repulsion in dust grain and plasma particles. To allow the collision we take $v_j^m > 0$, therefore, v_j^m can be expressed as

$$v_j^m = \left(-\frac{2Q_j\phi_D}{M_j} \right)^{\frac{1}{2}}. \quad (1.32)$$

Consider the velocity distribution function as Maxwellian, i.e.,

$$f_j(v_j) = N_j \left(\frac{M_j}{2\pi K_B T_j} \right)^{\frac{3}{2}} \exp\left(-\frac{M_j v_j^2}{2K_B T_j} \right), \quad (1.33)$$

where N_j is the particle number density. Now, substitute equation (1.30) and (1.33) in equation (1.31), to get a result for both situations.

For attractive potential ($Q_j\phi_D < 0$),

$$I_j = 4\pi r_d^2 N_j Q_j \left(\frac{K_B T_j}{2\pi M_j} \right)^{\frac{1}{2}} \left(1 - \frac{Q_j\phi_D}{K_B T_j} \right). \quad (1.34)$$

For repulsive potential ($Q_j\phi_D > 0$),

$$I_j = 4\pi r_d^2 N_j Q_j \left(\frac{K_B T_j}{2\pi M_j} \right)^{\frac{1}{2}} \exp\left(\frac{Q_j\phi_D}{K_B T_j} \right). \quad (1.35)$$

These situations are simple where the ions streaming is not involved [10]. This OLM theory is further extended to cylindrical dust grains and dust grains which are less symmetric than spherical and circular cylinders [19].

1.7.2 Photo-emission

When several photons having $h\nu$ energy greater in magnitude than photoelectric work function (w_f) of dust grain strikes on the dust grain surface then it releases photoelectrons. The photo-emission of the electron depends upon

- Wavelength (λ) of the incident photons
- Surface area of dust grains
- Properties of the dust grain material.

The photo-emission process makes dust grain positive with the associated positive charging current.

Suppose the photoelectric work function (w_f) of the material of dust grain is positive, i.e., for excitation of the electron, the incoming photon must have energy $h\nu > w_f + \frac{q_d e}{r_d}$. Therefore, maximum dust grain charge is roughly

$$q_d = (h\nu - w_f) \frac{r_d}{e}. \quad (1.36)$$

Since the dust grain surface is positive ($\phi_D > 0$) then some of the electrons come back to the dust grain surface and the photoelectrons having more energy will escape by overcoming the dust grain potential. Therefore, the net current determined by the balance between the photoelectrons comes back to the dust grain and photoelectrons escape from the dust grain surface.

$$I_p = \phi r_d^2 e J_p Q Y_p \exp\left(-\frac{e\phi_d}{K_B T_p}\right), \quad (1.37)$$

where J_p , Q , Y_p and T_p are photon flux, efficiency of the absorption for photons and average temperature. This current equation is valid only when photo-emitted electrons follow a Maxwellian distribution [10].

1.7.3 Radioactivity

Radioactivity is a process in which unstable atomic nuclei radiate (lose energy). This process in a body may cause a charging mechanism by the emission of charged species and due to primary accelerated species the secondary electrons also escape from the surface. In 1981, Whipple concludes that the amount of ordinary radioactive material in a body is insignificant for charging effects [20]. But on the other hand, Yanagita in 1977 indicates nova and supernova dust grains can have remarkable radioactive levels which are β emitters. The β emission from large dust grains can make it positively charged [10].

1.8 Non-isolated Dust Grains

Dust grain becomes non-isolated in the situation $r_d \ll a \ll \lambda_D$, which we called dusty plasma situation.

Since the charge neutrality condition is given as:

$$\frac{N_e}{N_i} = 1 - Z_d \frac{N_d}{N_i}, \quad (1.38)$$

where N_i and N_e are the particle number densities of positive ions and electrons. If $Z_d \frac{N_d}{N_i} \ll 1$, then dust particles would be considered as isolated, while for $Z_d \frac{N_d}{N_i} \approx 1$ then dust particles would be considered as non-isolated dust particles. Therefore, for the non-isolated case, N_d increases at the same time Z_d decreases rapidly. This will lead to the conclusion that particle number density increases in the non-isolated case which means that dust grains together have a large tendency towards electrons but the number of available electrons for dust particles decreases.

For negatively charged dust grain, the currents are:

$$I_e = -4\pi r_d^2 N_e e \left(\frac{K_B T_e}{2\pi M_e} \right)^{\frac{1}{2}} \exp\left(\frac{e\phi_d}{K_B T_e} \right), \quad (1.39)$$

and

$$I_i = -4\pi r_d^2 N_i e \left(\frac{K_B T_i}{2\pi M_i} \right)^{\frac{1}{2}} \exp\left(1 - \frac{e\phi_d}{K_B T_i} \right), \quad (1.40)$$

where $I_i \ll I_e$ because $M_e \ll M_i$, therefore the dust grain surface is negatively charged. Ion current is increasing and electron current is decreasing until $I_i = -I_e$, which implies that $I_e + I_i = 0$, we get. Using equations (1.39) and (1.40) in $I_e + I_i = 0$.

$$\left(\frac{T_i}{M_i} \right)^2 \left(1 - \frac{e\phi_d}{K_B T_i} \right) = \frac{N_e}{N_i} \left(\frac{T_e}{M_e} \right)^2 \exp\left(\frac{e\phi_d}{K_B T_e} \right).$$

By using charge neutrality condition, we get

$$\left(\frac{T_i M_e}{T_e M_i} \right)^{\frac{1}{2}} \left(1 - \frac{e\phi_d}{K_B T_i} \right) \exp\left(-\frac{e\phi_d}{K_B T_e} \right) = 1 - Z_d \frac{N_d}{N_i}, \quad (1.41)$$

where ϕ_d and Z_d are related as

$$Z_d = -\frac{\phi_D r_d}{e}. \quad (1.42)$$

Using equation (1.42) in (1.41) and take $T_e = T_i = T$

$$\begin{aligned} \left(1 - \frac{e\phi_d}{K_B T}\right) \exp\left(-\frac{e\phi_d}{K_B T}\right) &= \left(\frac{M_e}{M_i}\right)^{\frac{-1}{2}} \left(1 + \frac{\phi_d r_d n_d}{n_i e}\right), \\ 1 - \frac{e\phi_d}{K_B T} - \left(\frac{M_e}{M_i}\right)^{\frac{1}{2}} \left(1 + \frac{\phi_d r_d n_d}{n_i e}\right) \exp\left(\frac{e\phi_d}{K_B T}\right) &= 0, \\ 1 - \frac{e\phi_d}{K_B T} - \left(\frac{M_e}{M_i}\right)^{\frac{1}{2}} \left[1 + P \frac{e\phi_d}{K_B T}\right] \exp\left(\frac{e\phi_d}{K_B T}\right) &= 0, \end{aligned} \quad (1.43)$$

where $P = 4\pi N_d r_d \lambda_{D0}^2$ and $\lambda_{D0}^2 = \frac{K_B T}{4\pi N_i e^2}$. By solving this equation numerically we calculate ϕ_d and Z_d . By taking N_i , T and r_d constant then the variation in $\log P$ with $\frac{e\phi_d}{K_B T}$ shows that when n_d increase slowly (it mean that dust grain inter-space distance slowly decreases) and overshoot a critical value, the value of $-\frac{e\phi_d}{K_B T}$ starts to decay which indicates that the average dust grain charge Z_d starts to decrease.

1.9 Different types of Non-linear Structures

The nonlinear wave structure strongly depends on the type of nonlinearity. In general, three types of nonlinearities are discussed in plasma environments, i.e.,

- Scalar nonlinearities (Solitons, multi-solitons, envelop solitons, Shocks etc.)
- Vector nonlinearities (Vortices)
- Chaos (Chaotic evolution or behavior)

1.9.1 Solitons

Solitons are nonlinear and stable profiled dip or hump-shaped structure. Solitons maintain their shape despite dispersion and nonlinearity of medium. And it has self localized solutions of a nonlinear partial differential equation that takes into account the evolution of nonlinear systems. Before the mathematical representation, solitons are detected as pulsed type structures of density, potential, electric field, or some other

physical quantity in the medium.

One can define a soliton as a solitary wave having the following unique properties [43].

- Shape of solitons does not change, i.e. solitons are shaped invariant during their propagation. This property (shape invariant) of soliton has occurred in the plasma environment where dispersion and nonlinearity both are present.
- Solitons interact nonlinearly and during two soliton waves collision, the waves just pass through each other without changing the shape but phase shift can be occurred.
- Solitons are localized waves and a soliton vanishes asymptotically. For example if we have a localized structure of electrostatic potential $\phi(x, t)$ then we can impose condition i.e, $\phi(x, t) \rightarrow 0$ as $|x| \rightarrow \pm\infty$.

When wave phase dispersion and nonlinearity comes at the same phase then an isolated hump or dip like wave profile comes to existence called soliton with no rapid oscillations inside the packet . This type of soliton is called the aforementioned KdV type soliton because its dynamics are governed by Korteweg-de Vries (KdV) type equation. And when wave group dispersion balance the nonlinearity then another type of soliton formed which is known as envelope soliton. Envelope soliton is a localized modulated wave packet whose dynamics are governed by nonlinear Schrodinger equation (NLS). The KdV equation shows the dynamics of wave pulses itself, while on the other hand, the nonlinear Schrodinger equation controls the far-field dynamics of the amplitude of the almost monochromatic (narrow-banded) wave train propagating in a weakly nonlinear and strongly dispersive medium .

Solitons are abundantly in nature, such as in water (like Tsunami waves, referred to as solitons in literature) and in space, etc. A familiar example of solitons are moving clouds that are observed in Australia, Gulf of Carpentaria.

Nonlinear phenomena in nature are very common than linear phenomena. Since the very first time observation of nonlinear phenomena called solitary waves is made by John Scott Russell (Scottish naval architect and an engineer) during riding a horse

in the Union canal in Edinburgh in August 1834. He saw a hump of water somehow thirty feet long produced in a narrow canal that was traveling with constant speed without any change in its shape for a distance of about two miles. He observed the strange behavior of waves above the surface of the water and carry water along with it unlike the ordinary water wave having crest and trough. Therefore, Russel called this strange and unique wave a "solitary wave of translation". This is how the birth of nonlinear science (like solitons, envelope solitons, and shocks, etc) came into being.

In 1844 Russel reported his results based on several experiments to explore this unusual unique wave [44]. While next year in 1845, Airy published his analysis on such types of waves which contradicts the theory proposed by Russel [45]. In Airy's analysis, he finds that during propagation this wave does not maintain its shape. And also in 1847 Stokes showed that in nonviscous fluids, such type of waves could not exist [46]. After many years that is in 1865 Russel's work was confirmed by a French scientist named Bazin. For this purpose, Bazin performed many experiments in a canal close to Dijon. In years 1871 and 1876, Boussinesq and Rayleigh confirmed the existence of such types of waves in the absence of dissipation because of the decrease in the dispersion and increase in the velocity of the wave because finite-amplitude balances each other resulting in a wave of permanent form. In 1895 the well known Korteweg deVries equation was derived by Korteweg and deVries during their observations on competition between steepening and dispersion in traveling shallow water waves which confirmed the existence of solitary waves [47]. And in 1967 KdV equation was derived by Zabusky and Kruskal in the long-wavelength limit and found that when two waves interact with each other then they emerge with only change in their phase shift whereas their shape remains the same [48].

1.9.2 Shock Waves

The shock wave is a propagating disturbance which appears in a medium due to nonlinear and dissipative effects. The shock waves carry the energy and can also pass through the medium like liquids, solids, gases, and plasmas, and in some cases in absence of a material medium, like electromagnetic fields in free space. When state variables such as

velocity, density, etc. of the medium experience sudden changes because of a surface of discontinuity which propagates through the medium then such surface of discontinuity is termed as a shock wave. Shock waves can further be classified into two types, i.e. compressive (positive) shocks, and rarefactive (negative) shocks. Compressive shocks travel in a direction of the minimum density of the medium whereas rarefactive shocks propagate along the direction of maximum density of the medium [49].

Nonlinear shock waves are large-amplitude waves having the following properties.

- When a frame moves with the shock then subsonic velocity remains behind whereas supersonic velocity remains ahead of the shock.
- Change in velocity and strength of non-planar imploding (exploding) shocks depends on the distance from the center of origin. As the distance increases the velocity and strength decrease and vice versa.
- When a fluid is compressed because of a shock, its entropy increases.
- Formation of a steep wavefront across which the state variables change abruptly.
- Nonlinear superposition principle holds during the interactions and reflection of shock waves.

Formation of shock wave required damping or dissipative mechanism. The dissipation is provided by viscosity or thermal conductivity of the medium in ordinary fluids. But in plasmas, other processes also play an important role which appears because of collective effects, i.e. Landau damping, particle trapping in a potential well, and reflection. These processes are collision-less that engender the collision-less shock structures whose transition layer can be much smaller as compared to their mean free path. The earth bow shock is an example of collision-less shock structures.

A mathematical theory of shock waves was the first to predict the existence of shock waves [50]. And Toepler used a spark discharge in 1864 to produce shock waves [51]. Many researchers like Mach, Wentzel, and Salcher [52, 53] performed experiments on explosions and blast waves to determine the speed of shock waves by using the

soot method invented by Antolik [54] to investigate the shock wave interactions. Lord Rayleigh argued that the shock waves can be as thick as of the order of the ratio of specific gas viscosity and wave velocity [55]. The well-known Burger equation was derived by Bateman in 1905 [56] whereas Burger studied weak turbulence by using this equation and from then this equation is termed as Burger's equation [57]. This is a model equation for several dissipative and diffusion processes in convention dominated systems and is responsible for the formation of weak shocks. When dispersion plays a role along with nonlinearity, dissipation, and diffusion mechanisms on spatial and temporal scales then Burgers equation can be combined with Korteweg deVries equation to get KdV Burgers (KdVB) equation which has been derived in long-wavelength limits to obtain the wave dynamics for a variety of plasma systems.

1.10 Dusty Plasma in Space

Dust is an abundant particle that presents on large scale in space plasma. Interstellar clouds, circumstellar clouds, and the solar system contain dust particles in large numbers.

The space between the stars (i.e, interstellar space) is filled up by gas medium and dust particles. The collapse of massive molecular clouds can give birth to new stars which decrease the gas content of the interstellar medium. The dust grains in the interstellar clouds or circumstellar clouds are present in different forms, i.e. it may be dielectric (ice, silicates, etc) or metallic (graphite, magnetite, amorphous carbon, etc). In the interstellar clouds, certain parameters of dust-laden plasma are given as

Electron number density $n_e = 10^{-3}cm^{-3}$ to $10^{-4}cm^{-3}$

Temperature of electrons $T_e \simeq 12K$

Dust particles number density $n_d = 10^{-7}cm^{-3}$

Dust grain radius $r_d \simeq 0.2\mu m$

Neutrals neutral density $n_n \simeq 10^4cm^{-3}$

Debye screening radius $\frac{a}{\lambda_D} \leq 0.3$. [10]

Beside these, dusty plasma also presents in different region of the space, like

- Interplanetary space
- Comets
- Jupiter's ring system
- Saturn's ring system
- Uranian ring system
- Neptune's ring system
- Earth's atmosphere

1.10.1 Interplanetary Space

The space between the stars is not empty but occupied by photons (electromagnetic radiation), cosmic rays, hot plasma (electrons and ions), solar wind, magnetic field, and dust particles. The dust particles are distributed in the region of the inner solar system with the contribution of the asteroid belt which causes the zodiacal light. When the asteroids collide with the asteroid belt that can also produce interplanetary dust. The earth also receives the dust which is an accretion of interplanetary dust estimated 40,000 tonnes per year, and the interplanetary dust is also detected in the stratosphere. This interplanetary dust is been collected by NASA by their research aircraft for the past several decades. At the altitude of 18 kilometers to 20 kilometers, the dust particles have been detected. In the interplanetary space, the inside and outside interplanetary dust particles are shown in figure 1.1 respectively.

1.10.2 Comets

Comets are like stars but not the stars since it is the smallest members of the solar system. The comets have an important role in understanding the cosmic and solar systems. It has been said that during the first stages of our planet, the long period

comets may have transported water and organic materials which are necessary for the evolution of life. It has been said that the interaction of dust with solar electromagnetic radiation is the key which leads to the discovery of solar wind [11].

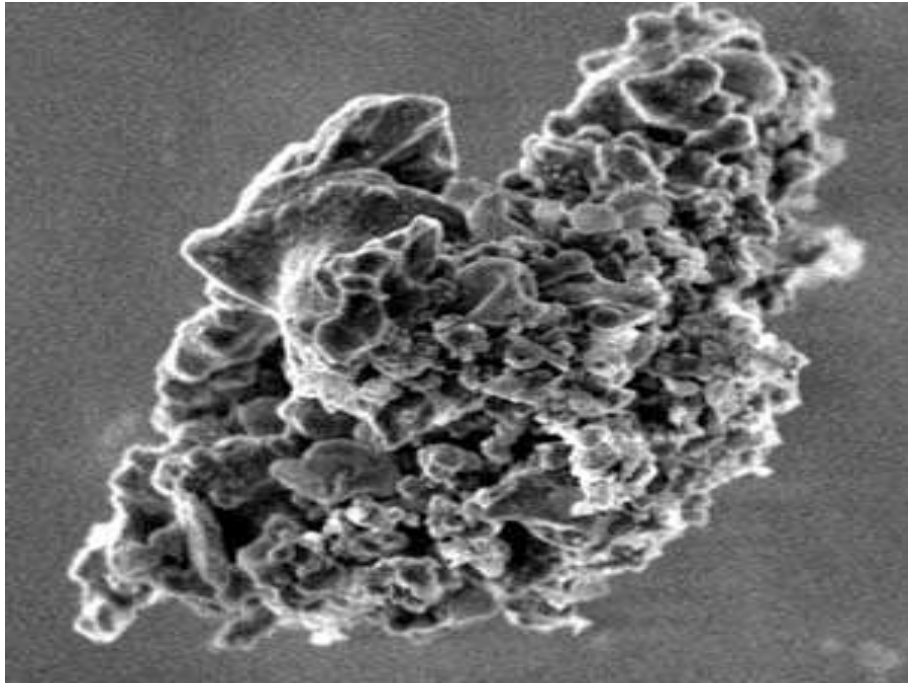


Figure 1.1: A view of comet Hale-Bopp showing.

Most comets are composed of three components, ahead, a nucleus, and a tail (dust tail or may be a simple plasma tail), and are considered as a globe of dust and ice. Coma and nucleus which in the middle of the comet less than 10km in diameter, form the head of the comet. Comet is usually surrounded by clouds of diffuse materials (coma), when the comet comes closer to the sun then the coma size increases and gets more brightness. When this distance decreases the comet develops a tail in the opposite direction of the sun from the head, and this tail is then expanded in millions of kilometers. However, when the comet is far away from the sun its material in the nucleus is in solid form. But when the distance between the comet and the sun decreases, the material in the comet nucleus gets warm and warm and then finally from a comet nucleus form a coma of gas and dust. The dust particles in the coma have the property to reflect more sunlight, while the gas in the coma absorbs ultraviolet light

and begin to fluorescence. Now, when this distance decreases further the fluorescence intensity becomes greater than dust particles reflected sunlight. Nearly at this stage, the hydrogen envelope is also formed due to the absorption of ultraviolet light that makes the hydrogen escape from the comet's gravity. This envelope which is formed due to the escape of hydrogen cannot be seen from the earth (due to the absorption of this light in our atmosphere) but can be detected by spacecrafts.

As the comet comes closer to the sun the material inside the head of the comet accelerates with different velocities (depend on the material's size and mass), due to the radiation pressure of the sun and solar wind. Therefore, the tail which contains dust particles accelerated slowly and become curved. The ions (which are lighter particles than dust) in the comet tail can accelerate more and look like a straight line. So, the ion tail extends away from the comet in opposite direction to the sun [10]. Figure 1.2, a view of comet Hale-Bopp showing two distinct tails, i.e thin blue plasma tail and broad white tail of dust particles.

1.10.3 Jupiter's Ring System

Jupiter's ring was firstly discovered by Voyager 1 that was basically in the search of Faint ring system. After Voyager 1, a more clear image was taken by Voyager 2. Jupiter's ring is composed of three basic components, i.e.,

- Main ring
- Halo ring
- Gossamer ring

The main ring is about 7×10^3 kilometers wide and their outer boundary is about 1.29×10^5 kilometers from the center of the planet . This ring also encompasses the orbits of the two small moons (Adrastea and Metis), which may act as a source for the dust that makes up most of the ring.

1.10.4 Saturn's Ring System

Saturn's ring was firstly discovered by Galileo (in 1610) using his telescope. This ring confused the researchers and astronomers of that time. Their confusion increased since the Voyager 1 and Voyager 2 image the ring system in 1980 and 1981, respectively. Voyager 1 closest approach at a distance of 6.42×10^4 kilometer while Voyager 2 closest approach is 4.1×10^4 kilometers, therefore, Voyager 2 observe the ring system at a higher resolution than Voyager 1 and report many unseen ringlets [12]. The main rings from the outward direction are known as A, B, and C rings. Rings A and B are divided by the Cassini Division, i.e, the largest gap in the rings. The fainter rings are also discovered recently which are called G, D, and E rings. D ring is extremely faint and also close to the planet. At the outer side of the A ring, there is another ring called the F ring. Saturn's ring is primarily composed of ice and range from micron to meters in size. The exciting characteristic observed by Voyager 1 and Voyager 2 in the ring system of Saturn was nearly radial spokes strength for the dust-plasma interaction study in the planetary magnetosphere. The spoke model is based on the consideration that spoke contains electro-statically floated micron and sub-micron dust size dust grain. In Saturn's ring, the features of the plasma and dust vary from one ring to another, i.e.,

E ring:

$$n_e = 10 \text{ cm}^{-3}$$

$$T_e = 10^5 \text{ K to } 10^6 \text{ K}$$

$$n_d = 10^{-7} \text{ cm}^{-3}$$

$$r_d \sim 1 \text{ } \mu\text{m}$$

$$\text{and } \frac{a}{\lambda_D} = 0.1 \text{ } \mu\text{m}$$

F ring:

$$n_e = 10 \text{ cm}^{-3}$$

$$T_e = 10^5 \text{ K to } 10^6 \text{ K}$$

$$n_d \leq 10 \text{ cm}^{-3}$$

$$r_d = 1 \text{ } \mu\text{m},$$

and $\frac{a}{\lambda_D} \leq 10^{-3}$

Spokes

$n_e = 0.1 \text{ cm}^{-3}$ to 10^2 cm^{-3}

$T_e \sim 10^4 \text{ K}$

$n_d \sim 1 \text{ cm}^{-3}$

$r_d \sim 1 \text{ }\mu\text{m}$

and $\frac{a}{\lambda_D} \leq 10^{-2}$ [10].

1.10.5 Uranian Ring System

Uranian ring system discovery was reported in the early few months of 1977 during an examination of an occultation by the planet. Before the planet, the blinking star (blink five times) was observed, and later its blinking is also observed five times. These blinking indicate that the planet was surrounded by five narrow rings. But this observation is not final, and some other observations show that there are actually nine major rings, i.e α , β , γ , η , δ , ϵ , 4, 5, and 6. In 1986 Voyager spacecraft took certain images of the ring system and it also notices that these rings are surrounded by a belt of dust particles. Some images taken by the Voyager spacecraft look brighter than their environment which indicates that there must be dust particles there because dust particles have a property that reflects sunlight [10].

1.10.6 Earth's Atmosphere

In the earth's atmosphere at an altitude of 80 km to 90 km, polar summer mesopause is located where the dust particles are detected [13]. In polar summer mesopause, the most puzzling phenomenon has been detected in 1885, i.e the formation of clouds known as "noctilucent clouds" (NLC). In the year 1957 to 1958 (International Geophysical Year), some other peculiarity of polar mesopause has been reported that it was much colder in summer than in winter, which indicates that NLCs were composed of ice (which is formed at very low temperature, even below 100K).

Besides these, there are many other theories that involve charge dust particles with a total charge density that is significant compare with electron or ion com-

ponent. These dust particles are highly charged (positively charged) by the photo-emission dust charging process. When the photo-emission process is negligible then the charging of dust particles is only due to the collection of plasma particles, therefore, the dust particles will get negatively charged [14].

1.11 Dusty Plasmas in Laboratories

Laboratory dusty plasma has some distinct characteristics from those of space and astrophysical dusty plasmas. The first thing which differentiates laboratory dusty plasma from space and astrophysical dusty plasma is the laboratory discharges that have geometric boundaries, and these boundaries structure, composition, temperature, and conductivity, etc affect the formation and transport of the dust grains. Second distinguish feature of a laboratory dusty plasma is the external circuit (needs to maintain the dusty plasma) which imposes spatiotemporally varying boundary conditions on the dusty discharge. Dust occurs in many laboratory devices, such as:

- Direct current (DC) discharges
- Radiofrequency (RF) discharges
- Fusion plasma devices etc.

1.11.1 DC and RF Discharge

Dust particles are traced in DC discharges having large quantities for the same gases under conditions of RF excitations. Here the dust particles are originated in the gas phase, for-example carbon monoxide (CO) or silane containing discharges. While, dust particles may originate from the sputtering of electrodes, for example, metals (most metals not all metals) and graphite, etc. The formation of dust particles also depends on the nature of gas, i.e in electronegative gas mixtures, the dust particles are formed more quickly. The dust particles also occur more rapidly in a gas mixture where silicon or carbon-like substrates are present, and electronegative free radicals

are obtained from silicon and carbon by the process of sputtering. The Radio-frequency (RF) discharges is a very effective trap for negative ions and for negatively charged dust particles. The electrons have more mobility power than positive ions due to the less mass from positive ions, therefore, the electrodes receive negative DC bias. Due to these mobility effects, an ambipolar electric field occurs in the radial direction where negative ions and dust particles are trapped. The physical properties of dust particles like growth, charge, position, and temperature, etc, which are formed in DC or RF discharges depend on many physical and chemical processes involved [15].



Figure 1.2: A view of comet Hale-Bopp showing two distinct tails.

1.11.2 Fusion Plasma Devices

It has been known for a long time that microscopic grains of solid matter (dust) exist in fusion devices. Although, interest is also developed recently in outcomes of plasma operation and performances [16]. The plasmas in fusion devices like Tokamaks and Stellarators etc are somehow contaminated by impurities (heavier than hydrogen isotopes) which are the fuel in fusion reactors. These impurities which

are known as dust particles are generated by different processes like desorption, arcing and sputtering, etc, and there are some other important mechanisms which are spallation and flaking of thin films of redeposited material (or the films which were grown intentionally) for wall conditioning purposes.

Recently, a different type of dust particles was collected from Tokamak experiment for technology oriented research 94 (TEXTOR-94) in which plasma-wall interactions are studied is a medium size tokamak, and this collection is done by means of the vacuum cleaner. The remaining rough particles were removed from the sticky bag of the vacuum cleaner by a coarse fraction. The coarse fraction basically contains the irregular size of dark or whitish particles (0.1 to 0.5 millimeter). Coarse particles may be found in different types and sizes like metal cuttings, spheres (diameter in between 0.01 mm and 0.1 mm), and irregularly formed pieces , etc [10].

Chapter 2

Mathematical Model

2.1 Mathematical Model

The fluid theory for the plasma system is modeled by fluid equations and Maxwell's equation. These equations then form a number of coupled partial differential equations, which is very complicated to solve exactly (analytically) rather than approximate methods. These approximate methods are either numerical or analytical like the asymptotic perturbative method. To solve the number of coupled partial differential equations numerically then strong command on some favorable programming languages are necessary like Fortran, C++, or some computational software packages like MATHEMATICA and MATLAB. The deeper understanding of the physical mechanisms and reliance of system behavior on different physical parameters over space (it may be Cartesian, spherical, or cylindrical, etc) scale and time scale, the analytical method is the best approach. Although, analytical and numerical approaches are needed to greatly investigate the dynamics of the plasma system.

Generally, two analytical methods, i.e., reductive perturbative method (RPM) and pseudo-potential method (PPM) are used to solve the number of coupled partial differential equations in the investigation of non-linear structure in plasma-like solitary waves and shock waves, etc. For the investigation of small amplitude nonlinear waves, the reductive perturbative method (RPM) is used while studying the arbitrary amplitude waves the pseudo-potential method (PPM) is used. Moreover, the RPM has some advantages over PPM, i.e., RPM is applied to study the non-planar nonlinear wave

structures and the study of time evolution of nonlinear waves. The final equation obtained through both the methods required numerical techniques.

2.1.1 Reductive Perturbative Method

A simple case for the perturbation method is the dynamical system whose model equation is an ordinary linear differential equation with some small parameter ϵ (which shows the strength of nonlinearity or weakness of dispersion) and the system is exactly solvable if this small parameter ϵ is set equal to zero. Then use the regular perturbative method to solve such a system by expanding the dependent variable in terms of ϵ like $X = X_0 + \epsilon X_1 + \epsilon^2 X_2 + \epsilon^3 X_3 + \dots$, where X , X_0 and ϵ are the dependent variable, the unperturbed quantity of dependent variable X and strength of nonlinearity respectively. Then putting these expansions back into the original equation and compare the terms for various orders of ϵ to obtain a set of equations for various orders, which can be solved to calculate different orders of the asymptotic solution.

Moreover, if the set of model equations explains a physical system and does not contain a small parameter, the perturbative methods are still used to solve the system if certain parameters of the systems are assumed to be either too small or too large. Then expand the different state-dependent variables of the system in terms of these small parameters which leads to getting the asymptotic solution. Considered a nonlinear oscillation with small amplitude and nonlinearity effect one can go through a perturbative solution, this weakness of amplitude and nonlinearity can be utilized to obtain a perturbative solution. Since the regular perturbative methods break for the highest order derivative occurs to be a multiple of ϵ and due to the existence of weak nonlinearity in the model equations, the regular perturbation method is also broke. Therefore, the solution obtained in this way becomes invalid over long spatial and temporal scales due to the presence of unbounded terms known as secular terms. To avoid such problems and make sure the logic of the solution over large scales the singular perturbation methods is used. In this method, the dependent variables and independent variables of time and space are expressed in terms of the small parameter ϵ and known as multiple-scale analysis. Different singular perturbation methods

are implemented which not only allow secularity free solution but also assemble the progressive effect of the nonlinearity over long space and time scales.

The reductive perturbative method (RPM) is also a singular perturbative method and seems to be the first use in 1960 by Gardner and Morikawa [33][34] to explore the nonlinear behavior of hydrodynamic waves in cold plasma. After that Washimi and Taniuti [35] used this method to derive KdV equation for small amplitude ion-acoustic waves and then generalized by Taniuti and Wei [36] to solve an immense category of weakly nonlinear and weakly dispersive and dissipative systems and successfully applied it to investigate different plasma systems. The method is known as a reductive perturbative method because it reduces the far-field behavior of a system of partial differential equations to the solution of a scalar, nonlinear evolution equation [37] like KdV, Burgers, or KdVB equations.

2.2 Korteweg de-Vries (KdV) Equation

The phenomenon described by Russell can be expressed by a non-linear Partial Differential Equation of the third order. A partial differential equation (PDE) is a mathematical equation that contains an unknown function of more than one variable as well as some derivatives of that function concerning the different independent variables. In practical applications where the PDE describes a dynamic process one of the variables has the meaning of the time (hence denoted by t) and the other (normally only up to 3) variable have the meaning of the space (hence denoted by x , y , and z).

Korteweg de-Vries (KdV) Equation is usually written as

$$u_t(x, t) + 6u(x, t)u_x(x, t) + u_{xxx}(x, t) = 0. \quad (2.1)$$

Where the short notations are express as

$$u_t(x, t) = \frac{\partial u(x, t)}{\partial t}; u_x(x, t) = \frac{\partial u(x, t)}{\partial x},$$

and

$$u_{xxx}(x, t) = \frac{\partial^3 u(x, t)}{\partial^3 x}.$$

This equation (2.1) is known as Korteweg-de Vries(KdV) equation and is named due to the paper written by Korteweg and de Vries which is published in 1895 [38]. This equation is nonlinear because due to the product shown in the second summand, and of third order because of the third derivative as highest present in this equation, and factor 6 is just a scaling number. And finally, Korteweg and de Vries found the solution for solitary waves in this way. For many decades this equation pays attention to many researchers and leads to quite important discoveries.

2.2.1 Exact Solution of Kd-V equation

Let $u = u(x, t)$ be a function of two variables x and t representing the space and time coordinates respectively. Then the general KdV equation is as follows.

$$u_t + 6uu_x + u_{xxx} = 0. \quad (2.2)$$

To solve this PDE we adopt the exact solution method, since this PDE is nonlinear and dispersive in nature. Considered $u(x, t) = z(x - ct) = f(\xi)$, where c is the phase velocity and $\xi = x - ct$. The wave equation $u_{tt} - c^2u_{xx}$ and which has a characteristic wave solution, i.e., $f(x + ct)$ and $f(x - ct)$. Therefore, we have

$$u(x, t) = z(x - ct) \equiv f(\xi), \quad (2.3)$$

here one can replace the parameter c by β and the function f by g . And by Substituting equation (2.3) in (2.2), we obtained the ordinary differential equation

$$-\beta \frac{dg}{d\xi} + 6g \frac{dg}{d\xi} + \frac{d^3g}{d\xi^3} = 0. \quad (2.4)$$

Taking single integration over ξ , the following equation is obtained

$$-\beta g + 3g^2 + \frac{d^2g}{d\xi^2} = C_1, \quad (2.5)$$

where C_1 is the constant of integration. Now multiply this equation with $\frac{dg}{d\xi}$ to obtain an expression for g

$$-\beta z \frac{dg}{d\xi} + 3z^2 \frac{dg}{d\xi} + \frac{d^2g}{d\xi^2} \frac{dg}{d\xi} = C_1 \frac{dg}{d\xi},$$

$$-\beta z dg + 3z^2 dg + \frac{d^2 g}{d\xi^2} dg = C_1 dg.$$

Hence, integrating over variable ξ

$$-\frac{\beta}{2}g^2 + g^3 + \frac{1}{2}\left(\frac{dg}{d\xi}\right)^2 = C_1 g + C_2, \quad (2.6)$$

where C_2 is the constant of integration. In this case apply boundary conditions i.e., $x \rightarrow \pm \infty$ we have $g \rightarrow 0$, $\frac{dg}{d\xi} \rightarrow 0$ and $\frac{d^2 g}{d\xi^2} \rightarrow 0$. From that we have, $C_1 = C_2 = 0$. Therefore, solution of (2.6) under these boundaries conditions is

$$\left(\frac{dg}{d\xi}\right)^2 = g^2(\beta - 2g). \quad (2.7)$$

Using separation of variable technique, we obtained the following result

$$\int_0^g \frac{d\xi}{\xi\sqrt{\beta - 2\xi}} = \int_0^\xi d\eta. \quad (2.8)$$

In this equation's lower limit 0 the generality cannot lose since the starting point can be transformed linearly. Use the transformation, i.e., $s = \frac{1}{2}\beta \operatorname{sech}^2 w$ and integrate the left side of equation (2.8), one can obtained the equation

$$\beta - 2\beta = \beta(1 - \operatorname{sech}^2 w) = \beta \tanh^2. \quad (2.9)$$

Using the identity $\cosh^2 - \sinh^2 = 1$, then

$$\frac{d\xi}{dw} = -\beta \left(\frac{\sinh w}{\cosh^3 w} \right). \quad (2.10)$$

Now the upper integration limit of the left hand integral of equation (2.8) due to the transformation $s = \frac{1}{2}\beta \operatorname{sech}^2 w$ becomes

$$w = \operatorname{sech}^{-1} \sqrt{\frac{2g}{\beta}}, \quad (2.11)$$

substituting equations (2.9)-(2.11) in equation (2.8), we obtained the following equation

$$\begin{aligned} \xi &= -\frac{2}{\sqrt{\beta}} \int_0^w \frac{1}{\operatorname{sech}^2 w \cdot \tanh w} \frac{\sinh w}{\cosh^3 w} dw \\ &= -\frac{2}{\sqrt{\beta}} \int_0^w \frac{\cosh^2 w \cdot \cosh w}{\sinh w} \frac{\sinh w}{\cosh^3 w} dw \\ &= -\frac{2}{\sqrt{\beta}} \int_0^w dw \\ &\equiv -\frac{2}{\sqrt{\beta}} w. \end{aligned}$$

By back substitution ξ , we get

$$\xi = -\frac{2}{\sqrt{\beta}} \operatorname{sech}^{-1} \sqrt{\frac{2g}{\beta}},$$

$$g(\xi) = \frac{\beta}{2} \operatorname{sech}^2 \left(\frac{\sqrt{\beta}}{2} \xi \right),$$

therefore, the final result is of the form

$$u(x, t) = \frac{\beta}{2} \operatorname{sech}^2 \left[\frac{\sqrt{\beta}}{2} (x - \beta t) \right]. \quad (2.12)$$

Equation (2.12) is the solution of KdV equation and describe the stationary bell shaped

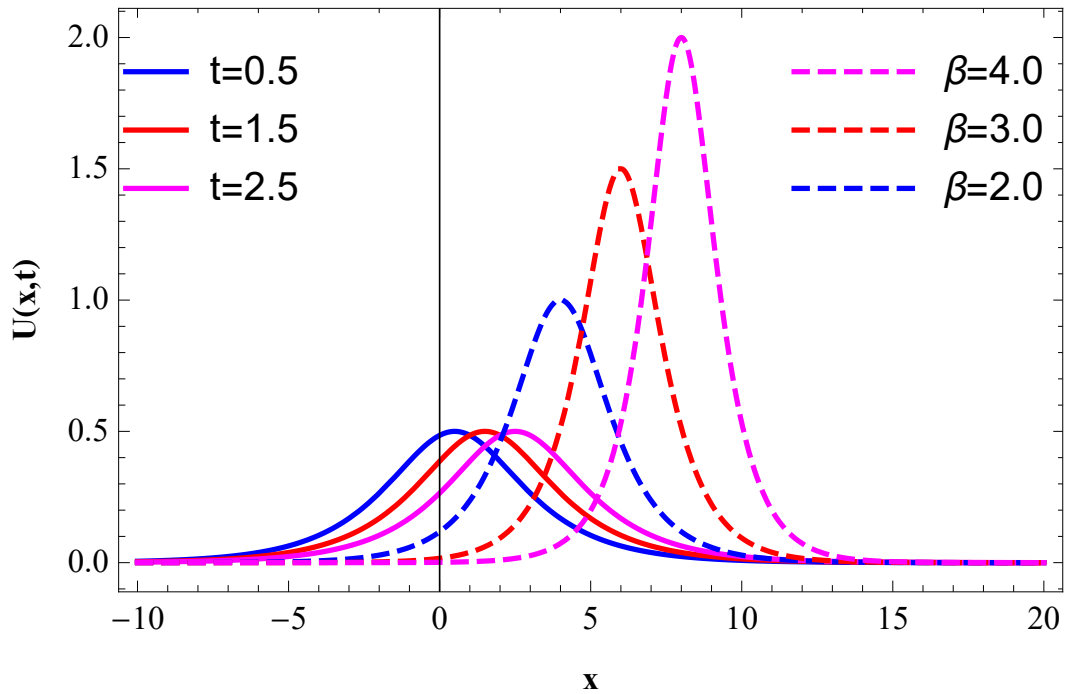


Figure 2.1: Propagation of KdV Solitons for two different values (a) Solid curves $\beta = 1$ and (b) Dashed lines $t = 2$

curved propagating with velocity β along x with width of the pulse $\Delta = \frac{2}{\sqrt{\beta}}$ without any change in its shape.

2.3 Burger Equation

Burger's equation is obtained from combining nonlinear wave motion with linear diffusion and is the simplest model for analyzing the combined effect of nonlinear advection and diffusion. The presence of viscous terms helps to terminate wave breaking and smooth out shock discontinuities which help to obtain a well behaved and smooth solution. Since the inviscid limit, the diffusion term becomes vanishingly small and the smooth viscous solutions converge non-uniformly to the appropriate discontinuous shock wave, leading to an alternative mechanism for analyzing conservative nonlinear dynamical processes. Burger in 1948 first succeeds in his equation to throw light on turbulence describing the interaction of two opposite effects of convection and diffusion.

2.3.1 Solution of Burger Equation

If the nonlinearity is balanced by the dissipation the resultant equation is the non-linear equation with diffusion term

$$\partial_t u + u \partial_x u - w \partial_{xx} u = 0. \quad (2.13)$$

This equation is well known Burger equation. Where by ∂_t we mean $\frac{\partial}{\partial t}$ and similar is the case for x , while by ∂_{xx} we mean $\frac{\partial^2}{\partial x^2}$ and $u = u(x, t)$. The equation (2.38) is composed of time evolution ($\partial_t u$), nonlinearity ($u \partial_x u$) and diffusion ($\partial_{xx} u$) terms. This is the simplest nonlinear model equation for diffusive waves in fluid like dynamics.

The effect of nonlinear term (uu_x) is shocking up that cause to break the wave while the diffusion term (vu_x) is like one occurring in heat equation. To find the travelling wave solution of following nonlinear equation, we considered

$$u(x, t) = h(x - ct) \equiv h(\xi), \quad (2.14)$$

where $\xi = x - ct$ and c is the phase velocity. One can also determine the phase velocity c and h . Therefore, by chain rule, i.e., $\frac{\partial u}{\partial t} = -ch'(\xi)$, $\frac{\partial u}{\partial x} = h'(\xi)$, $\frac{\partial^2 u}{\partial x^2} = h''(\xi)$

Now Substituting these expressions into equation (2.38), the following ordinary differential equation is obtained

$$-ch'(\xi) + h(\xi)h'(\xi) - vh''(\xi) = 0. \quad (2.15)$$

In equation (2.40), $h(\xi)h'(\xi) = \frac{1}{2}\frac{dh^2}{ds}$, after performing the integration with respect to ξ yields

$$\begin{aligned} -ch(\xi) + \frac{1}{2}h^2(\xi) - vh'(\xi) &= C_1, \\ 2v\frac{dh(\xi)}{d\xi} &= \left(h^2(\xi) - 2ch(\xi) - 2C_1\right), \\ 2v\frac{dh(\xi)}{d\xi} &= \left(h(\xi) - h_1(\xi)\right)\left(h(\xi) - h_2(\xi)\right), \end{aligned} \quad (2.16)$$

where C_1 is the constant of integration, $h_1 = c + \sqrt{c^2 + 2C_1}$ and $h_2 = c - \sqrt{c^2 + 2C_1}$. Assuming h_1 and h_2 are real and therefore, $h_1 > h_2$. After separation of variable integrate equation (2.16), we get the following equation

$$\begin{aligned} \frac{\xi}{2v} &= \int \frac{dh(\xi)}{\left(h(\xi) - h_1(\xi)\right)\left(h(\xi) - h_2(\xi)\right)}, \\ &= \frac{1}{h_1(\xi) - h_2(\xi)} \ln \frac{h_1(\xi) - h(\xi)}{h(\xi) - h_2(\xi)} \end{aligned}$$

Assuming $h_2(\xi) < h(\xi) < h_1(\xi)$, this will leads to the equation of the form

$$h(\xi) = \frac{h_1(\xi) + h_2(\xi)e^{\left(\frac{h_1(\xi) - h_2(\xi)}{2v}\right)\xi}}{1 + e^{\left(\frac{h_1(\xi) - h_2(\xi)}{2v}\right)\xi}}. \quad (2.17)$$

Or this equation may be write as

$$h(\xi) = h_2(\xi) + \frac{h_1(\xi) - h_2(\xi)}{1 + e^{\left(\frac{h_1(\xi) - h_2(\xi)}{2v}\right)\xi}}. \quad (2.18)$$

Equation (2.17) can be written as

$$\begin{aligned} h(\xi) &= \frac{1}{2}(h_1(\xi) + h_2(\xi)) + \frac{h_1(\xi) + h_2(\xi)e^{\left(\frac{h_1(\xi) - h_2(\xi)}{2v}\right)\xi}}{1 + e^{\left(\frac{h_1(\xi) - h_2(\xi)}{2v}\right)\xi}} - \frac{1}{2}(h_1(\xi) + h_2(\xi)), \\ &= \frac{1}{2}(h_1(\xi) + h_2(\xi)) - \frac{1}{2}(h_1(\xi) - h_2(\xi))\tanh\left[\frac{1}{4v}(h_1(\xi) - h_2(\xi))\xi\right]. \end{aligned}$$

This solution of Burger's equation is called shock structure solution because it looks like the actual shock wave profile as it connects the asymptotic states $h_1(\xi)$ and $h_2(\xi)$. When the Burger's equation solution does not contain the viscous term then a shock wave would be formed and at last, it breaks. The presence of the diffusion term stop the moderate distortion of the wave and it's breaking would occur by countering the non-linearity. Therefore, the nonlinear advection term and the linear diffusion term balance each other in the same fashion in real shock waves in the small region, which is the region where the gradient is steep. In this regard, the diffusion coefficient affects the waveform, i.e smaller the diffusion coefficient the sharper the transition layer between the two asymptotic values of the solution and vice versa. And finally traveling wave solution to equation (2.38) is

$$u(x, t) = c - \frac{1}{2}(h_1(\xi) - h_2(\xi)) \tanh \left[\frac{1}{4v} (h_1(\xi) - h_2(\xi)) (x - ct) \right]. \quad (2.19)$$

Now from $h_1(\xi)$ and $h_1(\xi)$ relation, we calculate the expression for c , i.e

$$c = \frac{1}{2}(h_1(\xi) + h_2(\xi)). \quad (2.20)$$

And for special case where $h_1(\xi) = 2$ and $h_2(\xi) = 0$, the travelling wave solution becomes

$$h_\xi = \frac{2}{1 + e^{\frac{\xi}{v}}} = 1 - \tanh\left(\frac{\xi}{2v}\right), \quad (2.21)$$

this solution is independent of time in space-time frame.

Since the traveling wave solution defines shock thickness, and one can obtained this thickness by multiplying a factor $e^{-\left(\frac{h_1(\xi)-h_2(\xi)}{2v}\right)\xi}$ with equation (2.17), i.e.,

$$h(\xi) = \frac{h_2(\xi) + h_1(\xi) e^{-\left(\frac{h_1(\xi)-h_2(\xi)}{2v}\right)\xi}}{1 + e^{-\left(\frac{h_1(\xi)-h_2(\xi)}{2v}\right)\xi}}. \quad (2.22)$$

And for a special case where $h_1(\xi) = 2$ and $h_2(\xi) = 0$, we have

$$h(\xi) = \frac{2e^{-\frac{\xi}{v}}}{1 + e^{-\frac{\xi}{v}}}. \quad (2.23)$$

In equation (2.22), the exponential term specify the existence of a thin layer of thickness σ , i.e., $\sigma = \frac{v}{h_1(\xi)-h_2(\xi)}$. This is basically the shock wave thickness which is approaching

to zero as $v \rightarrow 0$ (means that $h_1(\xi)$ and $h_2(\xi)$ is fixed). While on the other hand σ increases as $h_1(\xi) \rightarrow h_2(\xi)$ where v is fixed. This will leads us to an idea that if σ is small comparable with other typical length scales of the problem then the rapid shock transition can satisfactorily be approximated by a discontinuity.

2.4 Distribution Functions

In plasma, the plasma's species moving with random velocities and are affected by different parameters. To assign a specific velocity to individual species is very difficult. Therefore, the velocities of plasma species are distributed and the systems are best dealt with by considering the statistical approach called velocity distribution function. All physical information like macroscopic properties related to the plasma environment contains in the distribution function. In the simple case when plasma is in thermal equilibrium its distribution function is homogeneous, isotropic, and time-independent.

A volume element in phase space is a six dimensional cube at position $(\mathbf{r}, \boldsymbol{\nu})$ and is represented by $d^3\mathbf{r}d^3\nu$. Inside the volume the particles contained are $d^3\mathbf{r} = dx dy dz$ with velocities $d^3\nu = d\nu_x d\nu_y d\nu_z$ [22]. More generally with the addition of time coordinate the distribution function becomes the seven variable function, i.e., $\mathcal{F}(x, y, z, \nu_x, \nu_y, \nu_z, t)$, which gives the number of particles per unit volume in phase space. The particle number density is the write as

$$\begin{aligned} \mathcal{N}(\mathbf{r}, t) &= \int_{-\infty}^{\infty} d\nu_x \int_{-\infty}^{\infty} d\nu_y \int_{-\infty}^{\infty} d\nu_z \mathcal{F}(\mathbf{r}, \boldsymbol{\nu}, t), \\ &= \int_{-\infty}^{\infty} \mathcal{F}(\mathbf{r}, \boldsymbol{\nu}, t) d^3\nu, \\ &= \int_{-\infty}^{\infty} \mathcal{F}(\mathbf{r}, \boldsymbol{\nu}, t) d\boldsymbol{\nu}. \end{aligned}$$

And finally write in the normalized form

$$\int_{-\infty}^{\infty} \mathcal{F}(\mathbf{r}, \boldsymbol{\nu}, t) d\boldsymbol{\nu} = 1.$$

2.4.1 Maxwellian Distribution Function

In thermally equilibrium plasma the velocities of the particles disperse around the average velocity of the particles. But in stationary state plasma, the average velocity of the particles is zero and the distribution obeys statistical Gaussian distribution of errors [23].

$$h(\Delta x) = (\pi(\Delta x)^2)^{-\frac{1}{2}} \exp\left(-\frac{(\Delta x)^2}{\langle \Delta x \rangle^2}\right).$$

In plasma situation Δx equivalent to the x -direction velocity component (ν_x), and $\langle \Delta x \rangle$ show the variance from average velocity of particles, i.e, $\langle \nu_x \rangle$. For the N number of particles number density in thermal equilibrium, the one dimensional distribution function is

$$f(\nu_x) = N(\pi\langle \nu_x \rangle^2)^{-\frac{1}{2}} \exp\left(-\frac{(\nu_x)^2}{\langle \nu_x \rangle^2}\right).$$

More generally, in three dimensional space $\nu^2 = \nu_x^2 + \nu_y^2 + \nu_z^2$ the three dimensional Maxwellian distribution function is

$$f(\nu) = N(\pi\langle \nu \rangle^2)^{-\frac{3}{2}} \exp\left(-\frac{(\nu)^2}{\langle \nu \rangle^2}\right),$$

where ν is the thermal velocity of the plasma species having mass (m) and average thermal energy ($K_B T$) of plasma species, i.e $\langle \nu \rangle = \left(\frac{K_B T}{m}\right)^{\frac{1}{2}}$. Thus, the distribution function becomes

$$f(\nu) = N\left(\frac{m}{2\pi K_B T}\right)^{\frac{3}{2}} \exp\left(-\frac{m\nu^2}{2K_B T}\right), \quad (2.24)$$

where $\frac{m\nu^2}{2}$ is kinetic energy and by integrating equation (2.24) over velocity space gives density of the plasma and sketched in Fig. 2.2.

The Maxwellian distribution function depends on the ratio of kinetic energy and average thermal energy. If we take the distribution function for electrons species where there is any external potential is applied, i.e., $E = -\nabla\phi$. Thus the kinetic energy of electrons replaced by total energy, then the Maxwellian distribution of electrons becomes

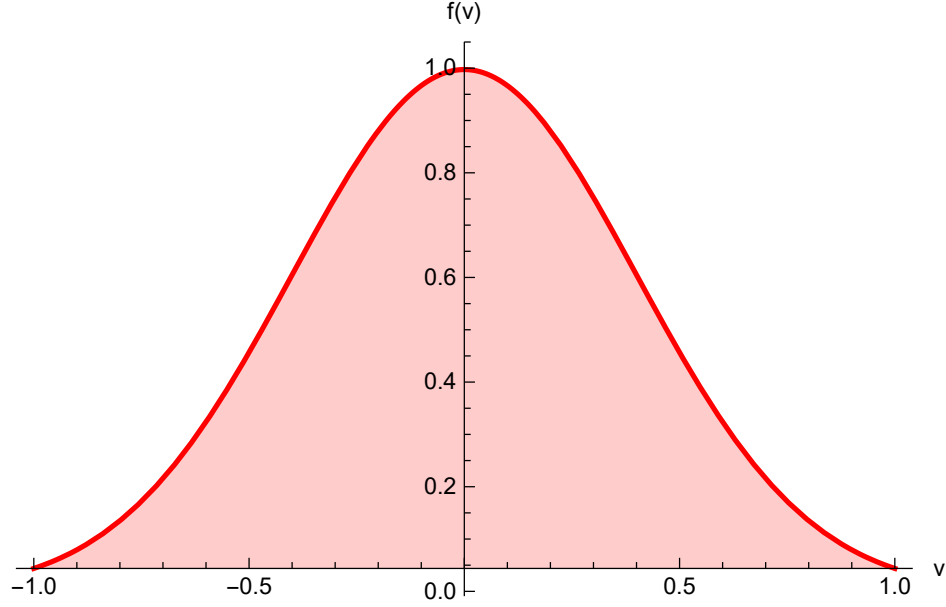


Figure 2.2: Maxwell Distribution Function

$$f_e(\nu) = N \left(\frac{m_e}{2\pi K_B T} \right)^{\frac{3}{2}} \exp \left(- \frac{U}{K_B T_e} \right). \quad (2.25)$$

While write the distribution function in the form of total energy (as variable of system) $U = \frac{m_e \nu^2}{2} + e\phi$, i.e.,

$$f(U) = 2 \left(\frac{2(U + e\phi)}{m_e} \right)^{\frac{1}{2}} f(\nu). \quad (2.26)$$

The equation (2.26) is known as Boltzmann distribution function [23]. And by integrating equation (2.25) we get the electron number density

$$n_e = n_0 \exp \left(- \frac{e\phi}{K_B T_e} \right). \quad (2.27)$$

2.4.2 Cairns Distribution Function

Cairns distribution is common non-maxwellian nature distribution function. It received the attention when Cairns *et al* in 1995 presented that the nature of ion acoustic solitary structures should modified to rarefactive in the presence of non-Maxwellian distribution of electrons [24], and mostly found in auroral zone [25, 26]. And their

structure which has upper and lower cavities has been observed by two different satellites, namely Freja satellite and Viking satellite [27, 28]. In foreshock and bow shock of earth [29, 30], proximity of the Moon [31] and upper Martian ionosphere [32] these non-thermal populations are detected. The Non-thermal velocity distribution function used by Cairan *et al* has the following form

$$f_s(\nu) = \frac{n_0}{(3\Gamma + 1)} (2\pi\nu_j^2)^{-\frac{1}{2}} \left(1 + \frac{\Gamma\nu^4}{\nu_j^4}\right) \exp\left(-\frac{(\nu^2 - \frac{2e\phi}{m_e})}{2\nu_j^2}\right), \quad (2.28)$$

where n_0 , ν_j and Γ are the equilibrium number density, velocity of j species in plasma and non-thermality parameter, respectively. We can switch to Maxwellian distribution by putting $\Gamma = 0$. For the electrons number density integrate equation (2.28) over velocity space, we get

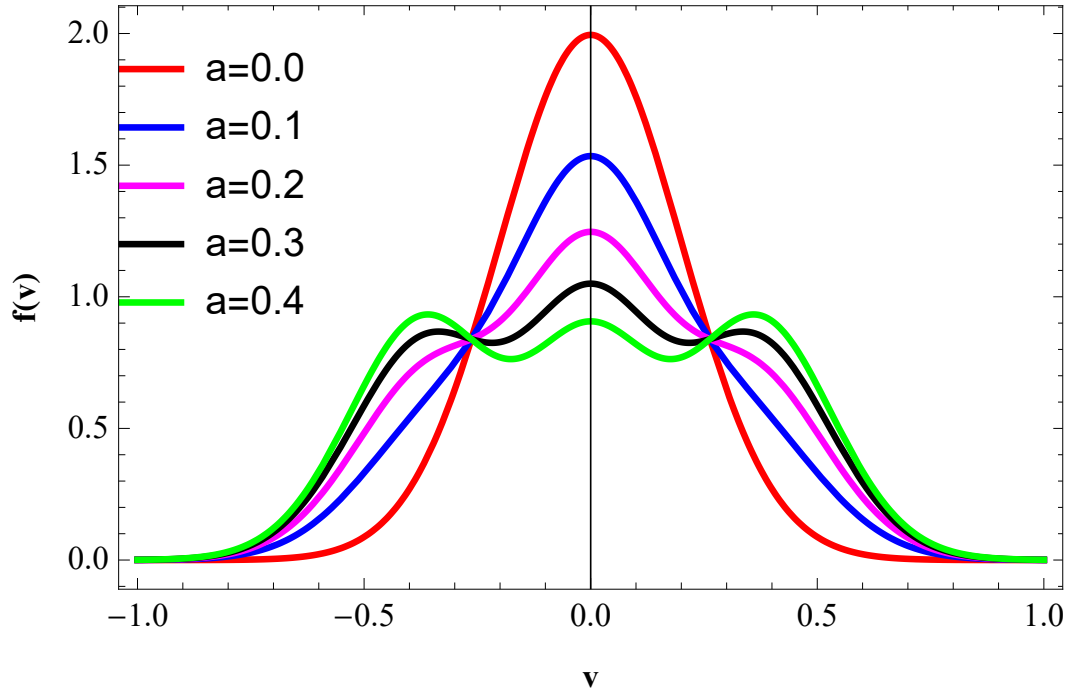


Figure 2.3: Cairn Distribution Function

$$n_e = n_{e0} \left[1 - \beta \frac{e\phi}{T_e} + \beta \left(\frac{e\phi}{T_e}\right)^2\right] \exp\left(\frac{e\phi}{T_e}\right), \quad (2.29)$$

where $\beta = \frac{4\Gamma}{1+3\Gamma}$. In fig(2.2) shows the plot for various values of the Cairns distribution function. The shoulders in the Cairns distribution function represents the behavior of

the non-thermal particles at low energies. It is double humped and is essentially an unstable distribution.

2.5 Linear Analysis of Plasma Waves

In general, plasma is known to be a nonlinear medium, although, linear waves has also an important role in plasma. To study small-amplitude perturbations in linear approximation, we assume and write variable quantities as a perturbed and unperturbed state of plasma, where we have to neglect nonlinear terms. Therefore, the linear differential equations are solved by either Fourier transformation or Laplace transformation. For Fourier analysis assume that perturbed quantities undergo sinusoidal oscillations and sinusoidal character, i.e., $e^{i(\mathbf{k}\cdot\mathbf{r}-\omega t)}$, can be taken into account to solve linear plasma waves. Where \mathbf{k} , \mathbf{r} , ω and t represents the wave vector, position vector, angular frequency and time respectively. Such kind of equations ends up with dispersion relation which relates the wave vector and angular frequency. In the linear regime, several waves can overlap each other without interacting and these waves travel without disturbing the medium. For linear theory, only small amplitude plasma waves are to be considered.

Now, we describe two different kinds of waves to understand the linear analysis of waves.

- Linear and non-dispersive
- Linear and dispersive

In linear and non-dispersive cases, one can consider the basic wave equation.

$$\frac{\partial u(x, t)}{\partial t} + v \frac{\partial u(x, t)}{\partial x} = 0. \quad (2.30)$$

The periodic solution of plane wave leads for equation (2.30) leads to

$$u(x, t) = e^{i(kx - \omega t)}. \quad (2.31)$$

The linear dispersion relation which is the relationship between angular frequency ω and wavenumber k is given by $\omega = vk$. Where v is the phase speed. This is a linear dispersion relation of a non-dispersive wave. The main aspect of such wave is that the initial pulse-type profile (which is made up of superposition of plane wave with different wavenumbers do not change the shape). The reason is that each superposed plane wave is traveling at the same speed.

In linear dispersive case, there is only some additional effects which modify the equation

$$\frac{\partial u(x, t)}{\partial t} + v \frac{\partial u(x, t)}{\partial x} + \sigma \frac{\partial^3 u(x, t)}{\partial x^3} = 0. \quad (2.32)$$

Assume the plane wave solution for equation (2.51) and dispersion relation for this case write as $\omega = vk - \sigma k^3$, this involves higher order in k , so it's basically nonlinear in k . For the given case the phase velocity and group velocity are respectively, $v_\phi = v - \sigma k^2$ and $v_g = v - 3\sigma k^2$. As the wave travels it can spread out because of velocity variation due to k . Which means that linear dispersive waves do not preserve their original shape.

2.5.1 Dust Acoustic Waves

The dust acoustic waves have been theoretically investigated by Rao *et al* in 1990 [39]. In these investigations, they take multi-component collision-less dusty plasma whose species are the electrons, ions, and negatively charged dust grains. The phase velocity of the dust acoustic waves is much smaller than the electron and ion thermal speeds. Consequently, the inertia-less electrons and ions establish equilibrium in the dust acoustic wave potential denoted by ϕ . The pressure gradient in this situation is balanced by the electric force, leading to Boltzmann electron and ion number density perturbation n_{j1} , which are, respectively,

$$n_{e1} \approx n_{e0} \frac{e\phi}{k_B T_e}, \quad (2.33)$$

and

$$n_{i1} \approx -n_{i0} \frac{e\phi}{k_B T_i}. \quad (2.34)$$

The main governing equation for the system is given as:

Continuity equation

$$\frac{\partial n_{d1}}{\partial t} + n_{d0} \nabla \cdot v_d = 0. \quad (2.35)$$

Momentum equation

$$\frac{\partial v_d}{\partial t} = -\frac{q_{d0}}{m_d} \nabla \phi - \frac{3k_B T_d}{m_d n_{d0}} \nabla n_{d1}. \quad (2.36)$$

And the system is closed by Poisson's equation

$$\nabla^2 \phi = 4\pi (en_{e0} - en_{i1} - q_{d0} n_{d1}). \quad (2.37)$$

In these equations (2.35) - (2.37), v_d is the fluid velocity, q_{d0} is the non-perturbed dust charge which is assumed to be constant. And n_{e1} , n_{i1} and n_{d1} are the number densities of electrons, ions and dust grains, respectively.

In the linear analysis of waves, one can obtain the dispersion relation. For this purpose we combine equations (2.35) and (2.36) and obtained

$$\left(\frac{\partial^2}{\partial t^2} - 3V_{td}^2 \nabla^2 \right) n_{d1} = \frac{n_{d0} q_{d0}}{m_d} \nabla^2 \phi. \quad (2.38)$$

Substituting n_{e1} and n_{i1} in the above equation, we get

$$\nabla^2 \phi = k_D^2 \phi - 4\pi q_{d0} n_{d1}, \quad (2.39)$$

where $k_D^2 = \frac{4\pi e^2 n_{e0}}{k_B T_e} + \frac{4\pi e^2 n_{i0}}{k_B T_i}$. And assuming $n_{d1} = \hat{n}_{d1} \exp(-i\omega t + i\mathbf{k} \cdot \mathbf{r})$ and $\phi = \hat{\phi} \exp(-i\omega t + i\mathbf{k} \cdot \mathbf{r})$, where ω and \mathbf{k} are the frequency and the wave vector, respectively. Now we Fourier transform equations (2.38) and (2.39), i.e., $\frac{\partial}{\partial t} = -i\omega$ and $\nabla = i\mathbf{k}$ and the combination of these equations will leads to dispersion relation for dust acoustic waves

$$1 + \frac{k_D^2}{k^2} - \frac{\omega_{pd}^2}{\omega^2 - 3k^2 V_{td}^2} = 0, \quad (2.40)$$

which gives the equation of form

$$\omega^2 = 3k^2 V_{td}^2 + \frac{k^2 C_D^2}{1 + k^2 \lambda_d^2}, \quad (2.41)$$

where $C_D = \omega_{pd} \lambda_D$ is the dust acoustic speed. Although, $\omega \gg kV_{td}$, we deduce from equation (2.41) the dust acoustic wave frequency

$$\omega = \frac{kC_D}{(1 + k^2 \lambda_d^2)^{\frac{1}{2}}}, \quad (2.42)$$

which in long wavelength limit, i.e., $k^2 \lambda_D^2 \ll 1$, the equation (2.42) reduced to

$$\omega = k Z_{d0} \left(\frac{n_{d0}}{n_{i0}} \right)^{\frac{1}{2}} \left(\frac{k_B T_i}{m_d} \right)^{\frac{1}{2}} \left[1 + \frac{T_i}{T_e} \left(1 - \frac{Z_{d0} n_{d0}}{n_{i0}} \right) \right]^{-\frac{1}{2}}, \quad (2.43)$$

when the dust grains are negatively charged. Equation (2.42) tells that the restoring force in the dust acoustic waves comes from the pressure of inertia-less electrons and ions. While the dust mass provides the inertia to support the waves. Frequency of the dust acoustic waves is much smaller than the dust plasma frequency. Using equation (2.43), the dust acoustic phase velocity, i.e., $V_p = \frac{\omega}{k}$ can be estimated if one knows the plasma and dust parameters [10].

2.5.2 Dust Ion Acoustic Waves

The dust ion acoustic waves were predicted for the first time by P. K. Shukla and Silin in 1992. The phase velocity of the dust ion acoustic waves is much smaller (larger) than the electron thermal speed (ion and dust thermal speeds). Here the electron number density perturbation associated with the dust ion acoustic waves is given by (2.33) while the ion number density perturbation n_{i1} is calculated from the ion continuity equation

$$\frac{\partial n_{i1}}{\partial t} + n_{i0} \nabla \cdot \mathbf{v}_i = 0, \quad (2.44)$$

and the ion momentum equation

$$\frac{\partial \mathbf{v}_i}{\partial t} = -\frac{e}{m_i} \nabla \phi - \frac{3k_B T_i}{m_i n_{i0}} \nabla n_{i1}, \quad (2.45)$$

where \mathbf{v}_i is the ion fluid velocity. By combining the continuity ion continuity and ion momentum equations, we get the following equation

$$\left(\frac{\partial^2}{\partial t^2} - 3V_{ti}^2 \nabla^2 \right) n_{i1} = \frac{n_{i0} e}{m_i} \nabla^2 \phi. \quad (2.46)$$

Equation (2.38) for the dust number density perturbation remains intact for the dust ion acoustic waves as well. However, for stationary dust grains, we have $n_{d1} \approx 0$ and the dust ion-acoustic waves appears on a time scale much shorter than the plasma

period, i.e., $\frac{2\pi}{\omega_{pd}}$. Assuming $\omega \gg kV_{ti}$, kV_{td} . One can combine equations (2.33), (2.37), (2.38) and (2.46) and Fourier transform the resultant equation in order to obtain the dust ion acoustic wave dispersion relation, i.e.,

$$1 + \frac{k_{de}^2}{k^2} - \frac{\omega_{pi}^2 + \omega_{pd}^2}{\omega^2} = 0. \quad (2.47)$$

Because of the large mass of dust grains, the ion plasma frequency ω_{pi} is much larger than the dust plasma frequency ω_{pd} . Therefore, by simplifying the equation (2.47), one can get the equation of the form

$$\omega^2 = \frac{k^2 C_s^2}{1 + k^2 \lambda_{De}^2}, \quad (2.48)$$

where $C_s = \omega_{pi} \lambda_{De} = \left(\frac{n_{i0}}{n_{e0}}\right)^{\frac{1}{2}} c_s$ and $c_s = \left(\frac{k_B T_e}{m_i}\right)^{\frac{1}{2}}$. In the long wavelength limit the equation (2.48) reduced to

$$\omega = k \left(\frac{n_{i0}}{n_{e0}}\right)^{\frac{1}{2}} c_s. \quad (2.49)$$

Equation (2.49) shows that the phase velocity of the dust ion-acoustic waves in a dusty plasma is larger than c_s because $n_{i0} > n_{e0}$ for negatively charged dust grains. The increase in the phase velocity is attributed to the electron density depletion in the background plasma so that the electron Debye radius becomes larger. As a result, there appears a stronger space-charge electric field which is responsible for the enhanced phase velocity of the dust ion-acoustic waves [10].

2.6 Non-linear Analysis of Plasma Waves

While on the other hand during the last four decades, growing attention has been given to nonlinear plasma waves [40, 41, 42]. If the plasma wave amplitude is large enough then nonlinearities cannot be ignored. When wave amplitude is large enough then waves start interacting with each other. These waves' interaction generates new waves of the same kind and similarly, waves of different types generate new waves. These nonlinearities, contribute towards the localization of produced waves, which result in various forms of structures such as solitons, shocks, and vortices, etc. Now, we describe

two different kind of waves to understand nonlinearities.

- Nonlinear and non-dispersive
- Nonlinear and dispersive

For non-linear and non-dispersive case, we take the non-dispersive wave equation, i.e.,

$$\frac{\partial u(x, t)}{\partial t} + v(u) \frac{\partial u(x, t)}{\partial x} = 0. \quad (2.50)$$

In equation (2.50) the term $v(u) \frac{\partial u(x, t)}{\partial x}$ makes the equation nonlinear and solution to this equation is $u(x, t) = u(x - v(u)t)$, where $v(u) = v + \alpha u^m$. Since $v(u)$ is an increasing function, which shows that wave travels faster when its amplitude grows. Therefore, the top of the wave travels faster than its base, which results in wave breaking and steepening and finally wave breaks and disappear completely.

The nonlinear and dispersive case is so interesting because such kind of situation give birth to solitary waves, which on specific case becomes solitons. Take the nonlinear and dispersive equation as equation

$$\frac{\partial u(x, t)}{\partial t} + v \frac{\partial u(x, t)}{\partial x} + \alpha u^m \frac{\partial u(x, t)}{\partial x} + \sigma \frac{\partial^3 u(x, t)}{\partial x^3} = 0. \quad (2.51)$$

In previous cases neither linear dispersive nor nonlinear dispersive wave is stable in nature but we see that solitary wave exist when the system has both nonlinearity and dispersion. In solitary wave the velocity at the top of wave and at base of wave is same. These nonlinearities, contribute towards localization of produced waves, which result in various forms of structures such as solitons, shocks and vortices etc.

2.6.1 Dust Acoustic Solitary Waves

In our physical problem, we take the plasma environment to contain electrons, positive ions, and negative dust species. The electrons and ions species particle number density are taken as Maxwellian and for simplicity take a one-dimensional problem. Therefore, the dynamics of low phase velocity, i.e. V_{Td} (thermal velocity of dust particles) $\ll V_p$

(plasma velocity) $\ll V_{Te}$ and V_{Ti} (thermal velocities of electron and ion, respectively). The one-dimensional dust acoustic solitary waves are governed by the following main equation of plasma.

Continuity equation

$$\frac{\partial n_d}{\partial t} + \frac{\partial n_d u_d}{\partial z} = 0. \quad (2.52)$$

Equation of motion

$$\frac{\partial n_d}{\partial t} + u_d \frac{\partial u_d}{\partial z} = \frac{\partial \phi}{\partial z}. \quad (2.53)$$

And the system is closed by Poisson's equation

$$\frac{\partial^2 \phi}{\partial z^2} = n_d + \mu_e n_e - \mu_i n_i, \quad (2.54)$$

where $\mu_e = \frac{n_{e0}}{Z_{d0} n_{d0}} = \frac{1}{\delta-1}$, $\mu_i = \frac{n_{i0}}{Z_{d0} n_{d0}} = \frac{\delta}{\delta-1}$ and $\delta = \frac{n_{i0}}{n_{e0}}$.

The normalized electron and ion number densities are, respectively,

$$n_e = \exp(\sigma_i \phi), \quad (2.55)$$

$$n_i = \exp(-\phi), \quad (2.56)$$

where $\sigma_i = \frac{T_i}{T_e}$ and the normalization scheme are introduced as

$$\text{Time (t)} \rightarrow \omega_{pd}^{-1} = \left(\frac{4\pi n_{d0} Z_d^2 e^2}{m_d} \right)^{-\frac{1}{2}}$$

$$\text{Space parameter (x)} \rightarrow \lambda_D = \left(\frac{K_B T_i}{4\pi n_{d0} Z_{d0} e^2} \right)^{\frac{1}{2}}$$

$$n_d \rightarrow n_{s0}, \quad u_d \rightarrow C_d = \left(\frac{Z_{d0} K_B T_i}{m_d} \right)^{\frac{1}{2}}$$

$$\text{And electrostatic wave potential } \phi \rightarrow \frac{K_B T_i}{e}$$

To study the small but finite amplitude nonlinear dust acoustic solitary (DAS) wave using the reduction perturbation technique, the independent variables are stretched as

$$\zeta = \epsilon^{\frac{1}{2}}(z - v_0 t), \quad (2.57)$$

and

$$\tau = \epsilon^{\frac{3}{2}} t, \quad (2.58)$$

where ϵ is a small parameter characterizing the strength of the nonlinearity or weakness of the amplitude or dispersion and v_0 is the soliton speed normalized by dust acoustic speed (C_d). The dependent variables are expanded as

$$n_d = 1 + \epsilon n_d^{(1)} + \epsilon^2 n_d^{(2)} + \dots, \quad (2.59)$$

$$u_d = \epsilon u_d^{(1)} + \epsilon^2 u_d^{(2)} + \dots, \quad (2.60)$$

$$\phi = \epsilon \phi^{(1)} + \epsilon^2 \phi^{(2)} + \dots \quad (2.61)$$

By using the chain rule the independent variable are stretched as

$$\begin{aligned} \frac{\partial}{\partial t} &= \frac{\partial}{\partial \zeta} \frac{\partial \zeta}{\partial t} + \frac{\partial}{\partial \tau} \frac{\partial \tau}{\partial t}, \\ &= \frac{\partial}{\partial \zeta} \frac{\partial}{\partial t} \epsilon^{\frac{1}{2}} (z - v_0 t) + \frac{\partial}{\partial \tau} \frac{\partial}{\partial t} \epsilon^{\frac{3}{2}} t, \\ &= -\epsilon^{\frac{1}{2}} v_0 \frac{\partial}{\partial \zeta}. \end{aligned} \quad (2.62)$$

And

$$\begin{aligned} \frac{\partial}{\partial z} &= \frac{\partial}{\partial \zeta} \frac{\partial \zeta}{\partial z} + \frac{\partial}{\partial \tau} \frac{\partial \tau}{\partial z}, \\ &= \frac{\partial}{\partial \zeta} \frac{\partial}{\partial z} \epsilon^{\frac{1}{2}} (z - v_0 t) + \frac{\partial}{\partial \tau} \frac{\partial}{\partial z} \epsilon^{\frac{3}{2}} t, \\ &= \epsilon^{\frac{1}{2}} \frac{\partial}{\partial \zeta}. \end{aligned} \quad (2.63)$$

Using equations (2.59) and (2.82) in equation (2.52), i.e. continuity equation

$$\begin{aligned} &\left(-\epsilon^{\frac{1}{2}} v_0 \frac{\partial}{\partial \zeta} + \epsilon^{\frac{3}{2}} \frac{\partial}{\partial \tau} \right) \left(1 + \epsilon n_d^{(1)} + \epsilon^2 n_d^{(2)} \right) + \epsilon^{\frac{1}{2}} \frac{\partial}{\partial \zeta} \left(1 + \epsilon n_d^{(1)} + \epsilon^2 n_d^{(2)} \right) \\ &\times \left(\epsilon u_d^{(1)} + \epsilon^2 u_d^{(2)} \right) = 0, \\ &-\epsilon^{\frac{1}{2}} v_0 \frac{\partial}{\partial \zeta} \left(1 + \epsilon n_d^{(1)} + \epsilon^2 n_d^{(2)} \right) + \epsilon^{\frac{3}{2}} \frac{\partial}{\partial \tau} \left(1 + \epsilon n_d^{(1)} + \epsilon^2 n_d^{(2)} \right) + \epsilon^{\frac{1}{2}} \frac{\partial}{\partial \zeta} \left(\epsilon u_d^{(1)} \right. \\ &\left. + \epsilon^2 u_d^{(2)} + \epsilon^3 u_d^{(3)} + \epsilon^2 n_d^{(1)} u_d^{(1)} + \epsilon^3 n_d^{(1)} u_d^{(2)} + \epsilon^3 n_d^{(2)} u_d^{(1)} \right) = 0, \end{aligned}$$

$$\begin{aligned}
& -v_0 \frac{\partial}{\partial \zeta} \left(\epsilon^{\frac{3}{2}} n_d^{(1)} + \epsilon^{\frac{5}{2}} n_d^{(2)} \right) + \frac{\partial}{\partial \tau} \left(\epsilon^{\frac{5}{2}} n_d^{(1)} + \epsilon^{\frac{7}{2}} n_d^{(2)} \right) + \frac{\partial}{\partial \zeta} \left(\epsilon^{\frac{3}{2}} u_d^{(1)} + \epsilon^{\frac{5}{2}} u_d^{(2)} \right) \\
& + \epsilon^{\frac{5}{2}} u_d^{(1)} n_d^{(1)} = 0.
\end{aligned} \tag{2.64}$$

Now using equations (2.59) - (2.63) in equation (2.53), i.e., equation of motion

$$\begin{aligned}
& \left(-\epsilon^{\frac{1}{2}} v_0 \frac{\partial}{\partial \zeta} + \epsilon^{\frac{3}{2}} \frac{\partial}{\partial \tau} \right) \left(\epsilon u_d^{(1)} + \epsilon^2 u_d^{(2)} \right) + \left(\epsilon u_d^{(1)} + \epsilon^2 u_d^{(2)} \right) \left(\epsilon^{\frac{1}{2}} \frac{\partial}{\partial \zeta} \right) \left(\epsilon u_d^{(1)} + \epsilon^2 u_d^{(2)} \right) \\
& = \epsilon^{\frac{1}{2}} \frac{\partial}{\partial \zeta} \left(\epsilon \phi^{(1)} + \epsilon^2 \phi^{(2)} \right), \\
& -\epsilon^{\frac{1}{2}} v_0 \frac{\partial}{\partial \zeta} \left(\epsilon u_d^{(1)} + \epsilon^2 u_d^{(2)} \right) + \epsilon^{\frac{3}{2}} \frac{\partial}{\partial \tau} \left(\epsilon u_d^{(1)} + \epsilon^2 u_d^{(2)} \right) + \left(\epsilon u_d^{(1)} + \epsilon^2 u_d^{(2)} \right) \frac{\partial}{\partial \zeta} \left(\epsilon^{\frac{3}{2}} u_d^{(1)} + \epsilon^{\frac{5}{2}} u_d^{(2)} \right) \\
& = \frac{\partial}{\partial \zeta} \left(\epsilon^{\frac{3}{2}} \phi^{(1)} + \epsilon^{\frac{5}{2}} \phi^{(2)} \right), \\
& -v_0 \frac{\partial}{\partial \zeta} \left(\epsilon^{\frac{3}{2}} u_d^{(1)} + \epsilon^{\frac{5}{2}} u_d^{(2)} \right) + \frac{\partial}{\partial \tau} \left(\epsilon^{\frac{5}{2}} u_d^{(1)} + \epsilon^{\frac{7}{2}} u_d^{(2)} \right) + \left(\epsilon^{\frac{5}{2}} u_d^{(1)} \frac{\partial}{\partial \zeta} u_d^{(1)} + \epsilon^{\frac{7}{2}} u_d^{(1)} \frac{\partial}{\partial \zeta} u_d^{(2)} \right) \\
& + \epsilon^{\frac{7}{2}} u_d^{(2)} \frac{\partial}{\partial \zeta} u_d^{(1)} = \frac{\partial}{\partial \zeta} \left(\epsilon^{\frac{3}{2}} \phi^{(1)} + \epsilon^{\frac{5}{2}} \phi^{(2)} \right).
\end{aligned} \tag{2.65}$$

At finally using equations (2.59) - (2.63) in equation (2.54), i.e., equation of Poisson.

$$\epsilon \frac{\partial^2}{\partial \zeta^2} \left(\epsilon \phi^{(1)} + \epsilon^2 \phi^{(2)} \right) = \left(1 + \epsilon n_d^{(1)} + \epsilon^2 n_d^{(2)} \right) + \mu_e n_e - \mu_i n_i. \tag{2.66}$$

Using equation (2.55) and (2.56) in equation (2.85), and expand the exponential terms

$$\begin{aligned}
\frac{\partial^2}{\partial \zeta^2} \left(\epsilon^2 \phi^{(1)} + \epsilon^3 \phi^{(2)} \right) & = \left(1 + \epsilon n_d^{(1)} + \epsilon^2 n_d^{(2)} \right) + \mu_e \left[1 + \sigma_i \left(\epsilon \phi^{(1)} + \epsilon^2 \phi^{(2)} \right) \right. \\
& \quad \left. + \frac{\sigma_i^2}{2} \left(\epsilon^2 \phi^{(1)2} + 2\epsilon^3 \phi^{(1)} \phi^{(2)} + \epsilon^4 \phi^{(2)2} \right) \right] - \mu_i \left[1 - \left(\epsilon \phi^{(1)} \right. \right. \\
& \quad \left. \left. + \epsilon^2 \phi^{(2)} \right) + \frac{1}{2} \left(\epsilon^2 \phi^{(1)2} + 2\epsilon^3 \phi^{(1)} \phi^{(2)} + \epsilon^4 \phi^{(2)2} \right) \right].
\end{aligned} \tag{2.67}$$

To the lowest order of ϵ , equations (2.83),(2.84) and (2.86) give

$$n_d^{(1)} = -\frac{\phi^{(1)}}{v_0^2}, \tag{2.68}$$

$$u_d^{(1)} = -\frac{\phi^{(1)}}{v_0}, \tag{2.69}$$

and

$$v_0 = \frac{1}{\sqrt{\mu_i + \sigma_i \mu_e}}. \quad (2.70)$$

To the next higher order ϵ , we obtained a set of equations

$$\frac{\partial n_d^{(1)}}{\partial \tau} - v_0 \frac{\partial n_d^{(2)}}{\partial \zeta} + \frac{\partial u_d^{(2)}}{\partial \zeta} + \frac{\partial}{\partial \zeta} \left(n_d^{(1)} u_d^{(1)} \right) = 0, \quad (2.71)$$

$$\frac{\partial u_d^{(1)}}{\partial \tau} - v_0 \frac{\partial u_d^{(2)}}{\partial \zeta} - \frac{\partial \phi^{(2)}}{\partial \zeta} + u_d^{(1)} \frac{\partial}{\partial \zeta} u_d^{(1)} = 0, \quad (2.72)$$

and

$$\frac{\partial^2 \phi^{(1)}}{\partial \zeta^2} - \frac{1}{v_0^2} \phi^{(2)} - n_d^{(2)} + \frac{1}{2} \left(\mu_i - \sigma^2 \mu_e \right) \phi^{(1)2} = 0. \quad (2.73)$$

Using equations (2.68) and (2.69) in equations (2.90) and (2.91), add these equations

$$\begin{aligned} -\frac{2}{v_0} \frac{\partial \phi^{(1)}}{\partial \tau} - v_0^2 \frac{\partial n_d^{(2)}}{\partial \zeta} + \frac{3}{v_0^2} \phi^{(1)} \frac{\partial \phi^{(1)}}{\partial \zeta} - \frac{\partial \phi^{(2)}}{\partial \zeta} &= 0, \\ \frac{\partial \phi^{(1)}}{\partial \tau} - \frac{3}{2v_0} \phi^{(1)} \frac{\partial \phi^{(1)}}{\partial \zeta} + \frac{v_0^3}{2} \frac{\partial n_d^{(2)}}{\partial \zeta} + \frac{v_0}{2} \frac{\partial \phi^{(2)}}{\partial \zeta} &= 0. \end{aligned} \quad (2.74)$$

Taking derivative of equation (2.92) with respect to ζ and multiply by $\frac{v_0^3}{2}$

$$\frac{v_0^3}{2} \frac{\partial^3 \phi^{(1)}}{\partial \zeta^3} - \frac{v_0}{2} \frac{\partial \phi^{(2)}}{\partial \zeta} - \frac{v_0^3}{2} \frac{\partial n_d^{(2)}}{\partial \zeta} + \frac{v_0^3}{2} \left(\mu_i - \sigma_i \mu_e \right) \phi^{(1)} \frac{\partial \phi^{(1)}}{\partial \zeta} = 0. \quad (2.75)$$

Addition of equations (2.93) and (2.94) which leads to KdV equation

$$\frac{\partial \phi^{(1)}}{\partial \tau} + A_s \phi^{(1)} \frac{\partial \phi^{(1)}}{\partial \zeta} + B_s \frac{\partial^3 \phi^{(1)}}{\partial \zeta^3} = 0. \quad (2.76)$$

Where A_s and B_s are non-linearity and dispersion terms, respectively. Where the value of non-linearity and dispersion are

$$A_s = \frac{v_0^3}{2} \left(\mu_i - \sigma_i^2 \mu_e - \frac{3}{v_0^4} \right), \quad (2.77)$$

and

$$B_s = \frac{v_0^3}{2}. \quad (2.78)$$

Again we have to transform the following independent variables ζ and τ , such as $\eta = \zeta - u_0 \tau$ and $\tau = \tau$. Where u_0 is normalized constant speed and following appropriate

boundary conditions for localized perturbations are $\phi \rightarrow 0$, $\frac{d\phi^{(1)}}{d\eta} \rightarrow 0$, $\frac{d^2\phi^{(1)}}{d\eta^2} \rightarrow 0$ and $\eta \rightarrow \pm\infty$. And obtained the stationary solution of the KdV equation (2.95)

$$\phi^{(1)} = \phi_0^{(1)} \operatorname{sech}^2 \left[\frac{\zeta - u_0\tau}{\Delta_w} \right], \quad (2.79)$$

where $\phi_0^{(1)}$ and Δ_w are the amplitude and width of the soliton, respectively, given as $\phi_0^{(1)} = \frac{3u_0}{A_s}$ and $\Delta_w = \sqrt{\frac{4B_s}{u_0}}$.

2.6.2 Dust Acoustic Shock Waves

In our physical problem we take plasma environment contain electrons, positive ions and negative dust species. The electrons and ions species particle number density are taken as Maxwellian and for simplicity take one dimensional problem. Therefore, the dynamics of low phase velocity, i.e. V_{Td} (thermal velocity of dust particles) $\ll V_p$ (plasma velocity) $\ll V_{Te}$ and V_{Ti} (thermal velocities of electron and ion, respectively). The one dimensional dust acoustic solitary waves are govern by the equations, i.e., (2.52), (2.54), (2.55), (2.56) and (P. K. Shukla and A. A. Mamun)[10]

$$(1 + \tau_n D_t) [n_d (\mathcal{D}_t u_d + \mathcal{V}_{dn} u_d - \frac{\partial \phi}{\partial z})] = \beta_d \frac{\partial^2 u_d}{\partial z^2}. \quad (2.80)$$

In equation (2.80) the $\mathcal{D}_t = \frac{\partial}{\partial t} + u_d \frac{\partial}{\partial z}$, \mathcal{V}_{dn} is normalized by the dust plasma frequency, τ_n is the viscoelastic relaxation time and normalized by the dust plasma period and β_d is the normalized longitudinal viscosity co-efficient and expressed as $(\frac{\tau_d}{m_d n_d 0 \lambda_d m^2}) [\eta_b + \frac{4\omega_b}{3}]$.

To derive a governing equation for dust acoustic shock waves, we have to employ the RPT (Reductive Perturbation Technique). For this purpose we introduce the stretched coordinates, i.e.,

$$\xi = \epsilon^{\frac{1}{2}} (z - u_0 t), \quad (2.81)$$

and

$$\tau = \epsilon^{\frac{3}{2}} t, \quad (2.82)$$

where ϵ is a small parameter characterizing the strength of the nonlinearity or weakness of the amplitude or dispersion. The dependent variables are expanded as

$$n_d = 1 + \epsilon n_d^{(1)} + \epsilon^2 n_d^{(2)} + \dots, \quad (2.83)$$

$$u_d = \epsilon u_d^{(1)} + \epsilon^2 u_d^{(2)} + \dots, \quad (2.84)$$

and

$$\phi = \epsilon \phi^{(1)} + \epsilon^2 \phi^{(2)} + \dots \quad (2.85)$$

Now substitute equations (2.82) - (2.85) in (2.52), (2.54), (2.55), (2.56) and (2.80) and obtain the following relations of lowest order of ϵ ,

$$u_d^{(1)} = -\frac{\phi^{(1)}}{v_0}, \quad (2.86)$$

$$n_d^{(1)} = -\frac{\phi^{(1)}}{v_0^2}, \quad (2.87)$$

$$v_0 = (\sigma_i \mu_e + \mu_i)^{-\frac{1}{2}}. \quad (2.88)$$

Now to the next high order in ϵ , we get

$$\frac{\partial n_d^{(1)}}{\partial \tau} - v_0 \frac{\partial n_d^{(2)}}{\partial \xi} + \frac{\partial}{\partial \xi} (n_d^{(1)} u_d^{(1)}) + \frac{\partial u_d^{(2)}}{\partial \xi} = 0, \quad (2.89)$$

$$\begin{aligned} (1 + \mathcal{V}_{dn} \tau_n) \frac{\partial u_d^{(1)}}{\partial \tau} - u_0 \frac{\partial u_d^{(2)}}{\partial \xi} - \frac{\partial \phi^{(2)}}{\partial \xi} + (1 - \mathcal{V}_{dn} \tau_n) u_d^{(1)} \frac{\partial u_d^{(1)}}{\partial \xi} \\ - \beta_{d0} \frac{\partial^2 u_d^{(1)}}{\partial \xi^2} = 0, \end{aligned} \quad (2.90)$$

and

$$\frac{\partial^2 \phi^{(1)}}{\partial \xi^2} - \frac{\phi^{(2)}}{u_0^2} - n_d^{(2)} = \frac{1}{2} (\sigma_i^2 \mu_e - \mu_i) \phi^{(1)2}. \quad (2.91)$$

By eliminating the second order quantities from Eqs. (2.89) to (2.91) and using the relation of Eqs. (2.86) to (2.88), we obtained the following expressions

$$-\frac{(1 + V_{dn} \tau_n)}{v_0^2} \frac{\partial \phi^{(1)}}{\partial \tau} - \frac{(V_{dn} \tau_n - 1)}{v_0^2} \phi^{(1)} \frac{\partial \phi^{(1)}}{\partial \xi} + \frac{\beta_{d0}}{v_0} \frac{\partial^2 \phi^{(1)}}{\partial \xi^2} = 0, \quad (2.92)$$

$$-\frac{1}{v_0^2} \frac{\partial \phi^{(1)}}{\partial \tau} + \frac{2}{v_0^3} \phi^{(1)} \frac{\partial \phi^{(1)}}{\partial \tau} = 0, \quad (2.93)$$

and

$$\frac{\partial^3 \phi^{(1)}}{\partial \xi^3} = (\sigma_i^2 \mu_e^2 - \mu_i) \phi^{(1)} \frac{\partial \phi^{(1)}}{\partial \xi} \quad (2.94)$$

After a short algebraic manipulations one can get the following KdV Burger equation, given as:

$$A^{-1} \frac{\partial \phi^{(1)}}{\partial \tau} + \phi^{(1)} \frac{\partial \phi^{(1)}}{\partial \xi} + \gamma_d \frac{\partial^3 \phi^{(1)}}{\partial \xi^3} = \mu_{da} \frac{\partial^2 \phi^{(1)}}{\partial \xi^2}. \quad (2.95)$$

Where $A = \frac{v_0^3 a_d}{2} \left(1 + \frac{V_{dn} \tau_n}{2}\right)^{-1}$, $\mu_{da} = \frac{\beta_{d0}}{a_d v_0^3}$, $\gamma_d = \frac{1}{a_d}$ and $a_d = \left(\frac{V_{dn} \tau_n - 3}{v_0^4 + \mu_i - \mu_e \sigma_i^2}\right)$. As $V_{dn} > 0$, $\tau_n > 0$, $\beta_{d0} > 0$ and $v_0 > 0$, therefore, the sign of A , γ_d and μ_{da} are determined by the sign of a_d . Where $a_d = (V_{dn} \tau_n - 3)(\mu_i + \sigma_i \mu_e)^2 - \sigma_i^2 \mu_e + \mu_i = \mu_e \left[(V_{dn} \tau_n - 3) \sigma_i^2 \mu_e - \sigma_i^2 \right] + \mu_i^2 \left(V_{dn} \tau_n - 3 + \frac{Z_d n_{d0}}{n_{i0}} \right) + 2(V_{dn} \tau_n - 3) \mu_i \mu_e \sigma_i$. It is clear that for strongly coupled dusty plasma with a significant background of neutrals. In such kind of situation we have $V_{dn} \tau_n \gg 1$, i.e., $a_d > 0$, which corresponds to $A > 0$, which corresponds to $A > 0$, $\mu_{da} > 0$ and $\gamma_d > 0$. While for a weakly coupled dusty plasma or a collision-less dusty plasma $V_{dn} \tau_n \rightarrow 0$, we have $a_d < 0$, which corresponds to $A < 0$, $\mu_{da} < 0$ and $\gamma_d < 0$.

2.6.3 Dust Ion Acoustic Shock Waves

In this section we have to present the one dimensional dust DIA shocks in an unmagnetized dusty plasma. The governing non-linear equations which are normalized are given as

$$\frac{\partial N_i}{\partial T} + \frac{\partial(N_i V_i)}{\partial Z} = 0, \quad (2.96)$$

$$\frac{\partial V_i}{\partial T} + V_i \frac{\partial V_i}{\partial Z} = -\frac{\partial \Phi}{\partial Z} - 3\sigma_i N_i \frac{\partial N_i}{\partial Z} + \eta_i \frac{\partial^2 V_i}{\partial Z^2}, \quad (2.97)$$

and

$$\delta \frac{\partial^2 \Phi}{\partial Z^2} = \exp(\Phi) - \delta N_i + (\delta - 1). \quad (2.98)$$

In the following equations V_i is the ion fluid speed which is normalized by the ion acoustic speed C_s , Φ is the electrostatic wave potential which is normalized by $\frac{k_B T_e}{e}$

and $\eta_i = \frac{\delta\mu_d}{\omega_{pi}\lambda_{De}^2}$ (here μ_d is the kinematic viscosity). Here the time and space variables are in units of the ion plasma period ω_{pi}^{-1} and the electron Debye length $\frac{\lambda_{De}}{\sqrt{\delta}}$, respectively.

Now to derive the governing equation for DIA shock waves, we expand the dependent variables in the following manner

$$\mathcal{N}_i = 1 + \epsilon\mathcal{N}_i^{(1)} + \epsilon^2\mathcal{N}_i^{(2)} + \dots, \quad (2.99)$$

$$\mathcal{V}_i = \epsilon\mathcal{V}_i^{(1)} + \epsilon^2\mathcal{V}_i^{(2)} + \dots, \quad (2.100)$$

and

$$\phi = \epsilon\phi^{(1)} + \epsilon^2\phi^{(2)} + \dots \quad (2.101)$$

Introducing the stretched coordinates as

$$\xi = \epsilon^{\frac{1}{2}}(Z - \mathcal{V}_0T), \quad (2.102)$$

and

$$\tau = \epsilon^{\frac{3}{2}}T, \quad (2.103)$$

where ϵ is a small parameter characterizing the strength of the non-linearity or weakness of the amplitude or dispersion.

Now substituting equations (2.99) - (2.103) into equations (2.96) - (2.98), we obtained the following expressions from the lowest order of ϵ

$$\Phi^{(1)} = \delta\mathcal{N}_i^{(1)}, \quad (2.104)$$

$$V_i^{(1)} = \mathcal{V}_0\mathcal{N}_i^{(1)}, \quad (2.105)$$

where $\mathcal{V}_0 = (\delta + 3\sigma_i)^{\frac{1}{2}}$. And to the next higher order in ϵ , we get the following expressions

$$\frac{\partial\mathcal{N}_i^{(1)}}{\partial\tau} - \mathcal{V}_0\frac{\partial\mathcal{V}_i^{(2)}}{\partial\xi} + \frac{\partial}{\partial\xi}(\mathcal{N}_iV_i) + \frac{\partial\mathcal{V}_i^{(2)}}{\partial\xi} = 0, \quad (2.106)$$

$$\begin{aligned} \frac{\partial\mathcal{V}_i^{(1)}}{\partial\tau} - \mathcal{V}_0\frac{\partial\mathcal{V}_i^{(2)}}{\partial\xi} + \mathcal{V}_i^{(1)}\frac{\partial\mathcal{V}_i^{(1)}}{\partial\xi} = & -\frac{\partial\Phi^{(1)}}{\partial\xi} + \eta_{d0}\frac{\partial^2\mathcal{V}_i^{(1)}}{\partial\xi^2} \\ & - 3\sigma_i\mathcal{N}_i\frac{\partial\mathcal{N}_i^{(1)}}{\partial\xi} - 3\sigma_i\frac{\partial\mathcal{N}_i^{(2)}}{\partial\xi}, \end{aligned} \quad (2.107)$$

and

$$\delta \frac{\partial^2 \Phi^{(1)}}{\partial \xi^2} = \frac{1}{2} \Phi^{(1)2} + \Phi^{(2)} - \mathcal{N}_i^{(2)} \delta, \quad (2.108)$$

where we have assumed $\eta_i = \epsilon^{\frac{1}{2}} \eta_{i0}$. By eliminating the second order quantities from equations (2.106) - (2.108) and using the lower order equations in it, we obtained the following equations

$$\begin{aligned} \frac{1}{\delta} \frac{\partial \Phi^{(1)}}{\partial \tau} + \frac{2\mathcal{V}_0}{\sigma^2} \Phi^{(1)} \frac{\partial \Phi^{(1)}}{\partial \xi} &= 0, \\ \frac{\mathcal{V}_0}{\delta} \frac{\partial \Phi^{(1)}}{\partial \tau} + \left(\frac{\mathcal{V}_0^2}{\delta^2} + \frac{3\sigma_i}{\delta^2} \right) \Phi^{(1)} \frac{\partial \Phi^{(1)}}{\partial \xi} &= \frac{\eta_{i0} \mathcal{V}_0}{\delta} \frac{\partial^2 \Phi^{(1)}}{\partial \xi^2}, \end{aligned}$$

and

$$\delta \frac{\partial^3 \Phi^{(1)}}{\partial \xi^3} - \Phi^{(1)} \frac{\partial \Phi^{(1)}}{\partial \xi} = 0.$$

After a short algebraic manipulation one can get the following KdV Burger equation

$$\mathcal{A}^{-1} \frac{\partial \Phi^{(1)}}{\partial \tau} + \Phi^{(1)} \frac{\partial \Phi^{(1)}}{\partial \xi} + \beta_i \frac{\partial^3 \Phi^{(1)}}{\partial \xi^3} - \mu_i \frac{\partial^2 \Phi^{(1)}}{\partial \xi^2}. \quad (2.109)$$

Where $\mathcal{A} = \frac{a_i}{2\mathcal{V}_0}$, $\beta_i = \frac{\delta^2}{a_i}$, $\mu_i = \frac{\mathcal{V}_0 \eta_{i0}}{a_i}$ and $a_i = \frac{(3\delta - \delta^2 + 12\sigma_i)}{\delta}$. The sign of the coefficients \mathcal{A} , β_i and μ_i are determined by the sign of a_i .

Now, we have replace $\Phi^{(1)}$ with new variable y , so the solution of the KdV Burger equation (2.113) can also be written in the following form,

$$\mathcal{A}^{-1} \frac{\partial y}{\partial \tau} + y \frac{\partial y}{\partial \xi} + \beta \frac{\partial^3 y}{\partial \xi^3} = \mu \frac{\partial^2 y}{\partial \xi^2}. \quad (2.110)$$

Transform the space variables $\zeta = \xi - U_0 \tau$, where U_0 is the normalized velocity of the shock waves and find a third order ordinary differential equation for $y(\zeta)$, and can be integrated once, yields

$$\beta \frac{d^2 y}{d\zeta^2} - \mu \frac{dy}{d\zeta} + \frac{1}{2} y^2 - \frac{U_0}{\mathcal{A}} y = 0. \quad (2.111)$$

Where we have to imposed the appropriate boundary conditions, namely, $y \rightarrow 0$, $\frac{dy}{d\zeta} \rightarrow 0$, $\frac{d^2 y}{d\zeta^2} \rightarrow 0$ at $\zeta \rightarrow \infty$. Now, one can easily describe the shock wave whose velocity is U_0 and related to the extreme values, i.e., $y(-\infty) - y(\infty) = Y$ by $Y = \frac{2U_0}{\mathcal{A}}$. Therefore, in the rest frame the normalized the normalized velocity of the shock waves is $(1 + \frac{AY}{2})$. The nature of the shock structure depend on the relation between the dispersive and dissipative parameters β and μ .

We first considered a situation where the dissipative term is dominant over the dispersive term. In such case, we can express equation (2.111) as

$$\left(y - \frac{U_0}{\mathcal{A}}\right) \frac{dy}{d\zeta} = \mu \frac{d^2y}{d\zeta^2}. \quad (2.112)$$

Now, one can easily integrated the equation (2.112) and using the coordinate that y is bounded as $\zeta \rightarrow \pm\infty$, to obtained the following equation

$$y = \frac{U_0}{\mathcal{A}} \left[1 - \tanh \left(\frac{U_0}{2\mathcal{A}\mu} (\xi - U_0\tau) \right) \right]. \quad (2.113)$$

This equation represents a monotonic shock solution with the shock speed (U_0), the shock height ($\frac{U_0}{\mathcal{A}}$), and the shock thickness ($\frac{A\mu}{U_0}$). The solution of shock is appeared due to the dissipative term, which is proportional to the viscosity coefficient.

Now, we have to discuss the effects of the dispersive term on the shock solution of equation (2.111). When μ is very small, the shock wave will have an oscillatory profile in which the first few oscillations at the wave front will be close to solitons moving with velocity U_0 . And when μ is increased and it is larger than a certain critical value μ_c then shock wave will have a monotonic behaviour. To determine the values of the dissipation coefficient μ corresponding to monotonic or oscillatory shock profiles, we investigate the asymptotic behaviour of the solution of equation (2.111) for $\zeta \rightarrow -\infty$. Therefore, one can substitute $y(\zeta) = y_0 + y_1(\zeta)$, where $y_1 \ll y_0$, into equation (2.111) and after that linearized it with respect to y_1 in order to obtained

$$\beta \frac{\partial^2 y_1}{\partial \zeta^2} - \mu \frac{\partial y_1}{\partial \zeta} + \frac{U_0}{\mathcal{A}} y_1 = 0. \quad (2.114)$$

The solution of the equation (2.114) are proportional to $\exp(p_s x)$, where p_s is given by

$$p_s = \frac{\mu}{2\beta} \pm \left(\frac{\mu^2}{4\beta^2} - \frac{U_0}{\mathcal{A}\beta} \right)^{\frac{1}{2}}. \quad (2.115)$$

This equation turns out that the shock wave has a monotonic profile for $\mu > \mu_c$ and an oscillatory profile for $\mu < \mu_c$, where $\mu_c = \left(\frac{4\beta U_0}{\mathcal{A}} \right)^{\frac{1}{2}}$. Thus, for $\mu < \mu_c$, the stationary solution of equation (2.110) is

$$y = y_0 + H \exp\left(\frac{\zeta' \mu}{2\beta}\right) \cos\left(\zeta' \sqrt{\frac{U_0}{\mathcal{A}\beta}}\right), \quad (2.116)$$

where $\zeta' = \zeta - U_0\tau$ and H is constant.

Chapter 3

Linear and Non-linear Analysis of Dust Acoustic Waves in Electronegative Halley Comet Plasma

3.1 Introduction

Since the early 1990s, there has been a great deal of interest in studying the physics of dusty (or complex) plasmas. Interest in this area of plasma physics has grown considerably over the last two decades. A dusty plasma is a usual electron and ion plasma with an additional charged component of micron- or sub-micron sized particulates. This extra component, which increases the complexity of the system even further, is responsible for the name "complex plasma". This complexity comes from the fact that the dust grain charge, mass, and size vary with space and time. Dusty plasmas are ubiquitous in nebulas, in asteroid zones, in interstellar clouds, in the planetary magnetosphere, as well as in cometary environments (e.g., cometary comae and tails), on the surfaces of Mars and Earth's moon, and in the Earth's polar mesosphere [58][59][60][61]. Charged dust particles are also encountered in the plasma-assisted manufacturing of semiconductor devices and in fusion reactors like Tokamaks, where they are regarded as a serious contamination problem. Unique and novel features of dusty plasmas when compared with the usual electron and ion plasmas are the existence of a new, ultra-low frequency regime for wave propagation and the highly charging of the grains which can fluctuate due to the collection of plasma currents

onto the dust surface. Dust grains become charged due to different processes, such as a collection of charged particles from the surrounding plasma, photo-ionization, secondary electron emission, sputtering by energetic ions, etc. Because of the high charge and large mass of the grain particulates compared to those of ions, new time and space scales come into play, giving rise to either new or modified waves and instabilities in the dusty plasmas. Not only the existing low-frequency waves are modified [74] but also new types of low-frequency dust-related waves are introduced such as the dust acoustic (DA) mode (weak coupling regime) [75], the dust lattice (DL) mode (strong coupling regime) [76] and dust Bernstein-Greene-Kruskal modes [79]. The dust acoustic (DA) wave is the most well studied of such new modes. It arises due to the restoring force provided by the plasma thermal pressure electrons and ions while the inertia is due to the dust mass.

Numerous observations indicate the presence of non-thermal electron and ion structures as ubiquitous in a variety of space plasma environments and measurements of their distribution functions revealed them to be highly non-isothermal [66]. Such non-thermal populations may arise due to the effect of external forces acting on the natural space environment plasmas or to the wave and particle interaction, which ultimately lead to non-Maxwellian distributions. Some recent theoretical work has focused on the effects of non-thermal ions on the dust acoustic (DA) waves [67] [68]. In this work, we addressed the problem of arbitrary amplitude solitary dust acoustic (DA) waves in a charge varying dusty plasma with non-thermal ions. Our results showed that in such a plasma, large-amplitude spatially localized dust acoustic (DA) waves can exist. Their spatial patterns are significantly modified by the presence of the non-thermal ion component. In particular, we have noticed that an addition of a small concentration of non-thermal ions may abruptly reduce the potential pulse amplitude and increase the net negative charge residing on the dust grain surface. The purpose of this work is to examine the combined effects of an oblique magnetic field and ion non-thermality on weak dust acoustic (DA) waves in a charge varying electronegative dusty plasmas.

This chapter is further organized in such a way that physical assumptions and

formulation of the problem are given in section (ii). The basic equations of the plasma and their normalization scheme are mention in section (iii). The non-linear Korteweg-de Vries (KdV) Burger equation is calculated in section (iv). The nature of the steady-state solution of the Korteweg-de Vries (KdV) Burger equation is discussed in section (v). The Comet Halley's numerical results are discussed in section (vi).

3.2 Physical Assumptions

The physical assumptions will help to formulate the physical problem which will later be justified by numerical values related to Halley's comet. These assumptions will help us in the explicit form of final results. Therefore, based on the following physical assumptions we proceed with our calculations.

- The magnetized electronegative dusty plasma is homogeneous, collision-less, and unbounded. In the plasma, species are electrons with particle number density " n_e ", positive ions with particle number density " n_p ", negative ions with particle number density " n_n " and mobile negatively charged dust grains with particle number density " n_d ". The dust grains are negatively charged and the charge varies continuously with time, i.e., non-steady charge variation. The constant magnetic field (\mathcal{B}) lies in the " $x - z$ " plane making an angle θ with the x-axis and, therefore, the wave propagation vector lies along the x-axis.
- At far upstream, there is a plasma flow \mathcal{V}_0 in the x direction, that is the direction of wave wave propagation. In equilibrium state plasma is quasi-neutral and described by $\phi = 0$, $n_e = n_{e0}$, $n_p = n_{p0}$, $n_n = n_{n0}$, $n_d = n_{d0}$ and $q_d = -\mathcal{Z}_d e$. Where, the subscript "0" and " \mathcal{Z}_{d0} " are the unperturbed quantities and dust grain charge number, respectively. Therefore, the quasi-neutrality condition is

$$n_{p0} = n_{e0} + n_{n0} + \mathcal{Z}_d n_{d0}. \quad (3.1)$$

- On the dust time scale, the electrons and negative ions are assumed to be in thermal equilibrium, with the densities

$$n_e = n_{e0} \exp\left(\frac{e\phi}{T_e}\right),$$

$$n_n = n_{n0} \exp\left(-\frac{e\phi}{T_n}\right).$$

In the following expressions, ϕ is the electrostatic potential, n_j represents the number densities where j represents the electrons and negative ion species, T_j is the temperature of the plasma species (electrons and negative ions), n_{e0} and n_{n0} are the unperturbed densities of electron and negative ion. These densities are not normalized, so their normalized form can be expressed as

$$n_e = n_{e0} \exp(\Phi), \quad (3.2)$$

$$n_- = n_{n0} \exp\left(\frac{\Phi}{\sigma_n}\right), \quad (3.3)$$

where, $\Phi (= \frac{e\phi}{T_e})$ is normalized plasma potential.

Now, to model the fast non-thermal positive ion distribution, we refer to a possible three dimensional equilibrium state ion velocity distribution function that solves the collision-less Vlasov equation with a population of fast particles [70].

$$f_p(v) = f_p(v_x, v_y, v_z) = \frac{n_{p0}}{(1+3a)} \left(\frac{1}{2\pi\mathcal{V}_{tp}^2}\right)^{\frac{3}{2}} \left[1 + a \left(\frac{v_x^2}{\mathcal{V}_{tp}^2} + 2\frac{e\phi}{T_p}\right)^2\right] \exp\left(-\frac{v_x^2 + v_y^2 + v_z^2}{2\mathcal{V}_{tp}^2} - \frac{e\phi}{T_p}\right), \quad (3.4)$$

here "a" is a parameter determining the number of non-thermal positive ions or energetic positive ions present in our plasma model. And $\mathcal{V}_{tp} = \sqrt{\frac{K_B T_p}{m_p}}$ is the positive ion thermal velocity.

The particle number density of positive ion is also calculated from equation (3.4), which is in the form

$$n_p(\phi) = n_{p0} \left[1 + \mathcal{G} \left(\frac{e\phi}{T_p} + \left(\frac{e\phi}{T_p}\right)^2\right)\right] \exp\left(-\frac{e\phi}{T_p}\right), \quad (3.5)$$

where, $\mathcal{G} = \frac{4a}{1+3a}$. Here one can note that to justify the validity of our theoretical model, we take a small deviation from the isothermal (Boltzmann) case ($a = 0$) for the positive ions, i.e., $0 < a < 0.15$.

- Here we presume that the dust grain having radius r_d is very much smaller than that of the electron gyro-radius ρ_e [69]. And the flow velocity of the dust is very less than the thermal velocities \mathcal{V}_{tj} , i.e., $\mathcal{V}_0 \ll \mathcal{V}_{tj}$, where j represents the plasma species, which is in our system be the electrons, positive ion and negative ion. As it has been pointed out by Taibany and Sabry [79], where the assumption, i.e., $r_d \ll \rho_e$ may be appropriate for a laboratory plasma that is used in weak magnetic fields. However, in the presence of a very strong magnetic field, the orbits of the magnetized plasma particles are confined to one dimension along the field lines, and thus the perturbed field does not come into play, and the problem of charging currents becomes independent of the magnetic field. The electron, negative ion, and positive ion charging currents, i.e., I_e , I_n and I_p for spherical dust grain with radius r_d are given by

$$I_e = J_e \exp\left[\Phi + Z(Q - 1)\right], \quad (3.6)$$

$$I_n = J_n \exp\left[\frac{\Phi + Z(Q - 1)}{\sigma_n}\right], \quad (3.7)$$

and

$$I_p = J_p \frac{1}{1 + 3a} \left\{ 1 + \frac{24a}{5} + \frac{16a}{3} \frac{\Phi}{\sigma_p} + 4a \frac{\Phi^2}{\sigma_p^2} - \frac{Z(Q - 1)}{\sigma_+} \left(1 + \frac{8a}{5} \frac{8a}{3} \frac{\Phi}{\sigma_p} + 4a \frac{\Phi^2}{\sigma_p^2} \right) \right\} \exp\left(-\frac{\Phi}{\sigma_p}\right) \quad (3.8)$$

where, $J_s = \pi r_0^2 e n_{s0} \sqrt{\frac{8T_s}{m_s}}$. In this expressions m_s , T_s are the mass of the sth plasma species and temperature of the sth plasma species. And "a" determining the number of non-thermal positive ions. And Z can be expressed as

$$Z = \frac{Z_{d0} e^2}{4\pi \epsilon_0 r_0 T_e},$$

where $4\pi \epsilon_0 r_0$ is the capacitance of spherical dust grain. And dust charge can be expressed as

$$q_d = q_d^{ed} + \delta q_d, \quad (3.9)$$

where $q_d^{ed}(= -Z_{d0}e)$ and δq_d are equilibrium dust charge and fluctuating dust charge, respectively. Therefore, the equation (3.9) becomes,

$$\begin{aligned} q_d &= -Z_{d0}e + \delta q_d, \\ \frac{q_d}{Z_{d0}e} &= -1 + \frac{\delta q_d}{Z_{d0}e}, \\ \frac{q_d}{Z_{d0}e} &= Q - 1, \end{aligned}$$

here, $Q = \frac{\delta q_d}{Z_{d0}e}$ which is normalized in units of equilibrium dust charge. Here and in the following $\Phi = \frac{e\phi}{T_e}$ is the normalized electrostatic potential, $\sigma_p = \frac{T_p}{T_e}$ and $\sigma_n = \frac{T_n}{T_e}$.

- Dust oscillation frequency ω_{pd} has a value, i.e., $\omega_{pd} = \sqrt{\frac{Z_{d0}^2 e^2 n_{d0}}{\epsilon_0 m_d}}$. And the ratio of dust oscillation frequency (ω_{pd}) to dust charging frequency (ν_{ch}) is finite, i.e., $\omega_{ch} = \frac{\omega_{pd}}{\nu_{ch}}$ is finite, i.e., $\omega_{ch} \sim O(1)$. Which is in contrast to the assumption that ω_{ch} is small but $\neq 0$, i.e., $\omega_{ch} \sim 0(\sqrt{\epsilon})$, where ϵ is the usual expansion parameter. While on the other hand, because of weak magnetic field, the ratio of dust cyclotron frequency $\Omega_d(= \frac{Z_{d0}eB_0}{m_d})$ to ω_{pd} , i.e., $\omega_{cd} = \frac{\Omega_d}{\omega_{pd}}$ is small but $\neq 0$, i.e., $\omega_{cd} \sim 0(\sqrt{\epsilon})$. Which is in contrast to assumption $\omega_{cd} \sim 0(1)$.

3.3 Model Equations

We considered homogeneous and collision-less magnetized dusty plasma comprising of electrons, and negative ions modeled via Boltzmann distribution and positive ions are modeled via Cairns distribution. The applied external magnetic field is such that $\mathcal{B} = \mathcal{B}_0 \cos \theta \hat{x} + \mathcal{B}_0 \sin \theta \hat{z}$ and the relative dust fluid velocity $\mathcal{V}_d(x) = \mathcal{V}_{dx} \hat{x} + \mathcal{V}_{dy} \hat{y} + \mathcal{V}_{dz} \hat{z}$. In order to make our equations dimensionless we have to normalized the continuity, momentum and Poisson's equations. And the nonlinear dynamics of low phase velocity DAW are governed by the normalized equations.

The normalization scheme is introduced as

$$\begin{aligned} \text{Time (t)} &\rightarrow \omega_{pd}^{-1} = \left(\frac{Z_{d0}^2 e^2 n_{d0}}{\epsilon_0 m_d} \right)^{-\frac{1}{2}}, \text{ Space parameter (x)} \rightarrow \lambda_D = \left(\frac{T_e}{4\pi e^2 \gamma n_{p0}} \right)^{\frac{1}{2}}, N_d \rightarrow \frac{n_d}{n_{d0}} \\ \text{and } v_d &\rightarrow C_d = \left(\frac{Z_{d0} T_e \alpha_d}{m_d} \right)^{\frac{1}{2}}. \text{ And electrostatic wave potential } \phi \rightarrow \frac{K_B T_i}{e}. \end{aligned}$$

During normalization we have $N_d = \frac{n_d}{n_{d0}}$, $\delta_d = \frac{T_d}{Z_{d0}T_e}$, $\Delta = 1 - \delta_p - \delta_n$, $\delta_p = \frac{n_{e0}}{n_{p0}}$, $\delta_n = \frac{n_{n0}}{n_{p0}}$, $\alpha_d = \frac{Z_{d0}n_{d0}}{\gamma n_{p0}}$ and $\gamma = \left(\delta_p + \frac{1}{\sigma_p} + \frac{\delta_n}{\sigma_n}\right)$. The dust particles are modeled via adiabatic pressure, i.e., $p_d = p_{d0}\left(\frac{n_d}{n_{d0}}\right)^{\gamma_d}$, where $\gamma_d = \frac{N+2}{N}$ such that N stand for the degree of freedom. For one dimensional case $N = 1$ and $\gamma_d = 3$. The equilibrium dust pressure is define as $p_{d0} = n_{d0}T_d$. Where T_d is dust temperature and γ_d is adiabatic index.

The set of equations which we have to deal with:

Continuity equation:

$$\frac{\partial n_d}{\partial t} + \vec{\nabla} \cdot (n_d \vec{v}_d) = 0.$$

Equation of motion:

$$m_d n_d \left[\frac{\partial \vec{v}_d}{\partial t} + (\vec{v}_d \cdot \vec{\nabla}) \vec{v}_d \right] = q_d n_d \left[-\vec{\nabla} \phi + \vec{v}_d \times \vec{\mathcal{B}} \right] - \vec{\nabla} p_d. \quad (3.10)$$

And the system is closed by Poisson's equation, i.e.,

$$\epsilon_0 \nabla^2 \phi = en_e + en_n - en_p - q_d n_d. \quad (3.11)$$

After a short algebraic manipulations one can get the following normalized equations.

$$\frac{\partial N_d}{\partial T} + \frac{\partial}{\partial X} (N_d \mathcal{V}_{dx}) = 0. \quad (3.12)$$

$$\frac{\partial}{\partial T} \mathcal{V}_{dx} + \mathcal{V}_{dx} \frac{\partial}{\partial X} \mathcal{V}_{dx} = -(Q-1) \left[\frac{1}{\alpha_d} \frac{\partial \Phi}{\partial X} - \omega_{cd} \mathcal{V}_{dy} \sin \theta \right] - \frac{\gamma_d \sigma_d}{\alpha_d} N_d^{\gamma_d-2} \frac{\partial}{\partial X} N_d. \quad (3.13)$$

or

$$\frac{\partial}{\partial T} \mathcal{V}_{dy} + \mathcal{V}_{dx} \frac{\partial}{\partial X} \mathcal{V}_{dy} = (Q-1) \omega_{cd} [\mathcal{V}_{dz} \cos \theta - \mathcal{V}_{dx} \sin \theta]. \quad (3.14)$$

or

$$\frac{\partial}{\partial T} \mathcal{V}_{dz} + \mathcal{V}_{dx} \frac{\partial}{\partial X} \mathcal{V}_{dz} = -(Q-1) \omega_{cd} (\mathcal{V}_{dy} \cos \theta). \quad (3.15)$$

and

$$\gamma \frac{\partial^2}{\partial X^2} = \delta_p \exp(\Phi) + \delta_n \exp\left(\frac{\Phi}{\sigma_n}\right) - \Delta(Q-1)N_d - \exp\left(-\frac{\Phi}{\sigma_p}\right) - \left[\mathcal{G}\left(\frac{\Phi}{\sigma_p} + \frac{\Phi^2}{\sigma_p^2}\right)\right] \exp\left(-\frac{\Phi}{\sigma_p}\right). \quad (3.16)$$

Normalized charged variable Q is determined by the charging equation:

$$\frac{dq_q}{dt} = \sum_{s=p,n,e} I_s, \quad (3.17)$$

$$\frac{dq_q}{dt} = I_p + I_n + I_e. \quad (3.18)$$

The normalized form of this equation is

$$\omega_{ch} \frac{dQ}{dT} = \frac{\sigma_p \beta_{ch}}{(1 + \sigma_p + \bar{\gamma}_2)} \left[\frac{1}{1 + 3a} \left\{ \left(1 - \frac{\mathcal{Z}Q}{\mathcal{Z} + \sigma_p}\right) \left(1 + \frac{8a}{5} + \frac{8a}{3} \frac{\Phi}{\sigma_p} + 4a \frac{\Phi^2}{\sigma_p^2}\right) + \frac{\sigma_p}{(\mathcal{Z} + \sigma_p)} \left(\frac{16a}{5} + \frac{8a}{3} \frac{\Phi}{\sigma_p}\right) \right\} \times \exp\left(-\frac{\Phi}{\sigma_p}\right) - A_p \exp(\Phi + \mathcal{Z}Q) - A_n \exp\left(\frac{\Phi + \mathcal{Z}Q}{\sigma_n}\right) \right], \quad (3.19)$$

where $\omega_{ch} = \frac{\omega_{pd}}{\nu_{ch}}$, and

$$\nu_{ch} = \frac{r_d}{\sqrt{2\pi}} \frac{\omega_{pp}^2}{\mathcal{V}_{tp}} \frac{\mathcal{Z} + \sigma_p}{\mathcal{Z}} \left[\frac{(1 + \sigma_p + \bar{\gamma}_2)}{\sigma_p \beta_{ch}} + \frac{a}{1 + 3a} \frac{7\mathcal{Z}}{5(\mathcal{Z} + \sigma_p)} \right],$$

$$\beta_{ch} = \frac{(\mathcal{Z} + \sigma_p)(1 + \sigma_p + \bar{\gamma}_2)}{\mathcal{Z}\sigma_p(1 + \mathcal{Z} + \sigma_p + \bar{\gamma}_1)},$$

$$\bar{\gamma}_1 = \frac{(\mathcal{Z} + \sigma_p)}{\mathcal{Z}} \left[\mathcal{Z}A_p + \mathcal{Z} \frac{A_n}{\sigma_n} + \frac{1}{1 + 3a} \left(1 + \frac{8a}{5}\right) \frac{\mathcal{Z}}{\mathcal{Z} + \sigma_p} \right] - 1 - \sigma_p - \mathcal{Z},$$

$$\bar{\gamma}_2 = \sigma_p \left[A_p + \frac{A_n}{\sigma_n} - \frac{1}{1 + 3a} \left(-\frac{1}{\sigma_p} + \frac{16a}{15\sigma_p} \left(\frac{1}{2} + \frac{\sigma_p}{\mathcal{Z} + \sigma_p}\right) \right) \right] - 1 - \sigma_p,$$

$$A_p = \frac{\delta_p \exp(-\mathcal{Z})}{(\mathcal{Z} + \sigma_p)} \left(\frac{\sigma_p m_p}{m_e}\right)^{\frac{1}{2}},$$

$$A_n = \frac{\delta_n \exp\left(\frac{-\mathcal{Z}}{\sigma_n}\right)}{(\mathcal{Z} + \sigma_p)} \left(\frac{\sigma_n \sigma_p m_p}{m_n}\right)^{\frac{1}{2}}.$$

At equilibrium the current balance equation, i.e., $\sum_{s=p,n,e} I_s = 0$, which yields

$$A_p = -A_n + \frac{1}{1 + 3a} \left(1 + \frac{8a}{5} + \frac{16a}{5} \frac{\sigma_p}{\mathcal{Z} + \sigma_p}\right). \quad (3.20)$$

Here one can also obtain the Maxwellian expression in the limit $a \rightarrow 0$.

3.4 Linear Analysis

In this section, we proceed toward the linear analysis of the problem. Generally, we cannot speculate that the non-linear coupling of frequencies will be missing. Although, if we limit ourselves to the situations, in which the oscillations are small and when we considered small amplitude waves, then we can linearize our model equations. After that, we look at the first-order expansion of equations in the term of small perturbation ignoring second and higher-order terms. Therefore, when two oscillating quantities are multiply even both are so small, we considered this as higher-order and neglect it.

3.4.1 DAWs in the Absence of Dust Charge Fluctuations

In dusty plasma, either we consider the dust charge fluctuation or not under certain conditions. When the dust charging frequency is very large as compared to dust acoustic frequency, then we take constant dust charge because the perturbation frequency cannot feel the dust charging effects. While on the other hand, when the dust charging frequency and dust acoustic frequency is comparable then we tackle the dust charge fluctuation.

Under the same physical assumptions except for the dust charge fluctuation, we obtained the following equation.

$$\mathcal{W}_D^4 - \mathcal{O}_i \mathcal{W}_D^2 + \mathcal{A}_3 \mathcal{D}_i k = 0, \quad (3.21)$$

where

$$\mathcal{O}_i = \mathcal{D}_i k + \mathcal{A}_3^2 + \mathcal{A}_1^2,$$

$$\mathcal{D}_i = \mathcal{A}_2 k + \frac{k \Delta}{\alpha_d \mathcal{F}_i} = 0,$$

$$\mathcal{F}_i = \gamma k^2 + \gamma - \frac{\mathcal{G}}{\sigma_p},$$

$$\mathcal{A}_1 = \omega_{cd} \sin \theta,$$

$$\mathcal{A}_2 = \frac{\sigma_d \gamma_d}{\alpha_d},$$

$$\mathcal{A}_3 = \omega_{cd} \cos \theta,$$

and $\mathcal{W}_D = \omega - k\mathcal{V}_0$ also known as a Doppler frequency. Now, by using quadratic formula, we get the following expression

$$\mathcal{W}_D^2 = \mathcal{I}_1, \quad (3.22)$$

and

$$\mathcal{W}_D^2 = \mathcal{I}_2. \quad (3.23)$$

Where in equations (3.22) and (3.23), we have

$$\mathcal{I}_1 = \frac{1}{2} \left[\mathcal{O}_i + \sqrt{\mathcal{O}_i^2 - 4\mathcal{A}_3^2 \mathcal{D}_i k} \right],$$

and

$$\mathcal{I}_2 = \frac{1}{2} \left[\mathcal{O}_i - \sqrt{\mathcal{O}_i^2 - 4\mathcal{A}_3^2 \mathcal{D}_i k} \right].$$

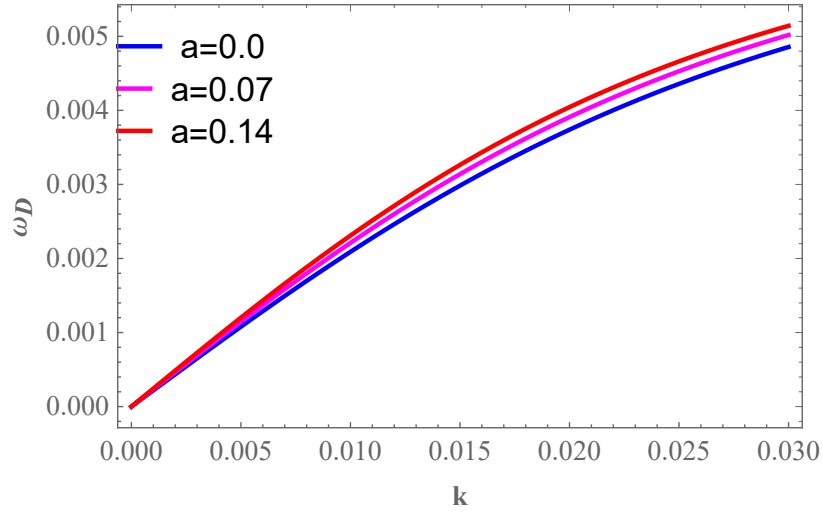


Figure 3.1: Variation of Doppler frequency (ω_D) against wave number (k) for different value of non-thermal parameter " a ".

3.4.2 Growth Rate

For the growth rate of a specific wave mode we have

$$\mathcal{W}_D^2 - \mathcal{I}_2 = 0,$$

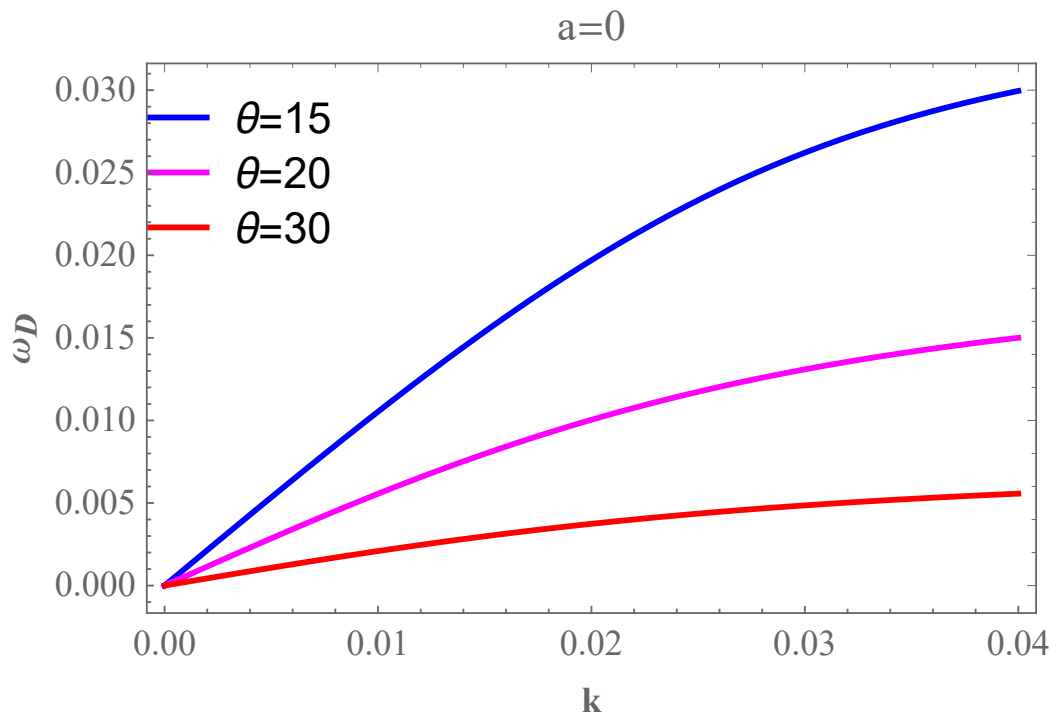


Figure 3.2: Variation of Doppler frequency (ω_D) against wave number (k) for different value of obliqueness of the magnetic field θ .

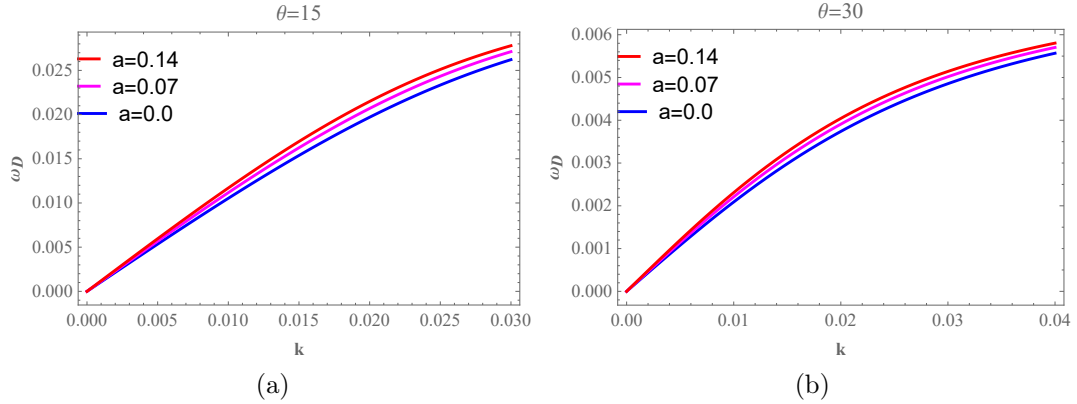


Figure 3.3: Variation of Doppler frequency (ω_D) against wave number (k) for different value of non-thermal parameter "a" at fixed obliqueness of magnetic field θ . The left panel represents $\theta = 5$ and the right panel represents $\theta = 30$.

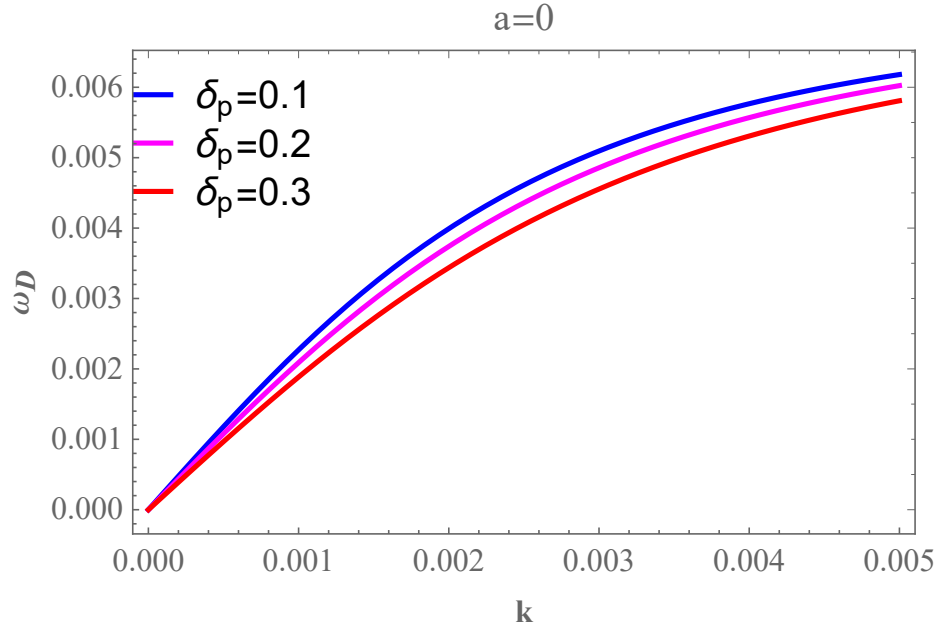


Figure 3.4: The profile of Doppler frequency (ω_D) against wave number (k) for different value of density ratio δ_p . The other parameters are $\theta = 30$ and $a = 0$.

Now, putting the value of \mathcal{W}_D and introduce $\omega = \omega_r + \iota\mathcal{X}$, we get the following equation

$$\omega_r^2 - \mathcal{X}^2 + 2\iota\omega_r\mathcal{X} - 2\omega_r k\mathcal{V}_0 - 2\iota\mathcal{X}k\mathcal{V}_0 + \mathcal{C}_i = 0,$$

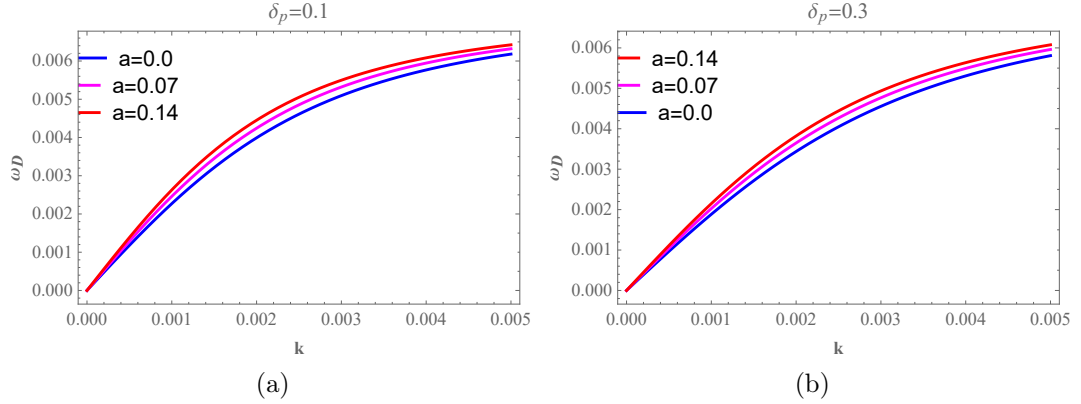


Figure 3.5: The behavior of Doppler frequency (ω_D) versus wave number (k) for different values of non-thermal parameter "a" with fixed density ratio δ_p . The left panel shows $\delta_p = 0.1$ and right panel shows $\delta_p = 0.3$.

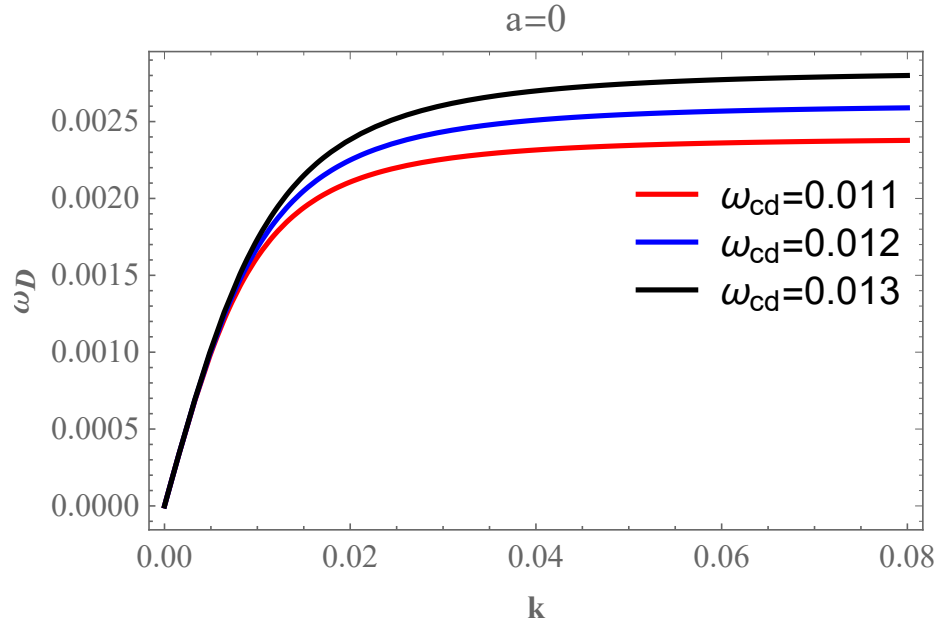


Figure 3.6: The profile of Doppler frequency (ω_D) against wave number (k) for different value of normalized dust cyclotron frequency ω_{cd} . The other parameters are $\theta = 30$ and $a = 0$.

where $C_i = k^2 \mathcal{V}_0^2 - \mathcal{I}_1$. Therefore, for \mathcal{I}_1 the growth rate is

$$\mathcal{X}_2 = \pm \frac{1}{2} \left[\sqrt{-\mathcal{O}_i - (\mathcal{O}_i^2 - 4\mathcal{A}_3^2 \mathcal{D}_i k)^{\frac{1}{2}}} \right]. \quad (3.24)$$

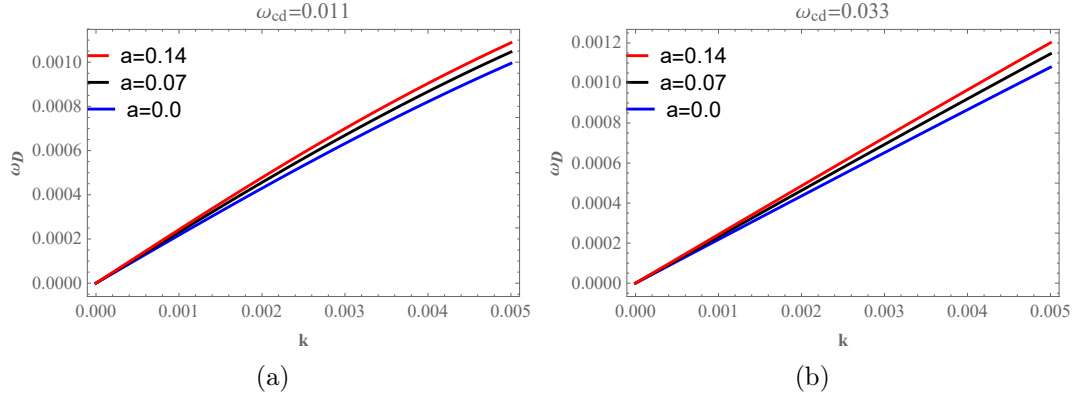


Figure 3.7: The profile of Doppler frequency (ω_D) against wave number (k) for different values of non-thermal parameter " a " with fixed normalized dust cyclotron frequency ω_{cd} . The left panel shows the $\omega_{cd} = 0.011$ and right panel shows the $\omega_{cd} = 0.033$.

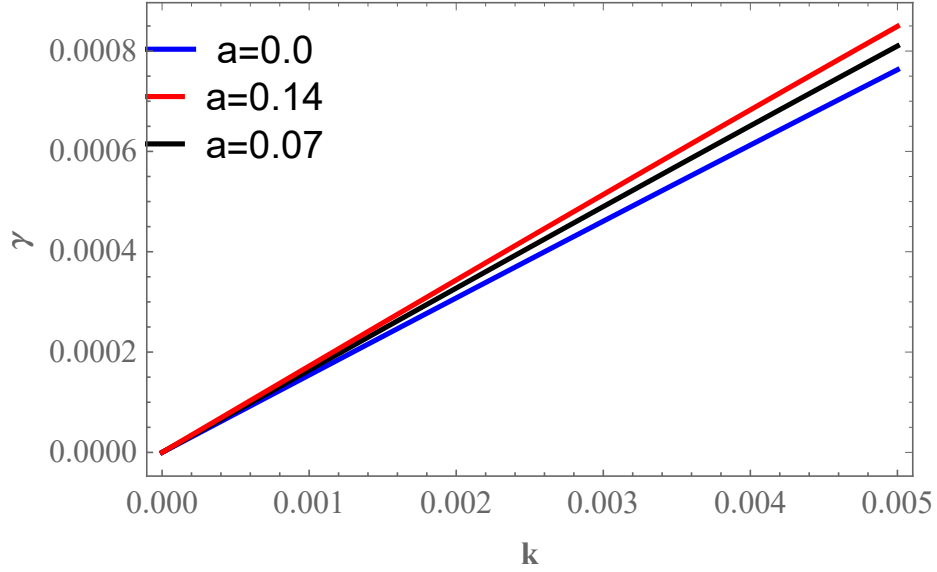


Figure 3.8: Plot of growth rate (γ) as a function of wave number (k) for different values of non-thermal parameter " a ".

Similarly, for \mathcal{I}_2 where $\mathcal{C}_i = k^2 \mathcal{V}_0^2 - \mathcal{I}_2$, we have the following expression

$$\mathcal{X}_1 = \pm \frac{1}{2} \left[\sqrt{(\mathcal{O}_i^2 - 4\mathcal{A}_3^2 \mathcal{D}_i k)^{\frac{1}{2}} - \mathcal{O}_i} \right]. \quad (3.25)$$

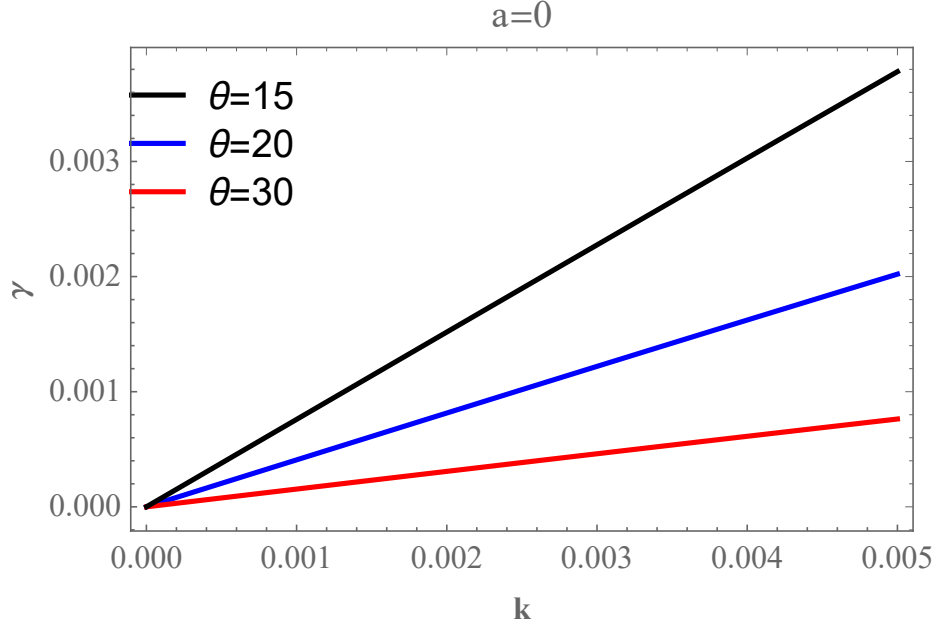


Figure 3.9: Plot of growth rate (γ) as a function of wave number (k) for different values of magnetic field obliqueness θ .

3.4.3 DAWs in the Presence of Dust Charge Fluctuations

In this section of linear analysis, we take dust charge fluctuations. As we take dust charge fluctuations which means that the dust charging frequency and dust acoustic frequency is comparable.

Under the same physical assumptions including the dust charge fluctuations, we obtained the following expression

$$\mathcal{W}_D^4 - \mathcal{T}_i \mathcal{W}_D + \mathcal{E}_i = 0, \quad (3.26)$$

where

$$\mathcal{E}_i = \mathcal{A}_2 \mathcal{A}_3^2 k^2 - \frac{\mathcal{A}_3^2 k^2 \Delta}{\alpha_d \left(\frac{\Delta \mathcal{J}_i}{\mathcal{H} - i\mathcal{U}} - \mathcal{F}_i \right)},$$

$$\mathcal{T}_i = \mathcal{A}_3^2 + \mathcal{A}_1^2 + \mathcal{A}_2 k^2 - \frac{k^2 \Delta}{\alpha_d \left(\frac{\Delta \mathcal{J}_i}{\mathcal{H} - i\mathcal{U}} - \mathcal{F}_i \right)},$$

$$\mathcal{H} = \frac{\mathcal{Z}}{(1+3a)(\mathcal{Z} + \sigma_p)} + \frac{8a\mathcal{Z}}{5(1+3a)(\mathcal{Z} + \sigma_p)} + A_p \mathcal{Z} + \frac{A_n \mathcal{Z}}{\sigma_n},$$

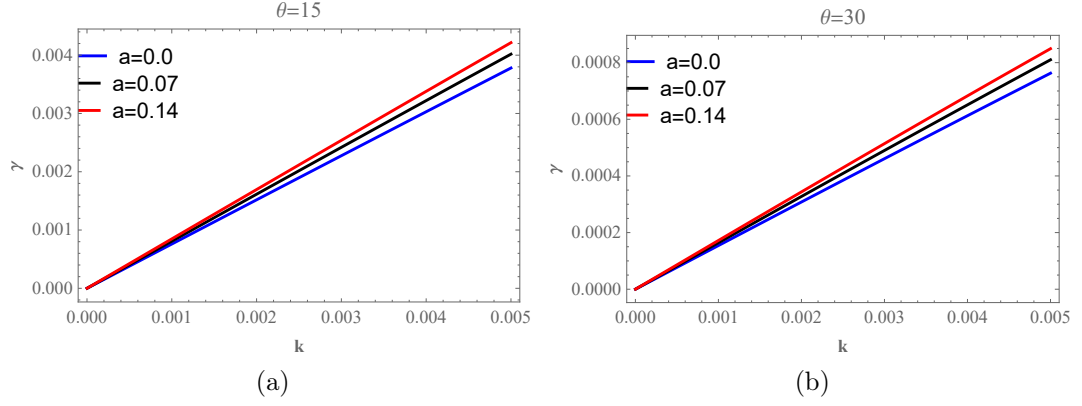


Figure 3.10: The behavior of growth rate (γ) against wave number (k) for different value of non-thermal parameter " a " with fixed magnetic field obliqueness θ . The left panel shows $\theta = 15$ and right panel shows $\theta = 30$.

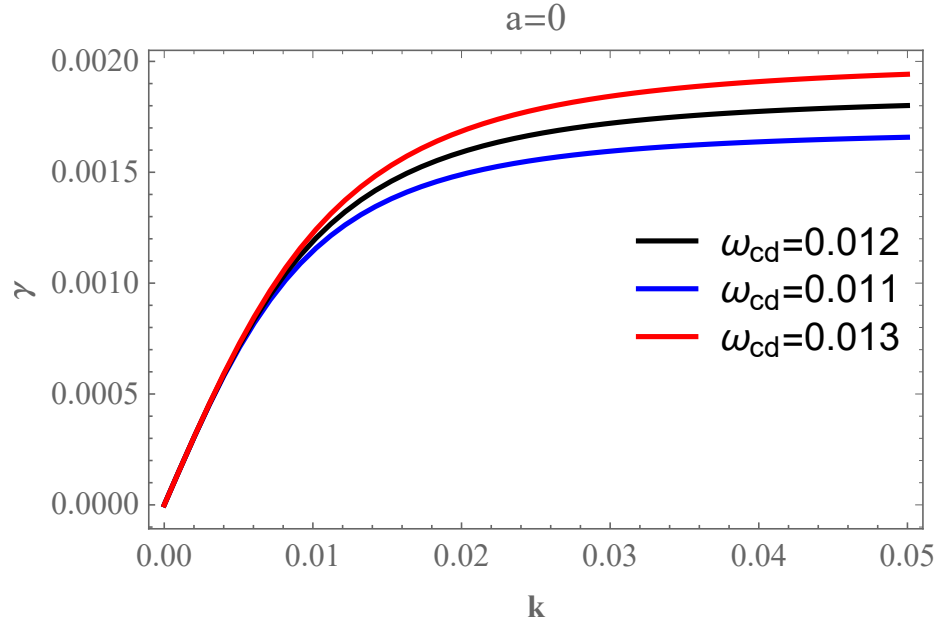


Figure 3.11: The variation of growth rate (γ) versus wave number (k) for different values of normalized dust cyclotron frequency ω_{cd} .

$$\mathcal{J}_i = \frac{8a}{3\sigma_p(1+3a)} - \frac{1}{\sigma_p(1+3a)} - \frac{8a}{5\sigma_p(1+3a)} + \frac{8a}{3(\mathcal{Z} + \sigma_p)(1+3a)},$$

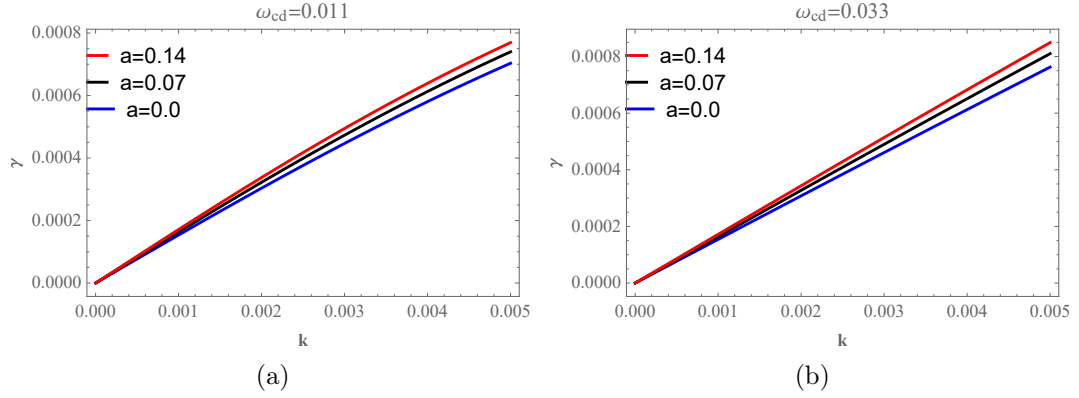


Figure 3.12: The variation of growth rate (γ) as a function of wave number (k) for different values of non-thermal parameter "a" at fixed normalized dust cyclotron frequency ω_{cd} . The left panel shows $\omega_{cd} = 0.011$ and the right panel shows $\omega_{cd} = 0.033$.

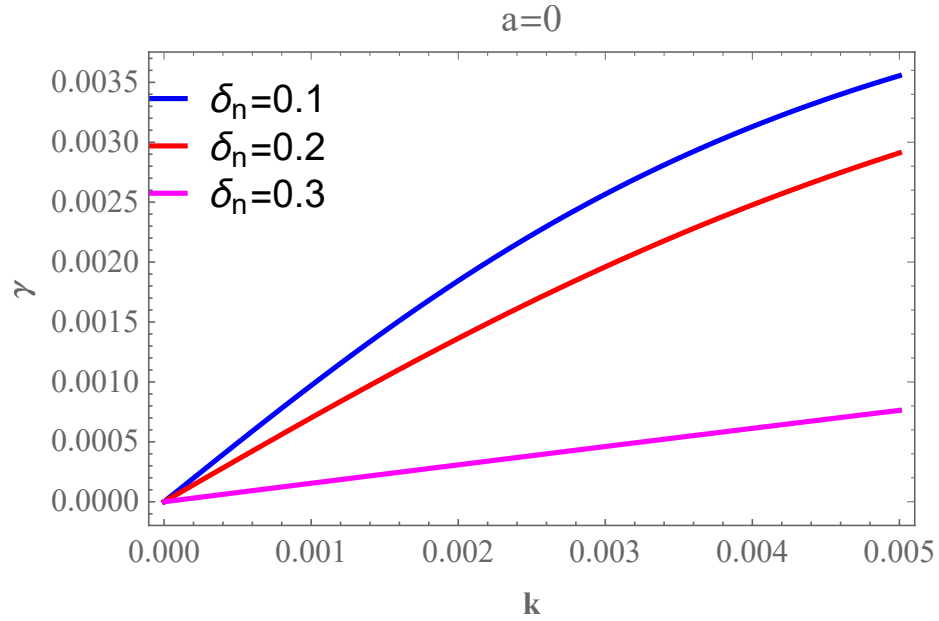


Figure 3.13: Plot of growth rate (γ) versus wave number (k) for different values of density ratio δ_n .

and

$$\mathcal{U} = \frac{\omega\omega_{ch}(1 + \sigma_p + \bar{\gamma}_2)}{\sigma_p\beta_{ch}}.$$

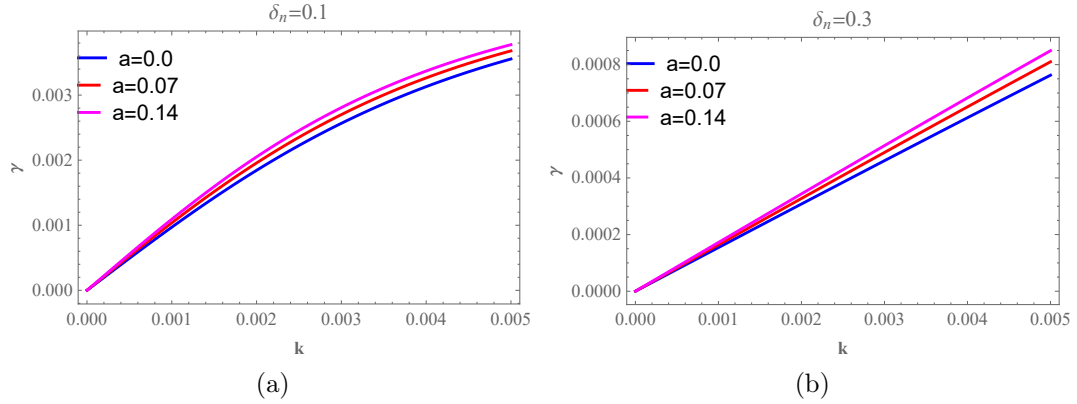


Figure 3.14: The behavior of growth rate (γ) versus wave number (k) for different values of non-thermal parameter "a" at fixed density ratio δ_n . The left plot shows $\delta_n = 0.1$ and the right plot shows $\delta_n = 0.3$.

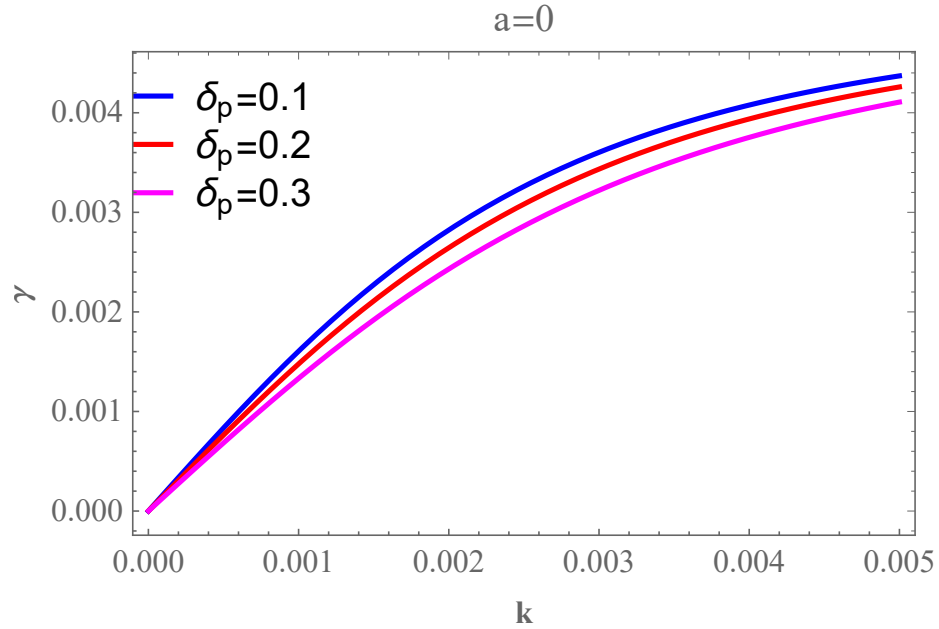


Figure 3.15: The profile of growth rate (γ) against wave number (k) for different value of density ratio δ_p . The other parameters are $\theta = 30$ and $a = 0$.

3.5 Derivation of Non-linear Evaluation Equation

In this section, we proceed toward the study of small but finite amplitude nonlinear dust acoustic waves using the standard Reductive Perturbation Technique (RPT).

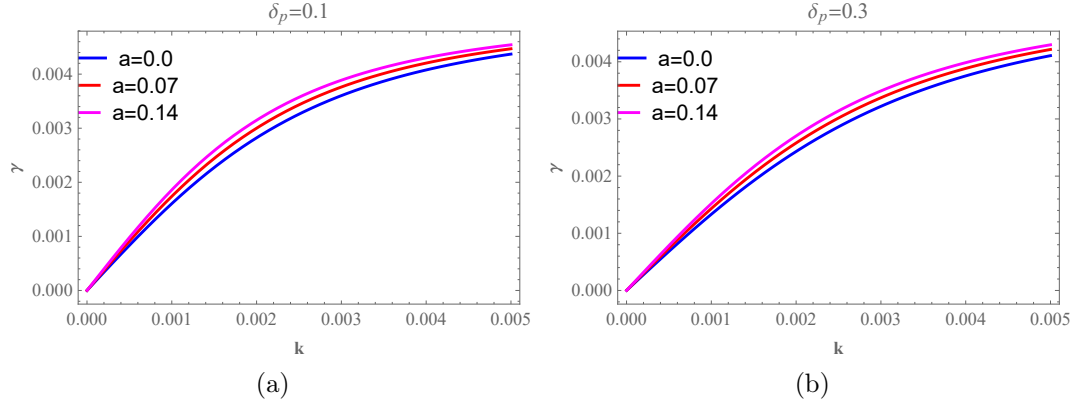


Figure 3.16: The profile of growth rate (γ) versus wave number (k) for different value of non-thermal parameter "a" at fixed density ratio δ_p . The left panel shows $\delta_p = 0.1$ and the right panel shows $\delta_p = 0.3$.

The independent variables are stretched as:

$$\xi = \epsilon(X - V_{ph}T), \quad (3.27)$$

and

$$\tau = \epsilon^2 T. \quad (3.28)$$

In equation (3.27), V_{ph} represents the normalized phase velocity of linear dust acoustic wave (DAW). And ϵ is a small parameter characterizing the strength of the non-linearity or weakness of the amplitude or dispersion.

The independent variable by using chain rule are stretched as:

$$\begin{aligned} \frac{\partial}{\partial T} &= \frac{\partial}{\partial \xi} \frac{\partial \xi}{\partial T} + \frac{\partial}{\partial \tau} \frac{\partial \tau}{\partial T}, \\ &= \frac{\partial}{\partial \xi} \frac{\partial}{\partial T} \epsilon(X - V_{ph}T) + \frac{\partial}{\partial \tau} \frac{\partial}{\partial T} \epsilon^2 T, \\ &= \epsilon^2 \frac{\partial}{\partial \tau} - \epsilon V_{ph} \frac{\partial}{\partial \xi}. \end{aligned} \quad (3.29)$$

And

$$\begin{aligned}
\frac{\partial}{\partial X} &= \frac{\partial}{\partial \xi} \frac{\partial \xi}{\partial X} + \frac{\partial}{\partial \tau} \frac{\partial \tau}{\partial X}, \\
&= \frac{\partial}{\partial \xi} \frac{\partial}{\partial X} \epsilon (X - V_{ph} T) + \frac{\partial}{\partial \tau} \frac{\partial}{\partial X} \epsilon^2 T, \\
&= \epsilon \frac{\partial}{\partial \xi}.
\end{aligned} \tag{3.30}$$

The dynamical variables are expanded in the power series of ϵ as follow:

$$f = f_0 + \epsilon f^{(1)} + \epsilon^2 f^{(2)} + \epsilon^3 f^{(3)} + \dots, \tag{3.31}$$

and

$$\mathcal{V}_{dy} = \epsilon^{\frac{3}{2}} \mathcal{V}_{dy}^{(1)} + \epsilon^{\frac{5}{2}} \mathcal{V}_{dy}^{(2)} + \dots \tag{3.32}$$

In equation (3.31) f shows the some dynamical variables, i.e., $f = N_d, \mathcal{V}_{dx}, \mathcal{V}_{dz}, \Phi$ and Q . Where $f^{(0)} = 1$ for N_d , $f^{(0)} = \mathcal{V}_0$ for \mathcal{V}_{dx} and $f^{(0)} = 0$ for \mathcal{V}_{dz}, Φ and Q , respectively. It is also noted that stretching expressions for velocity variables $\mathcal{V}_{dx}, \mathcal{V}_{dy}$ and \mathcal{V}_{dz} in term of ϵ have been chosen following Kakutani and Ono [71].

Thus dependent variable can be expanded in the following fashion.

$$\begin{aligned}
N_d &= 1 + \epsilon N_d^{(1)} + \epsilon^2 N_d^{(2)} + \epsilon^3 N_d^{(3)} + \dots, \\
\mathcal{V}_{dx} &= \mathcal{V}_0 + \epsilon \mathcal{V}_{dx}^{(1)} + \epsilon^2 \mathcal{V}_{dx}^{(2)} + \epsilon^3 \mathcal{V}_{dx}^{(3)} + \dots, \\
\mathcal{V}_{dz} &= \epsilon \mathcal{V}_{dz}^{(1)} + \epsilon^2 \mathcal{V}_{dz}^{(2)} + \epsilon^3 \mathcal{V}_{dz}^{(3)} + \dots, \\
\Phi &= \epsilon \Phi^{(1)} + \epsilon^2 \Phi^{(2)} + \epsilon^3 \Phi^{(3)} + \dots, \\
Q &= \epsilon Q^{(1)} + \epsilon^2 Q^{(2)} + \epsilon^3 Q^{(3)} + \dots, \\
V_{dy} &= \epsilon^{\frac{3}{2}} V_{dy}^{(1)} + \epsilon^{\frac{5}{2}} V_{dy}^{(2)} + \dots.
\end{aligned} \tag{3.33}$$

Due to the assumption (v) for consistent perturbation expansion, it is assumed that,

$$\omega_{ch} = \frac{\Omega_d}{\omega_{pd}} = O(\sqrt{\epsilon}). \tag{3.34}$$

Now, substituting Eqs. (3.29), (3.30) and (3.33) in Eqs. (3.12), (3.13), (3.14), (3.15), (3.16) and (3.19).

We obtained the following relations in the lowest power of ϵ :

$$\mathcal{V}_{dx}^{(1)} = -\Lambda N_d^{(1)}, \quad (3.35)$$

$$\mathcal{V}_{dz}^{(1)} = -\tan \theta N_d^{(1)}, \quad (3.36)$$

$$\mathcal{V}_{dy}^{(1)} = -\frac{\Lambda^2 \sin \theta \sec^2 \theta}{\omega_{cd}} \frac{\partial N_d^{(1)}}{\partial \xi}, \quad (3.37)$$

$$\Phi^{(1)} = \alpha_d \left(-\Lambda^2 \sec^2 \theta + \frac{\gamma_d \sigma_d}{\alpha_d} \right), \quad (3.38)$$

$$Q^{(1)} = \beta_{ch} \alpha_d \left(\Lambda^2 \sec^2 \theta - \frac{\gamma_d \sigma_d}{\alpha_d} \right) N_d^{(1)}. \quad (3.39)$$

From the comparison of Poisson's equation, we obtained a relation

$$\begin{aligned} & \frac{\delta_n}{\sigma_n} \Phi^{(1)} + \delta_p \Phi^{(1)} + \frac{1}{\sigma_p} \Phi^{(1)} - \Delta(Q^{(1)} - N_d^{(1)}) - \frac{\mathcal{G}}{\sigma_p} \Phi^{(1)} = 0, \\ & \Phi^{(1)} \left(\frac{\delta_n}{\sigma_n} + \delta_p + \frac{1 - \mathcal{G}}{\sigma_p} \right) - \Delta(Q^{(1)} - N_d^{(1)}) = 0, \\ & \Delta Q^{(1)} = \left(\frac{\delta_n}{\sigma_n} + \delta_p + \frac{1 - \mathcal{G}}{\sigma_p} \right) + \Delta N_d^{(1)}, \\ & Q^{(1)} = \frac{\alpha_d}{\Delta} \left(-\Lambda^2 \sec^2 \theta + \frac{\gamma_d \sigma_d}{\alpha_d} \right) \left(\frac{\delta_n}{\sigma_n} + \delta_p + \frac{1 - \mathcal{G}}{\sigma_p} \right) N_d^{(1)} + \Delta N_d^{(1)}, \\ & = \left\{ 1 - \frac{\mathcal{Z}_{d0} n_{d0}}{\Delta \gamma n_{p0}} \left(\Lambda^2 \sec^2 \theta - \frac{\gamma_d \sigma_d}{\alpha_d} \right) \left(\frac{\delta_n}{\sigma_n} + \delta_p + \frac{1 - \mathcal{G}}{\sigma_p} \right) \right\} N_d^{(1)}, \\ & = \left\{ 1 - \frac{\mathcal{Z}_{d0} n_{d0}}{n_{p0} \left(\delta_p + \frac{1}{\sigma_p} + \frac{\delta_n}{\sigma_n} \right) \left(1 - \delta_p - \delta_n \right)} \left(\Lambda^2 \sec^2 \theta - \frac{\gamma_d \sigma_d}{\alpha_d} \right) \left(\frac{\delta_n}{\sigma_n} + \delta_p + \frac{1}{\sigma_p} \right) \right. \\ & \quad \left. + \frac{\mathcal{Z}_{d0} n_{d0} \frac{\mathcal{G}}{\sigma_p}}{n_{p0} \left(\delta_p + \frac{1}{\sigma_p} + \frac{\delta_n}{\sigma_n} \right) \left(1 - \delta_p - \delta_n \right)} \left(\Lambda^2 \sec^2 \theta - \frac{\gamma_d \sigma_d}{\alpha_d} \right) \right\} N_d^{(1)}, \end{aligned}$$

using the quasi-neutrality condition, we obtained

$$\begin{aligned} Q^{(1)} = & \left\{ 1 - \frac{\mathcal{Z}_{d0} n_{d0}}{n_{p0} \left(1 - \frac{n_{e0}}{n_{p0}} - \frac{n_{e0}}{n_{p0}} \right)} \left(\Lambda^2 \sec^2 \theta - \frac{\gamma_d \sigma_d}{\alpha_d} \right) \right. \\ & \left. - \frac{\mathcal{Z}_{d0} n_{d0} \frac{\Gamma}{\sigma_p}}{n_{p0} \left(1 - \frac{n_{e0}}{n_{p0}} - \frac{n_{e0}}{n_{p0}} \right) \left(1 - \delta_p - \delta_n \right)} \left(\Lambda^2 \sec^2 \theta - \frac{\gamma_d \sigma_d}{\alpha_d} \right) \right\} N_d^{(1)}, \end{aligned}$$

and after a short algebraic manipulations one can get the following expression

$$Q^{(1)} = \left\{ 1 - \left(\Lambda^2 \sec^2 \theta - \frac{\gamma_d \sigma_d}{\alpha_d} \right) + \frac{\frac{\mathcal{G}}{\sigma_p}}{\left(\delta_p + \frac{1}{\sigma_p} + \frac{\delta_n}{\sigma_n} \right)} \left(\Lambda^2 \sec^2 \theta - \frac{\gamma_d \sigma_d}{\alpha_d} \right) \right\} N_d^{(1)}. \quad (3.40)$$

Now, compare Eqs. (3.39) and (3.40)

$$\left\{ 1 - \left(\Lambda^2 \sec^2 \theta - \frac{\gamma_d \sigma_d}{\alpha_d} \right) + \frac{\frac{\mathcal{G}}{\sigma_p}}{n_{p0} \left(\delta_p + \frac{1}{\sigma_p} + \frac{\delta_n}{\sigma_n} \right)} \left(\Lambda^2 \sec^2 \theta - \frac{\gamma_d \sigma_d}{\alpha_d} \right) \right\} = \beta_{ch} \alpha_d \left(\Lambda^2 \sec^2 \theta - \frac{\gamma_d \sigma_d}{\alpha_d} \right),$$

$$1 + \frac{\frac{\mathcal{G}}{\sigma_p}}{\left(\delta_p + \frac{1}{\sigma_p} + \frac{\delta_n}{\sigma_n} \right)} \left(\Lambda^2 \sec^2 \theta - \frac{\gamma_d \sigma_d}{\alpha_d} \right) = (1 + \beta_{ch} \alpha_d) \left(\Lambda^2 \sec^2 \theta - \frac{\gamma_d \sigma_d}{\alpha_d} \right),$$

$$1 = (1 + \beta_{ch} \alpha_d) \left(\Lambda^2 \sec^2 \theta - \frac{\gamma_d \sigma_d}{\alpha_d} \right) - \frac{\frac{\mathcal{G}}{\sigma_p}}{\gamma} \left(\Lambda^2 \sec^2 \theta - \frac{\gamma_d \sigma_d}{\alpha_d} \right),$$

$$1 = \left(\Lambda^2 \sec^2 \theta - \frac{\gamma_d \sigma_d}{\alpha_d} \right) \left(1 + \beta_{ch} \alpha_d - \frac{\frac{\mathcal{G}}{\sigma_p}}{\gamma} \right),$$

$$1 = \Lambda^2 \sec^2 \theta \left(1 + \beta_{ch} \alpha_d - \frac{\frac{\mathcal{G}}{\sigma_p}}{\gamma} \right) - \frac{\gamma_d \sigma_d}{\alpha_d} \left(1 + \beta_{ch} \alpha_d - \frac{\frac{\mathcal{G}}{\sigma_p}}{\gamma} \right),$$

$$1 + \frac{\gamma_d \sigma_d}{\alpha_d} \left(1 + \beta_{ch} \alpha_d - \frac{\frac{\mathcal{G}}{\sigma_p}}{\gamma} \right) = \Lambda^2 \sec^2 \theta \left(1 + \beta_{ch} \alpha_d - \frac{\frac{\mathcal{G}}{\sigma_p}}{\gamma} \right),$$

$$\frac{1}{\left(1 + \beta_{ch} \alpha_d - \frac{\frac{\mathcal{G}}{\sigma_p}}{\gamma} \right)} + \frac{\gamma_d \sigma_d}{\alpha_d} = \Lambda^2 \sec^2 \theta,$$

$$\Lambda^2 = \frac{1}{\sec^2 \theta} \left\{ \frac{\gamma_d \sigma_d}{\alpha_d} + \frac{1}{\left(1 + \beta_{ch} \alpha_d - \frac{\frac{\mathcal{G}}{\sigma_p}}{\gamma} \right)} \right\},$$

$$\Lambda = \cos \theta \left\{ \frac{\gamma_d \sigma_d}{\alpha_d} + \frac{1}{\left(1 + \beta_{ch} \alpha_d - \frac{\frac{\mathcal{G}}{\sigma_p}}{\gamma} \right)} \right\}^{\frac{1}{2}},$$

$$\Lambda = \mathcal{V}_{ph} - \mathcal{V}_0 = \cos \theta \left\{ \frac{\gamma_d \sigma_d}{\alpha_d} + \frac{1}{k} \right\}^{\frac{1}{2}}. \quad (3.41)$$

Eq. (3.41) shows the linear dust acoustic wave (DAW) phase velocity and where $k = \left(1 + \beta_{ch} \alpha_d - \frac{\frac{\mathcal{G}}{\sigma_p}}{\gamma} \right)$

The first order analysis only shows that the initial disturbance propagates and nonlinear, dissipation, dispersion, and/or geometrical convergence effects have not yet come into play. These effects appear in the next higher-order equations as given below:

$$\frac{\partial N_d^{(1)}}{\partial \tau} + \frac{\partial N_d^{(1)} \mathcal{V}_{dx}^{(1)}}{\partial \xi} = - \frac{\partial (\Lambda N_d^{(2)} + \mathcal{V}_{dx}^{(2)})}{\partial \xi}, \quad (3.42)$$

$$\begin{aligned} \frac{\partial \mathcal{V}_{dx}^{(1)}}{\partial \tau} + \mathcal{V}_{dx}^{(1)} \frac{\partial \mathcal{V}_{dx}^{(1)}}{\partial \xi} + \frac{1}{\alpha_d} \left(Q^{(1)} \frac{\partial \Phi^{(1)}}{\partial \xi} + \gamma_d \sigma_d (\gamma_d - 2) N_d^{(1)} \frac{\partial N_d^{(1)}}{\partial \xi} \right) \\ = \frac{1}{\alpha_d} \frac{\partial (\Phi^{(2)} - \gamma_d \sigma_d N_d^{(2)})}{\partial \xi} - \Lambda \frac{\partial \mathcal{V}_{dx}^{(2)}}{\partial \xi} + \omega_{ch} (Q^{(1)} \mathcal{V}_{dx}^{(1)} - \mathcal{V}_{dy}^{(2)}) \sin \theta, \end{aligned} \quad (3.43)$$

$$\Lambda \frac{\partial \mathcal{V}_{dy}^{(1)}}{\partial \xi} + \omega_{ch} Q^{(1)} (\mathcal{V}_{dx}^{(1)} \sin \theta - \mathcal{V}_{dz}^{(1)} \cos \theta) = \omega_{ch} (\mathcal{V}_{dx}^{(2)} \sin \theta - \mathcal{V}_{dz}^{(2)} \cos \theta), \quad (3.44)$$

$$\frac{\partial \mathcal{V}_{dz}^{(1)}}{\partial \tau} + \mathcal{V}_{dx}^{(1)} \frac{\partial \mathcal{V}_{dz}^{(1)}}{\partial \xi} = - \Lambda \frac{\partial \mathcal{V}_{dz}^{(2)}}{\partial \xi} - \omega_{ch} (Q^{(1)} \mathcal{V}_{dy}^{(1)} - \mathcal{V}_{dy}^{(2)}) \cos \theta, \quad (3.45)$$

$$\Phi^{(2)} + \frac{\left(\delta_p + \frac{\delta_n}{\sigma_n^2} - \frac{1}{\sigma_p^2} \right)}{2 \left(\gamma - \frac{g}{\sigma_p} \right)} \Phi^{(1)^2} - \frac{\Delta \left(Q^{(2)} - N_d^{(2)} + Q^{(1)} N_d^{(1)} \right)}{2 \left(\gamma - \frac{g}{\sigma_p} \right)} = 0. \quad (3.46)$$

From the comparison of charging equation one can get the equation of the form

$$\begin{aligned} \Lambda \omega_{ch} \frac{\partial}{\partial \xi} Q^{(1)} = - \Phi^{(2)} \beta_{ch} - Q^{(2)} + \frac{\sigma_p \beta_{ch}}{2(1 + \sigma_p + \bar{\gamma}_2)} \left\{ - \mathcal{Z}^2 (1 + B_n) Q^{(1)^2} \right. \\ \left. + \left(\frac{1 - \sigma_p^2 (1 + B_n)}{\sigma_n^2} - K_1 \right) \Phi^{(1)^2} + 2 \mathcal{Z} \left(\frac{1 - \sigma_p (\mathcal{Z} + \sigma_p) (1 + B_n)}{\sigma_p (\mathcal{Z} + \sigma_p)} - K_2 \right) Q^{(1)} \Phi^{(1)} \right\}, \end{aligned} \quad (3.47)$$

where

$$K_1 = \frac{a}{(1 + 3a)} \left(\frac{11}{15\sigma_p^2} + \frac{32}{15\sigma_p (\mathcal{Z} + \sigma_p)} \right),$$

$$K_2 = \frac{a}{(1 + 3a)} \left(\frac{61\mathcal{Z}}{15\sigma_p (\mathcal{Z} + \sigma_p)} \right),$$

and

$$B_n = A_n \frac{(1 - \sigma_n^2)}{\sigma_n^2} + \frac{a}{(1 + 3a)} \left(\frac{-7}{5} + \frac{16\sigma_p}{5(\mathcal{Z} + \sigma_p)} \right).$$

Finally, eliminating all the second order quantities from Eqs. (3.42) - (3.47) and using the relations (3.35) - (3.40), we obtained the following KdVB equation

$$\frac{\partial N_d^{(1)}}{\partial \tau} - \mathcal{A} N_d^{(1)} \frac{\partial N_d^{(1)}}{\partial \xi} - \mathcal{B} \frac{\partial^3 N_d^{(1)}}{\partial \xi^3} - \mathcal{D} \frac{\partial^2 N_d^{(1)}}{\partial \xi^2} = 0. \quad (3.48)$$

The coefficients of non-linearity \mathcal{A} , dispersion \mathcal{B} and Burger term \mathcal{D} are as follows:

$$\mathcal{A} = \frac{\cos^2 \theta}{2\Lambda} \left[\frac{\gamma_d \sigma_d}{\alpha_d} (\gamma_d + 1) + \frac{3}{k} - \frac{1}{k^2} \left(3\alpha_d \beta_{ch} + \frac{\alpha_d (\delta_p + \frac{\delta_n}{\sigma_n^2} - \frac{1}{\sigma_p^2})}{\gamma k} + \frac{\sigma_p \alpha_d^2 \beta_{ch} (C + K_3)}{(1 + \sigma_p + \bar{\gamma}_2) k} \right) \right], \quad (3.49)$$

where

$$\mathcal{C} = (1 + B_-) (\mathcal{Z} \beta_{ch} - 1)^2 + \frac{2\mathcal{Z} \beta_{ch}}{\sigma_p (\mathcal{Z} + \sigma_p)} - \frac{1}{\sigma_n^2}, \quad (3.50)$$

$$\mathcal{B} = \frac{\sin^2 \theta \cos \theta}{2\omega_{cd}^2} \left(\frac{\gamma_d \sigma_d}{\alpha_d} + \frac{1}{k} \right)^{\frac{3}{2}}, \quad (3.51)$$

$$\mathcal{D} = \frac{\alpha_d \beta_{ch} \omega_{ch} \cos^2 \theta}{2k^2} = \frac{\alpha_d \beta_{ch} \cos^2 \theta}{2k^2} \left(\frac{\omega_{pd}}{\nu_{ch}} \right), \quad (3.52)$$

and

$$K_3 = \frac{a}{(1 + 3a)} \left(\frac{11}{15\sigma_p^2} - \frac{2(16 - 61\mathcal{Z} \beta_{ch})}{15\sigma_p (\mathcal{Z} + \sigma_p)} \right). \quad (3.53)$$

The Burger term ν_{ch} implies the possibility of the existence of a shock-like structure. And for parallel propagation, i.e., $\theta = 0$, the dispersion term vanishes, i.e., $\mathcal{B} = 0$, and the nonlinear dust acoustic wave is governed by the so-called Burger equation

$$\frac{\partial N_d^{(1)}}{\partial \tau} - \mathcal{A} N_d^{(1)} \frac{\partial N_d^{(1)}}{\partial \xi} - \mathcal{D} \frac{\partial^2 N_d^{(1)}}{\partial \xi^2} = 0. \quad (3.54)$$

3.6 Stationary Solution: Generation of Shock Wave

It is well known that the Kortewege-de Vries (KdV) Burger equation describes the shock wave profile. The criteria for the formation of the shock wave is that the coefficient of the Burger term \mathcal{D} which arises due to the non-steady dust charge variation should be

positive, i.e., $\mathcal{D} > 0$. Otherwise, it would not be possible to get a stable solution to the Burger equation. A particular solution of the above KdV-Burger equation (3.48)

$$N_d^{(1)}(\xi, \tau) = -\frac{3\mathcal{D}^2}{25\mathcal{A}\mathcal{B}} \left[1 + \tanh \frac{\mathcal{D}}{10\beta} \left(\frac{6\mathcal{D}^2}{25\mathcal{B}}\tau - \xi \right) \right]^2. \quad (3.55)$$

While for the parallel propagation, i.e., $\theta = 0$, the dispersive term vanishes and one can easily obtain the following analytical solution of the Burger's equation (3.54) subject to the boundary conditions $N_d^{(1)}(\xi, \tau)$, $\frac{\partial N_d^{(1)}(\xi, \tau)}{\partial \eta} \rightarrow 0$ as $\eta \rightarrow -\infty$, which exhibits monotonic shock solution.

$$N_d^{(1)}(\xi, \tau) = \mathcal{N} \left[1 + \tanh \left(\frac{\eta}{L_w} \right) \right], \quad (3.56)$$

where $\mathcal{N} = \frac{\mathcal{V}_f}{\mathcal{A}}$ is the initial shock amplitude and $L_w = \frac{2\mathcal{D}}{\mathcal{V}_f}$ is the shock width. And in the absence of charge fluctuation, i.e., $\nu_{ch} = 0$, the KdVB equation (3.48) reduced to a KdV like equation

$$\frac{\partial N_d^{(1)}}{\partial \tau} - \mathcal{A}N_d^{(1)} \frac{\partial N_d^{(1)}}{\partial \xi} - \mathcal{B} \frac{\partial^3 N_d^{(1)}}{\partial \xi^3} = 0, \quad (3.57)$$

which admits a solitary solution of the form

$$N_d^{(1)}(\xi, \tau) = \mathcal{N} \operatorname{sech}^2 \left(\frac{\eta}{\Delta_w} \right), \quad (3.58)$$

where, \mathcal{N} and $\Delta_w = \sqrt{\frac{4\beta}{\mathcal{V}_f}}$ represents the amplitude and the width of the solitary wave, respectively. However, for steady state numerical solution transforming to the wave frame $\eta = \mathcal{V}_f\tau + \xi$ the KdV-Burger equation (3.48) with $\psi = N_d^{(1)}(\xi, \tau)$ reduce to the following expression

$$\frac{d^2\psi}{d\eta^2} = \left(\frac{\mathcal{V}_f}{\beta} \right) \psi - \left(\frac{\mathcal{A}}{2\mathcal{B}} \right) \psi^2 - \left(\frac{\mathcal{D}}{\beta} \right) \frac{d\psi}{d\eta}. \quad (3.59)$$

The Eq. (3.59) has two fixed points, i.e., $(0, 0)$ and $(\frac{2\mathcal{V}_f}{\alpha}, 0)$. However, $\psi = N_d^{(1)}$ can be calculated by numerical integration. Here the Mach number is defined as the ratio of dust acoustic (DA) wave velocity \mathcal{V}_a to the linear dust acoustic (DA) wave velocity. The DAW velocity \mathcal{V}_a is expressed as

$$\mathcal{V}_a = \mathcal{V}_0 - (\mathcal{V}_{ph} - \epsilon\mathcal{V}_f), \quad (3.60)$$

and the linear DAW velocity Λ which is expressed in equation (3.41). Therefore, the Mach number is indicated as

$$\mathcal{M} = \frac{\mathcal{V}_a}{\Lambda}. \quad (3.61)$$

3.7 Parametric Analysis

Horanyi and Mendis [72][73] investigated the trajectories of micron and sub-micron sized dust grains that are expected to be released from the cometary nucleus. It was shown that the electromagnetic forces associated with the motion of the grains (which are electrically charged by the plasma environment) through the magnetized plasma play an important role in their dynamics. The different spacecrafts like Vega 1, Vega 2, and Giotto has the observation on comets which tells that Comet Halley is composed of electrons, ice dust grains, different positive and negative ions. These positive and negative ions are usually (H^+, H^-) , (O^+, O^-) , (Si^+, Si^-) , (OH^+, OH^-) etc. Considered the positive and negative ions are (Si^+, Si^-) and pure ice dust grains for the numerical analysis of present findings [74][75][76][77]. The approximate physical parameters of Comet Halley which is approximate 10^4 km away from the nucleus are $n_{p0} \sim 2 \times 10^6$ m⁻³, $n_{d0} \sim 1$ m⁻³, $T_e = \sim 100$ eV, $m_p = m_n \sim 1.6726 \times 10^{-27}$ kg, $B_0 \sim 7.5 \times 10^{-3}$ Tesla, $r_0 \sim 5\mu m$ and $\gamma_d \sim \frac{5}{3}$. It is also noted that the ratio of the mass of positive ion and mass of the negative ion, i.e., $Q = \frac{m_+}{m_-}$ may have a strong influence on the spatial patterns of ion-acoustic solitons in electronegative dusty plasma which is recently reported by Taibany and Tribeche[78].

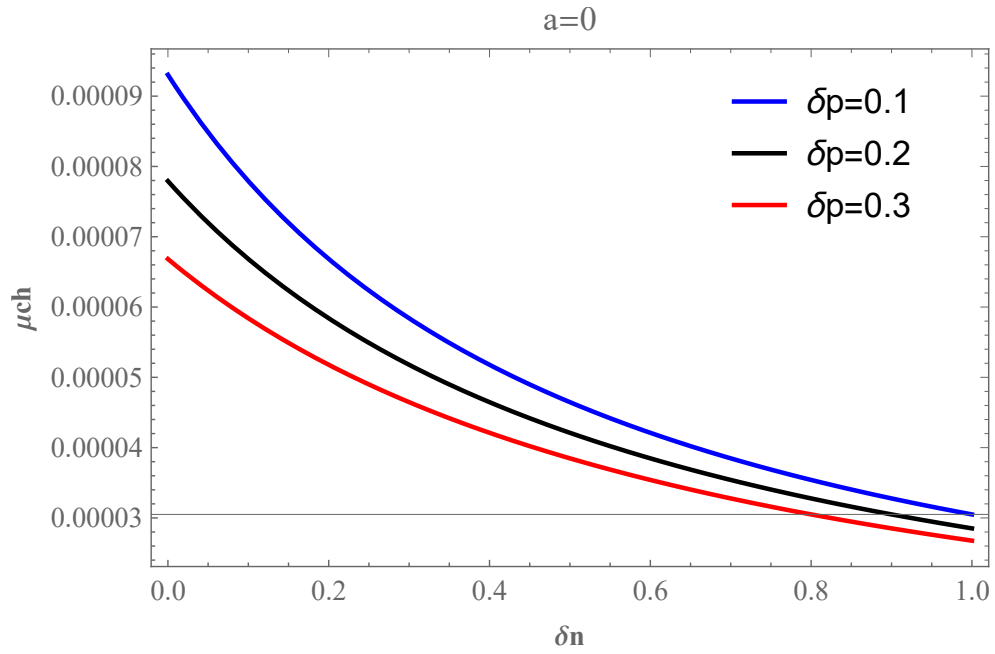


Figure 3.17: Variation of dissipative term (μ_{ch}) against density ratio (δ_n) for different value of density ratio δ_p . The other parameters are $\theta = 30$ and $a = 0$.

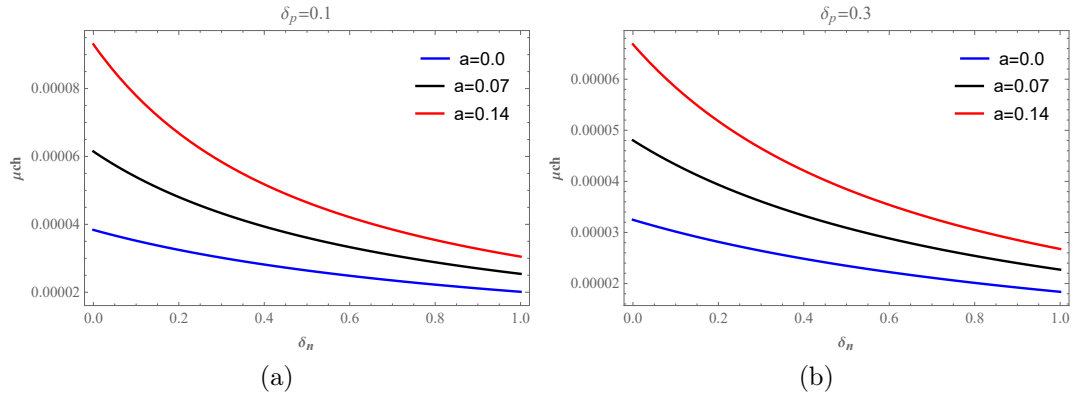


Figure 3.18: Plot of dissipative term (μ_{ch}) against density ratio (δ_n) for different values of non-thermal parameter "a" at fixed density ratio δ_p . The plot (a) shows $\delta_p = 0.1$ and plot (b) shows $\delta_p = 0.3$.

Chapter 4

Discussions and Conclusions

4.1 Discussions

Figure 3.1 indicates that when the population of Cairn distributed positive ions increases the Doppler frequency increases as well. The blue line refers to the Maxwellian case. Figure 3.2 and figure 3.3 manifests the effect of increasing magnetic field obliqueness (θ) for the Doppler frequency. It is observed that by increasing the magnetic field obliqueness θ the Doppler frequency is also increases and vice versa. And when the population of Cairn distributed positive ions increases the Doppler frequency increases. Now, to check the effects of the population of Cairn distributed positive ions, the density ratio of electrons and energetic positive ions we have to plot figure 3.4 and figure 3.5. It is noticed that by increasing the density ratio of electrons and energetic positive ions the Doppler frequency decreases. While by increasing the Cairn distributed positive ion population the Doppler frequency is increasing. Similarly, figure 3.6 and figure 3.7 shows the Doppler frequency variation against k , which indicates that the Doppler frequency increases by the increase of normalized cyclotron frequency ω_{cd} and similarly by enhancing the non-thermal Cairn distributed positive ions the Doppler frequency increases as well. The growth rate also increases with an increase in the Cairn distributed positive ion population. Variation in normalized cyclotron frequency means that there are variations in a magnetic field.

In figure 3.8 manifests the effect of an increasing Cairn distributed positive ion population. It indicates that by increasing the non-therm parameter the growth rate also

increases. On the other hand, if the magnetic field obliqueness (θ) is increasing then the growth rate is decreasing. The magnetic field obliqueness effects are shown in figure 3.9. Figure 3.11, 3.12, 3.13, 3.14, 3.15 and 3.16 manifests the effects of normalized dust cyclotron frequency (ω_{cd}), electrons and Cairn distributed positive ions density ratio, and negative and Cairn distributed positive ions density ratio. It shows that when the normalized dust cyclotron frequency increases the growth rate is also increases while increasing the electrons and Cairn distributed positive ions density and negative and Cairn distributed positive ions density the growth rate is decreasing. The increase of non-thermal parameter in all these cases will increase the growth rate.

Figure 3.17 and 3.18 explore the effects of electrons and Cairn distributed positive ions ratio and the population of Cairn distributed positive ions. It is also noticed that the ratio of electrons and Cairn distributed positive ions population plays a crucial role in the dissipation term. It is observed that in a particular case when the ratio of electrons and Cairn distributed positive ions density increases the dissipation term effects are decreases. While, the population of energetic positive ions for a particular case, i.e., $\delta_p = 0.1$, $\delta_p = 0.2$ and $\delta_p = 0.3$ will increase the variations of dissipative term. Figure 4.1 manifests that with the increase in obliqueness of the magnetic field the dissipative term decay rapidly. While an increase in Cairn distributed positive ions population for a specific obliqueness of the magnetic field (θ) shown in figure 4.2, indicates that the dissipation term is increases.

Figure 4.3 demonstrates an increase in the population of Cairn distributed positive ions for soliton structure. It is noticed that the increasing population of Cairn distributed positive ions plays a crucial role that the amplitude of the solitons is decreasing with increasing Cairn distributed positive ions population. While on the other hand, the shoulders of the solitons broadened. The broadness of the soliton shoulders or wings indicates that the population of Cairn distributed positive ions increase the dispersion term. The figure 4.4 manifests the effect of increasing normalized dust cyclotron frequency ω_{cd} . It is observed that by increasing the normalized dust cyclotron frequency ω_{cd} the soliton shoulders or wings shrinks but the amplitude remains the same. The figure 4.5 shows that how the shoulders of the solitons spread with the increase of Cairn

distributed positive ions population. The figures 4.6, 4.7, 4.8 and 4.9 indicates that the amplitude of the soliton is increased with the increase of the ratio of electrons and Cairn distributed positive ions density and the ratio of negative and Cairn distributed positive ions while the shoulders of the solitons are shrinks. The figures 4.10 and 4.11 manifests the effects of increasing the obliqueness of the magnetic field and population of Cairn distributed positive ions. It is observed that by increasing the obliqueness of the magnetic field the amplitude, as well as the shoulders of the solitons, get smaller. While, by increasing the population of Cairn distributed positive ions the amplitude, as well as the shoulders of the solitons, get smaller.

Figure 4.12 demonstrates an increase in the population of Cairn distributed positive ions for monotonic shock structure. It is noticed that the strength and amplitude of the shock decrease with the increase in the non-thermal population of positive ions. While increasing the density ratio of negative and energetic positive ions and density ratio of electrons and Cairn distributed positive ions increases the strength and amplitude of the monotonic shock elaborated in figures 4.13 and 4.15. If the population of Cairn distributed positive ions increases the strength and amplitude of the monotonic shock is decreases, shown in figures 4.14 and 4.16.

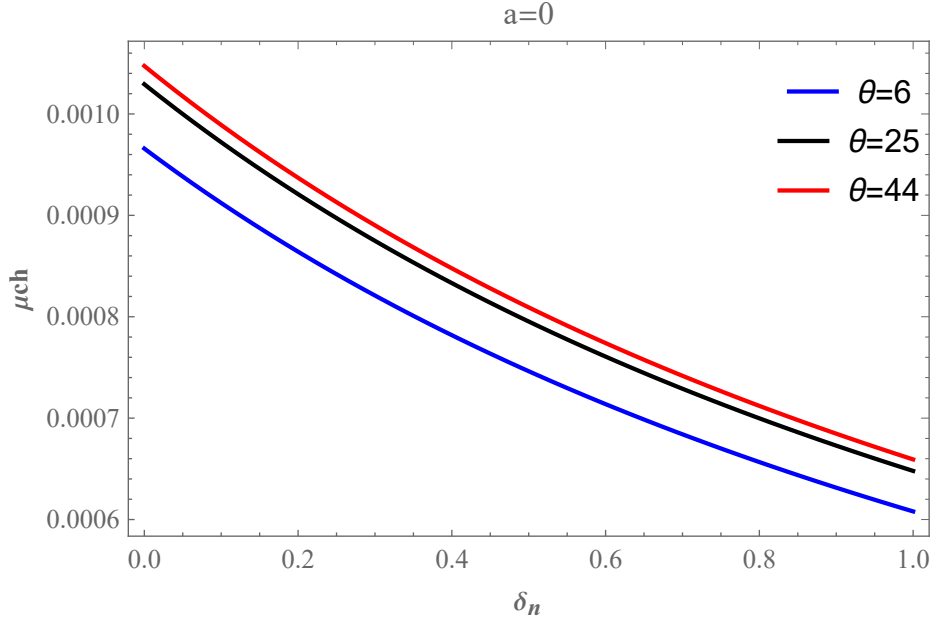


Figure 4.1: The effect of dissipative term (μ_{ch}) against density ratio (δ_n) for different values of obliqueness of magnetic field θ .

4.2 Conclusions

In this project, we have investigated the linear and non-linear analysis of dust acoustic waves with the application on the Halley comet. In the linear analysis regime, we have investigated the Doppler's frequency and growth rate for the constant dust charge variation. Besides this, we derived the relation for dust charge variation. To investigate the Doppler's frequency, we have observed that by increasing the population of energetic positive ions, the Doppler's frequency has also increased. Whereas, an increase in the obliqueness of the magnetic field has decreased the Doppler's frequency. Likewise, it was also observed that the density ratio of electrons and energetic positive ions (δ_p) played a crucial role, i.e., the increase in δ_p has decreased the Doppler's frequency. Similarly, the effects of normalized dust cyclotron frequency on Doppler's frequency cannot be ignored. It was observed that the small deviations in normalized dust cyclotron frequency led to a great increase in the Doppler's frequency.

Moreover, to investigate the growth rate, it has been found that by enhancing the

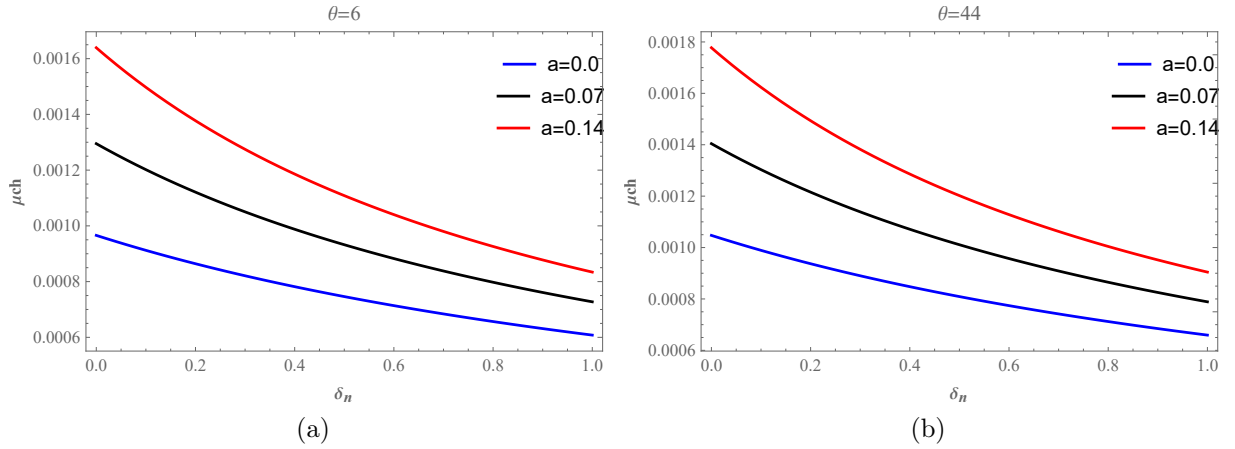


Figure 4.2: The effect of dissipative term (μ_{ch}) versus density ratio (δ_n) for different value of different values of non-thermal parameter "a" at fixed magnetic field obliqueness θ . The left panel shows $\theta = 6$ and right panel shows $\theta = 44$.

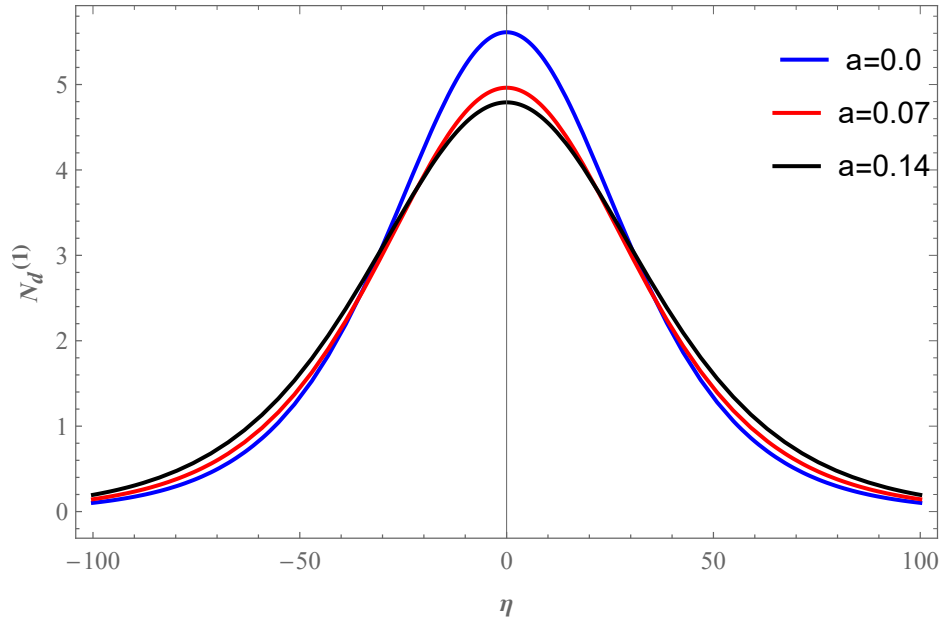


Figure 4.3: The KdV solitons are plotted for different values of non-thermal parameter "a" at fixed obliqueness of magnetic field $\theta = 30$.

population of energetic positive ions the growth rate increases. On the other hand, increasing the obliqueness of the magnetic field the growth rate decreases. However,

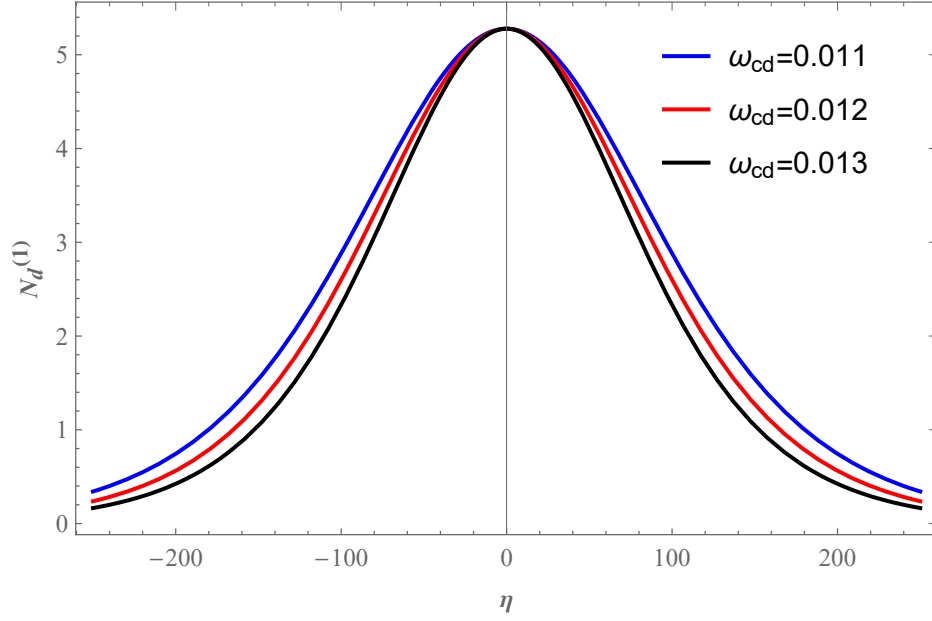


Figure 4.4: The profile of KdV solitons for different value of non-thermal parameter "a" at fixed obliqueness of magnetic field that is $\theta = 30$.

the increase in the normalized dust cyclotron frequency or the magnitude of the applied magnetic field leads to an increase in the growth rate. Also, both ratios of electrons versus energetic positive ions and negative ions versus energetic positive ions play a crucial role in the growth rate. A small deviation in both ratios led us to a great change in the growth rate. It was revealed that an increase in both the density ratios decreased the growth rate.

In the non-linear analysis regime, we have derived the KdVB equation. For the parallel propagation, i.e., $\theta = 0$, the dispersive term vanishes, and the KdVB equation is reduced to Burger's equation. This Burger's equation led us to the monotonic dust acoustic shock structure. While, in the absence of charge fluctuation, the KdVB equation was reduced to a KdV like -equation which admits a solitary solution. The dissipative term plays an important role in Burger's equation. This dissipative term decreases when the density ratio of electrons versus energetic positive ions increases. While the dissipative term increases with the enhancement of energetic positive ions population. Moreover, by increasing the obliqueness of the magnetic field the dissipative term decays gradu-

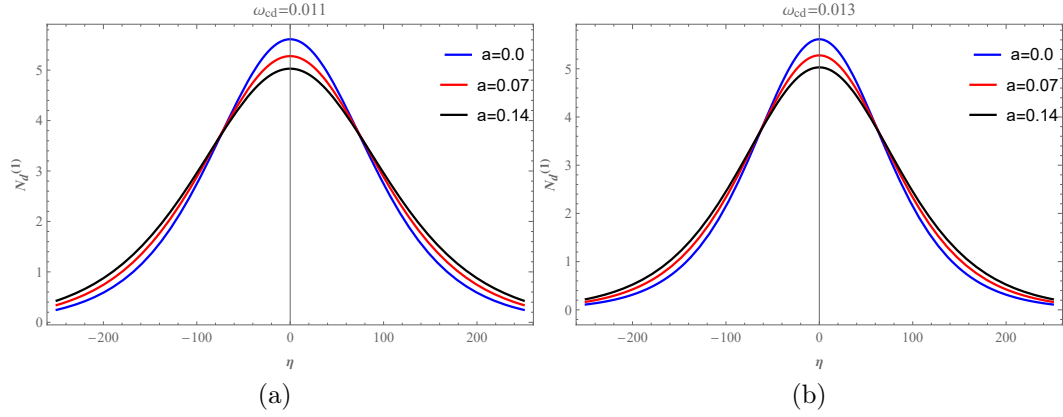


Figure 4.5: The profile of KdV solitons for different value of non-thermal parameter "a" at fixed normalized dust cyclotron frequency ω_{cd} . The plot (a) shows $\omega_{cd} = 0.011$ and plot (b) shows $\omega_{cd} = 0.013$

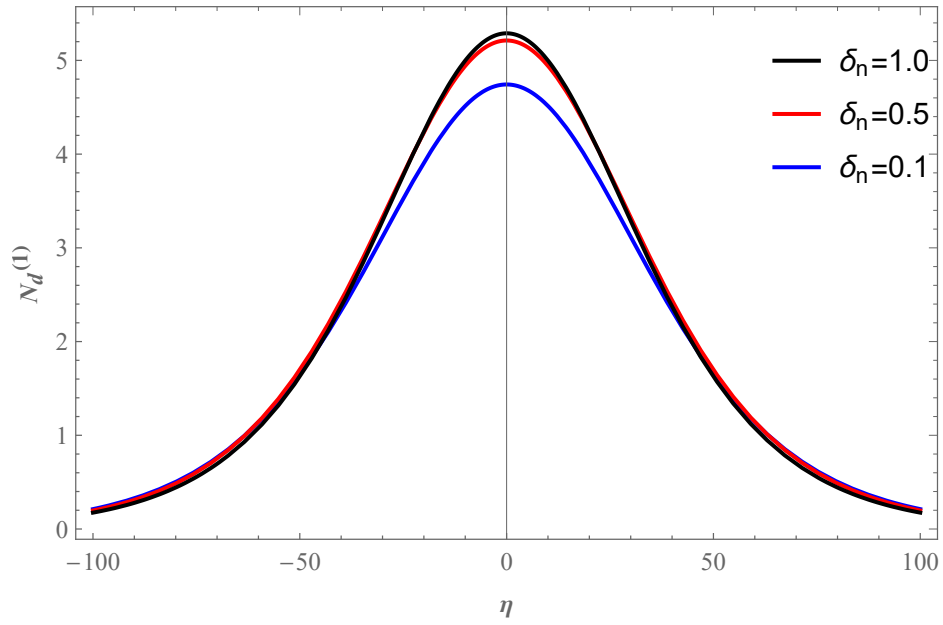


Figure 4.6: The behavior of KdV solitons are plotted for different values of negative ions and positive ions density ratio δ_n . The blue solid curve corresponds to $\delta_n = 0.1$, the red solid curve corresponds to $\delta_n = 0.5$ and the black solid curve corresponds to $\delta_n = 1$ at fixed obliqueness of magnetic field $\theta = 30$.

ally. The KdV soliton has been investigating, and it is found that by increasing the

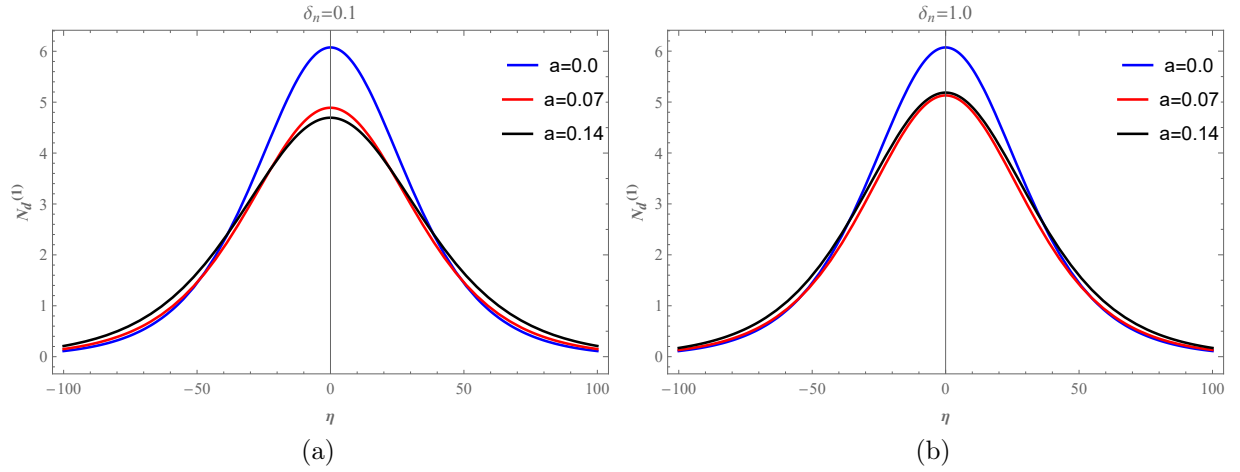


Figure 4.7: The behavior of KdV solitons for different values of non-thermal parameter "a" at fixed negative ions and positive ions density ratio δ_n . The left panel shows $\delta_n = 0.1$ and right panel shows $\delta_n = 1.0$.

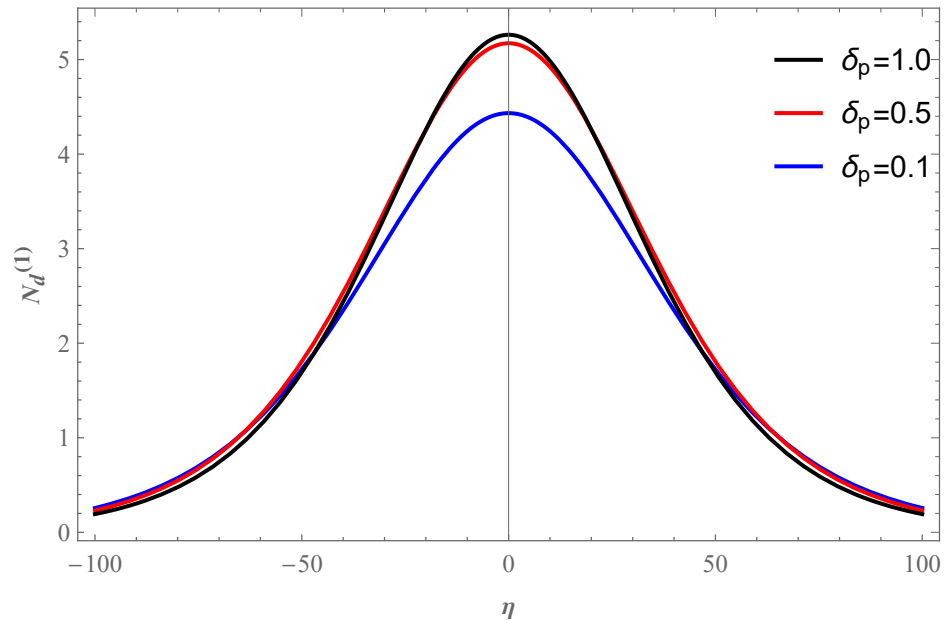


Figure 4.8: The profile of KdV solitons for different value of electrons and positive ions density ratio δ_p at fixed obliqueness of magnetic field $\theta = 30$.

population of energetic positive ions the amplitude of the soliton decreases while its width or shoulders increase. However, the increase in the normalized dust cyclotron fre-

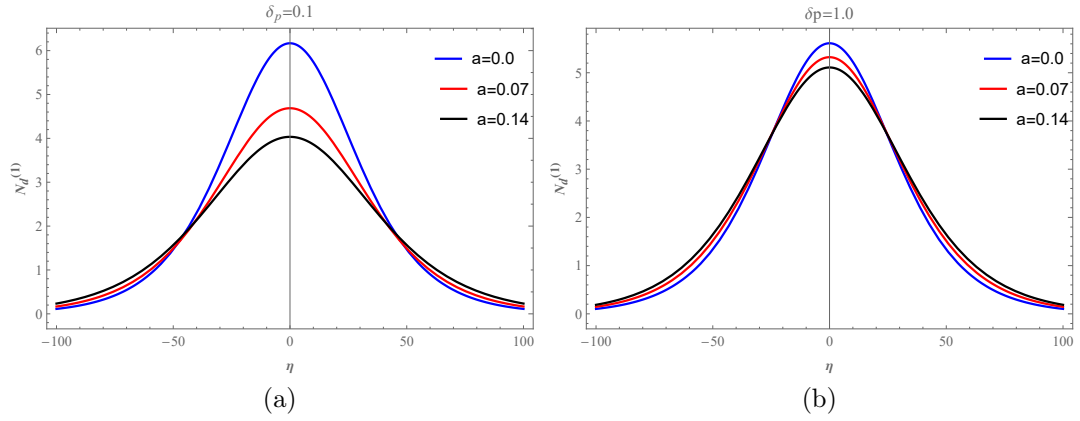


Figure 4.9: The profile of KdV solitons for different values of non-thermal parameter "a" at fixed electrons and positive ions density ratio δ_p . The left panel shows $\delta_p = 0.1$ and right panel shows $\delta_p = 1.0$.

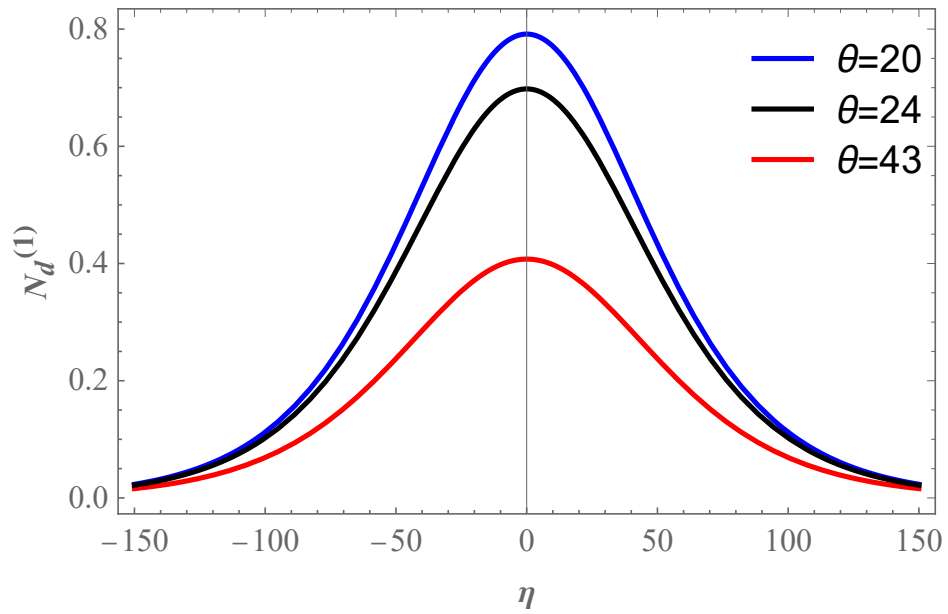


Figure 4.10: The profile of KdV solitons are plotted for different values of obliqueness of magnetic field θ .

quency or the magnitude of the applied magnetic field led to the decrease in the width of soliton while its amplitude remains unaffected. It is also observed that by increasing the density ratio of electrons versus energetic positive ions the amplitude of the soliton

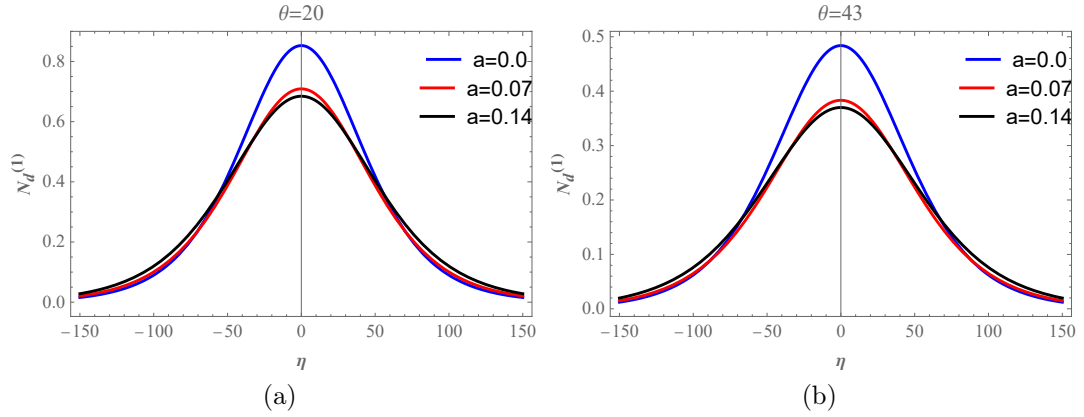


Figure 4.11: The profile KdV solitons are plotted for different value of obliqueness of magnetic field θ . The left panel shows $\theta = 20$ and right panel shows $\theta = 44$.

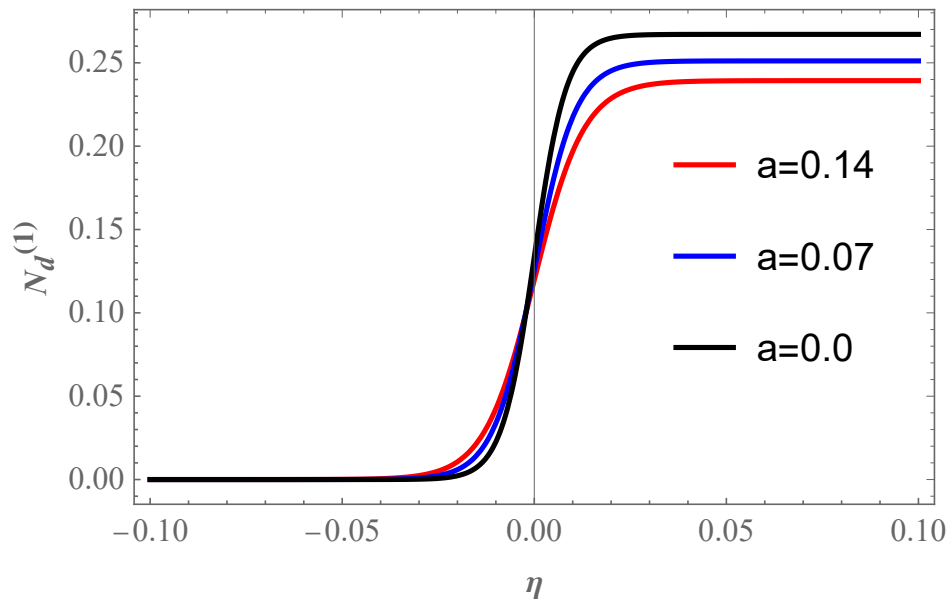


Figure 4.12: The profile of monotonic dust-acoustic shocks are plotted for different value of non-thermal parameter " a ".

increases but the width or shoulder of the soliton decreases. Similarly, for the density ratio of negative ions versus energetic positive ions population the amplitude of the soliton increases but the width or shoulder of the soliton decreases. Moreover, in our system, the obliqueness of the magnetic field has a very important role. Therefore, it

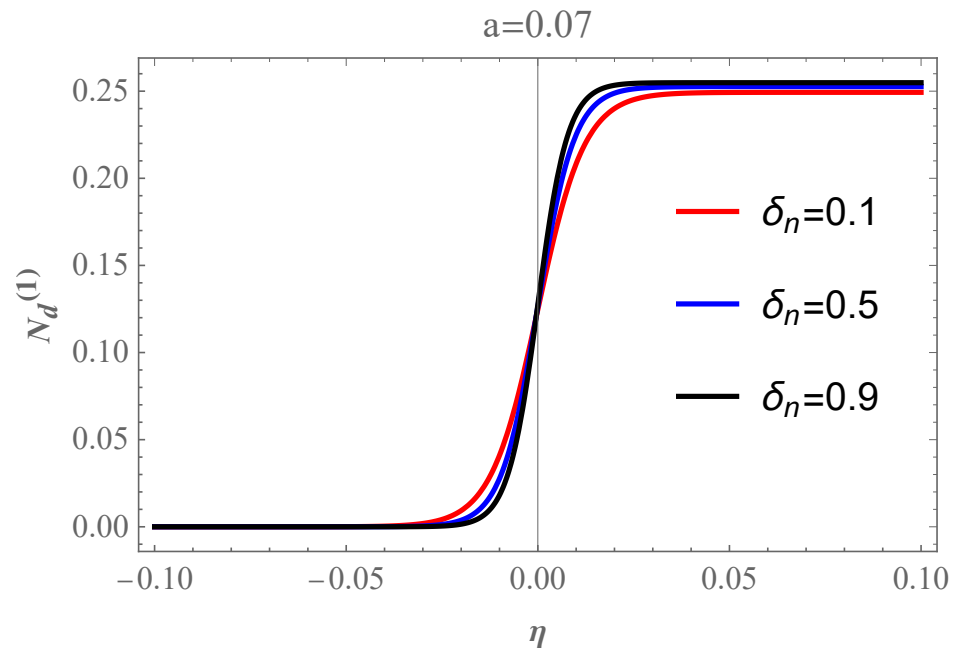


Figure 4.13: The behavior of monotonic dust-acoustic shocks are plotted for different value of negative and positive ions density ratio δ_n at fixed non-thermal parameter $a = 0.07$.

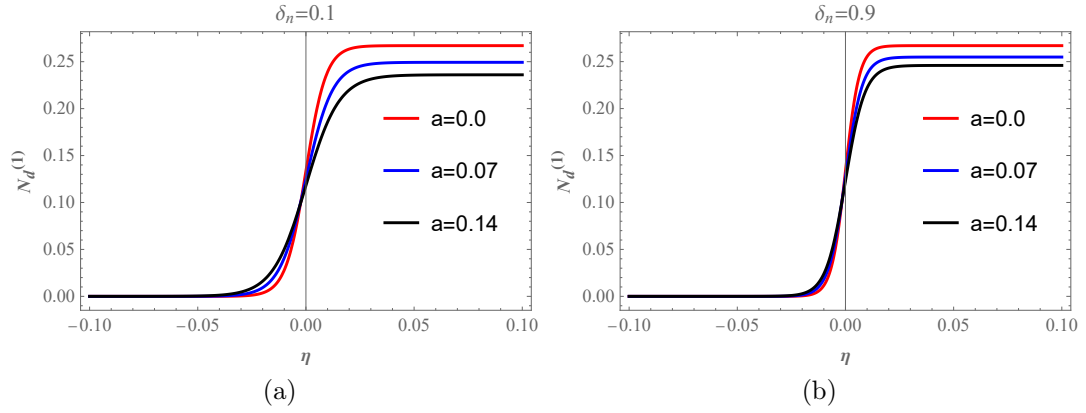


Figure 4.14: The behavior of monotonic dust-acoustic shocks are plotted for different values of non-thermal parameter "a" at fixed density ratio δ_n .

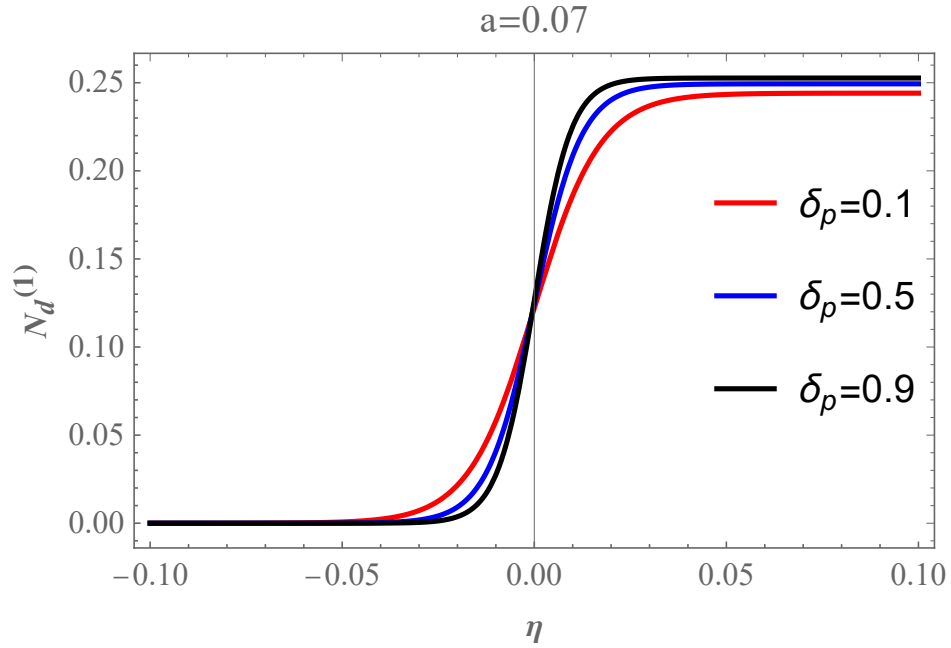


Figure 4.15: The profile of monotonic dust-acoustic shocks are plotted for different values of electrons and positive ions density ratio δ_p at fixed non-thermal parameter $a = 0.07$.

is observed that by enhancing the obliqueness of the magnetic field the amplitude, as well as the width of the soliton, decreases.

Since for the parallel propagation, the dissipative term vanishes, and our system is gov-

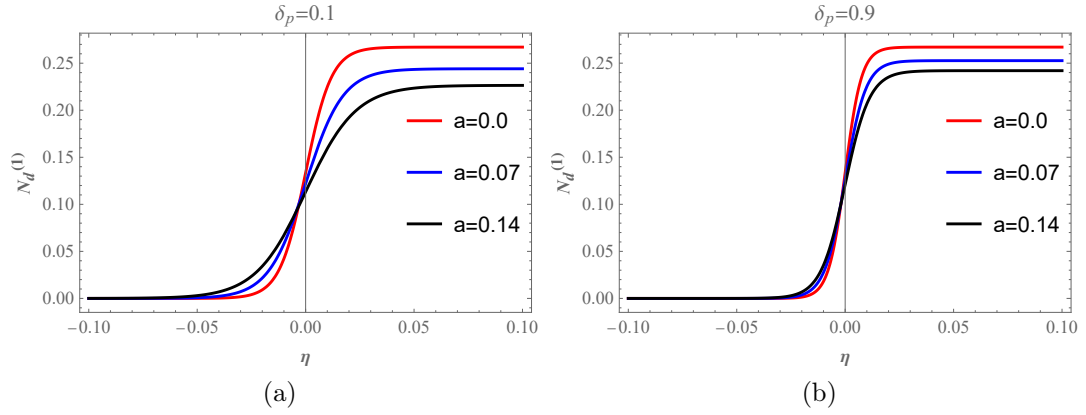


Figure 4.16: The profile of monotonic dust-acoustic shocks are plotted for different value of non-thermal parameter "a" at fixed electrons and positive ions density ratio δ_p . The left plot shows $\delta_p = 0.1$ and right plot shows $\delta_p = 0.9$.

erned by Burger's equation. This Burger's equation gave the monotonic dust acoustic shock structure. To investigate the monotonic shock structures, it is interestingly found that by enhancing the energetic positive ions population the shock amplitude decreases. While, to investigate the different densities ratios, i.e., electrons density versus energetic (Cairns distributed) positive ions density and negative ions versus energetic (Cairns distributed) positive ions, it is observed that both the density ratios increase the amplitude of the monotonic dust acoustic shock.

Bibliography

- [1] L. Tonks and I. Langmuir, *Phys. Rev.* *33* 195, 1929.
- [2] I. Langmuir, *Proc. Natl. Acad. Sci. U S A.* *14* 627, 1928.
- [3] F. F. Chen, Introduction to Plasma Physics and Controlled Fusion Volume 1, 2nd edition, *Plenum Press New York*, 1984.
- [4] A. Piel, Plasma physics an introduction to laboratory, space, and fusion plasmas, *Springer, Heidelberg German*, 2010.
- [5] J. R. Goldston and P. H. Rutherford, Introduction to plasma physics, *IOP Publishing, London*, 1995.
- [6] G. Manfredi, How to model quantum plasmas, *Fields Inst. Commun.*, 2005.
- [7] Tsytovich, V. N., S. V. Vladimirov, G. E. Morfill, and J. Goree, Theory of collision-dominated dust voids in plasmas, *Physical Review E* *63*, no. 5 056609, 2001.
- [8] Tsytovich, Vadim N., Gregor Morfill, Sergey V. Vladimirov, and Hubertus M. Thomas, Elementary physics of complex plasmas, *Springer Science and Business Media Vol. 731*, 2007.
- [9] J. Goree, G. E. Morfill, V. N. Tsytovich, and S. V. Vladimirov, Theory of dust voids in plasmas, *Phys. Rev. E* *59*, 7055, 1999.
- [10] P. K. Shukla, A. A. Mamun, Introduction to Dusty Plasma Physics, *Institute of Physics Publishing*, 2002.

- [11] D.A. Mendis and M. Horanyi ,DUSTY PLASMA EFFECTS IN COMETS: EXPECTATIONS FOR ROSETTA *American Geophysical Uniong*, 2013.
- [12] Angrum, Andrea, The Voyager Planetary Mission, *NASA web site*, 2015.
- [13] Cho, John YN and Michael C. Kelley,Polar mesosphere summer radar echoes: Observations and current theories, *Reviews of Geophysics* 243-265, 1993.
- [14] Havens, Karl E, Size structure and energetics in a plankton food web, *Oikos* 346-358, 1998.
- [15] Garscadden. A, Ganguly. B. N, Haaland P. D, and J. Williams, Overview of growth and behaviour of clusters and particles in plasmas, *Plasma Sources Science and Technology*, 1994.
- [16] Tsytovich. V. N, Dust plasma crystals, drops, and clouds, *Physics-Uspexhi*, 40(1), p.53, 1997.
- [17] Northrop, T.G., Dust plasmas, *Physica Scripta*, 45(5), p.475 1992.
- [18] J. E. Allen, Probe theory-the orbital motion approach, *Physica Scripta*, 45(5), p.497 1992.
- [19] Laframboise and Parker, probe design for orbitlimited current collection, *The Physics of Fluids*, 16(5), pp.629-636 1973.
- [20] Whipple, Potentials of surfaces in space, *Reports on progress in Physics*, 44(11), p.1197 1981.
- [21] F. F. Chen, Numerical computations for ion probe characteristics in a collisionless plasma, *Journal of Nuclear Energy. Part C, Plasma Physics, Accelerators, Thermonuclear Research*, 7(1), p.47 1965.
- [22] J.A. Bittencourt, Fundamentals of plasma physics, *Springer Science and Business Media*, 2013.

- [23] W. Baumjohann, R.A. Treumann, Basic space plasma physics, *World Scientific Publishing Company*, 2012.
- [24] R. A. Cairns, A. A. Mamun, R. Bingham, R. Bostrom, R. O. Dendy, C. M. C. Nairn and P. K. Shukla, *Geophys. Res. Lett.* *22*, 2709, 1995.
- [25] R. Lundin, L. Eliasson, B. Hultquist, and K. Stastewicz, *Geophys. Res. Lett.* *14*, 443, 1987.
- [26] D. S. Hall, C. P. Chaloner, D. A. Bryant, D. R. Lepine, J. Trikakis, *Geophys. Res.* *96*, 7869, 1991.
- [27] R. Bostrom, *IEEE Trans. Plasma Sci.* *20*, 756, 1992.
- [28] P. O. Dovner, A. I. Eriksson, R. Bostrom and B. Holback, *Geophys. Res. Lett.* *21*, 1827, 1994.
- [29] J. R. Asbridge, S. J. Bame, and I. B. Strong, *J. Geophys. Res.* *73*, 5777, 1968.
- [30] W. C. Feldman, R. C. Anderson, S. J. Bame, S. P. Gary, J. T. Gosling, D. J. McComas, M. F. Thomsen, G. Paschmann, and M. M. Hoppe, *J. Geophys. Res.* *88*, 96, 1983.
- [31] Y. Futaana, S. Machida, Y. Saito, A. Matsuoka, and H. Hayakawa, *J. Geophys. Res.* *108*, 1025, 2003.
- [32] R. Lundin, A. Zakharov, R. Pellinen, H. Borg, B. Hultqvist, N. Pissarenko, E. M. Dubinin, S. W. Barabash, I. Liede, and H. Koskinen, *Nature London* *341*, 609, 1989.
- [33] C. S. Gardner and G. K. Morikawa, Similarity in the asymptotic behavior of collision-free hydromagnetic waves and water waves, *New York. Inst. of Mathematical Sciences*, 1960.

- [34] C. S. Gardner and G. K. Morikawa, The effect of temperature on the width of a small amplitude, solitary wave in a collision-free plasma, *Communications on Pure and Applied Mathematics*, (1965) 35-49.
- [35] Washimi and Taniuti, Propagation of ion-acoustic solitary waves of small amplitude, *Physical Review Letters*, (1966) 996.
- [36] Taniuti and Wei, Reductive perturbation method in nonlinear wave propagation, *I. Journal of the Physical Society of Japan*, 1968.
- [37] L. Debnath, Nonlinear Partial Differential Equations for Scientists and Engineers, *Birkhauser Boston*, 2005.
- [38] Korteweg and De Vries, On the change of form of long waves advancing in a rectangular canal, and on a new type of long stationary waves, *Philosophical Magazine and Journal of Science*, 1895.
- [39] N. N. Rao, P. K. Shukla and M. Yu Yu, Dust-acoustic waves in dusty plasmas, *Planetary and space science*, 1990.
- [40] J. Weiland, Collective Modes in Inhomogeneous plasma, *IOP, New York*, 2000.
- [41] A. Hasegawa, Plasma instabilities and nonlinear effects, *Springer, Berlin*, 1975.
- [42] Younas khan et al, On the existence and formation of small amplitude electrostatic double layer structure in nonthermal dusty plasma, *Contributions to Plasma Physics*, 2020.
- [43] A. Scott, Encyclopedia of nonlinear science, *Routledge*, 2006.
- [44] J. S. Russel, Report on Waves, *Rep. 14th Meet. British Assoc. Adv. Sci*, 1844.
- [45] G. B. Airy, Tide and Waves, *Fellowes, London*, 1845.
- [46] G. G. Stokes, Report on recent researches in hydrodynamics (Chapter on waves), *Cambridge, London*, 1846.

- [47] D. J. Korteweg, De Vries, On the change of form of long waves advancing in a rectangular canal, and on a new type of long stationary waves, *London, Edinburgh, and Dublin Philosophical Magazine and Journal of Science*, 1895.
- [48] N. J. Zabusky and Porter, Soliton, *Scholarpedia*, 2010.
- [49] G. Ben-Dor, D. Igra and T. Elperin, Handbook of Shock Waves, Vol. 1, *Academic Press, San Diego*, 2001.
- [50] P. O. K. Krehl, History of Shock Waves, Explosions and Impact, A Chronological and Biographical Reference, *Springer-Verlag Berlin*, 2009.
- [51] A. Toepler, Beobachtungen nach einer neuen optischen Methode, *M. Cohen and Sohn, Bonn*, 1864.
- [52] E. Mach and J. Wentzel, Sitzungsber. Kaiserl. Akad. Wiss. Wien 92, *Abth. II*, 1864.
- [53] E. Mach and J. Wentzel, Sitzungsber. Kaiserl. Akad. Wiss. Wien 95, *Abth. IIa*, 1887.
- [54] K. Antolik, *Ann. Phys, II*, 1874.
- [55] K. Antolik, Aerial plane waves of finite amplitude, *Proceedings of the Royal Society of London*, 1910.
- [56] H. Bateman, Some recent researches on the motion of fluids, *PMonthly Weather Review 43*, 1915.
- [57] J. M. Burgers, A mathematical model illustrating the theory of turbulence, *Advances in applied mechanics*, 1948.
- [58] C. K. Geortz, Dusty plasmas in the solar system, *Reviews of Geophysics*, 1989.
- [59] D. A. Mendis and Marlene Rosenberg, Cosmic dusty plasma, *Annual Review of Astronomy and Astrophysics*, 1994.

- [60] M. Horanyi, Charged dust dynamics in the solar system, *Annual Review of Astronomy and Astrophysics*, 1996.
- [61] A. A. Mamun and P. K. Shukla, Cylindrical and spherical dust ion-acoustic solitary waves, *physics of plasmas*, 2002.
- [62] P. K. Shukla and V. P. Silin, Dust ion-acoustic wave, *PhyS*, 1992.
- [63] N. N. Rao, P. K. Shukla and M. Yu YU, Dust-acoustic waves in dusty plasmas, *Planetary and space science*, 1990.
- [64] F. Melandso, Lattice waves in dust plasma crystals, *Physics of Plasmas*, 1996.
- [65] M. Tribeche, H. Reguia and T. H. Zerguini, Effects of electron depletion on non-linear dusty plasma oscillations, *Physics of Plasmas*, 2000.
- [66] R. Lundin et al, First measurements of the ionospheric plasma escape from Mars oscillations, *Nature*, 1989.
- [67] S. Ghosh et al, Instability of dust acoustic wave due to non-thermal ions in a charge varying dusty plasma, *Physics of plasmas*, 2004.
- [68] Li-Ping Zhang and Ju-Kui Xue, Shock wave in magnetized dusty plasmas with dust charging and non-thermal ion effects, *Physics of plasmas*, 2005.
- [69] S. Ghosh, Z. Ehsan, and G. Murtaza, Dust acoustic shock wave in electronegative dusty plasma: Roles of weak magnetic field, *Physics of Plasmas* 2008.
- [70] R. A. Cairn., et al, Electrostatic solitary structures in non-thermal plasmas, *Geophysical Research Letters* 22.20, 1995.
- [71] T. Kakutani and H. Ono, Weak non-linear hydromagnetic waves in a cold collision-free plasma, *Journal of the physical society of Japan*, 1969.
- [72] M. Horanyi and D. A. Mendis, The effects of electrostatic charging on the dust distribution at Halley's comet, *The Astrophysical Journal*, 1986.

- [73] M. Horanyi and D. A. Mendis, Trajectories of charged dust grains in the cometary environment, *The Astrophysical Journal*, 1985.
- [74] A. Wekhof, Negative ions in comets, *The moon and the planets*, 1981.
- [75] I. M. Podgorny, E. M. Dubinin and P. L. Isrealevich, The estimates of the magnetic field in Halley's comet, *The moon and the planets*, 1982.
- [76] G. H. Schwehm and B. Kneissel, Optical and physical properties and dynamics of dust grains released by Comet Halley, *The Comet Halley. Dust and Gas Environment*, 1981.
- [77] Neil Divine et al, The Comet Halley dust and gas environment, *Space science reviews*, 1986.
- [78] Taibany and M. Tribeche, Nonlinear ion-acoustic solitary waves in electronegative plasmas with electrons featuring Tsallis distribution, *Physics of Plasmas*, 2012.
- [79] W. F. El-Taibany and R. Sabry, Dust-acoustic solitary waves and double layers in a magnetized dusty plasma with nonthermal ions and dust charge variation, *Physics of plasmas*, 2005.

Appendix